Dear editor and referees,

At this time when the news dominated by pandemic, we hope you and your family are healthy and safe. Let's get through the epidemic and welcome spring together. Our sincere apologies for the slow reply. The situation is not clear yet, we have to keep our social distance and self isolated at home. It causes difficulties to communicate, both person to person and data transfer. Our data is stored at the office, and the building is locked down most of the time. That's why we have to take longer time to make revisions for the manuscript.

Thank you for your valuable comments on our manuscript. First, we would like to express our sincere appreciation for your professional and insightful remarks on our paper. These comments are all valuable and have helped us to improve the quality of our paper. We have studied each comment and have made substantial changes. We hope our modifications will satisfy you and referees. Thank you for attaching importance to our work, and the dataset has been downloaded 2203 times (https://zenodo.org/record/3378912#.XmwrCXK-s2w) and the method of data set paper has been cited by two papers. We have received many thanks from many users for our dataset. Thanks again.

Sincerely,

Kebiao Mao, et al.

Response to referees

Response to referee #1

This is an excellent work with great significance for regional climate, environment and sustainability studies. The absence of complete and continuous time series LST datasets have challenged thermal studies for centuries. The dataset provided in this study is able to support the spatio-temporal analysis of climate change in China, and also the related sustainability assessment. The structure of the paper is well-organized, and the analysis based on the dataset is also sufficient.

Response: We would like to express our sincere appreciation to Anonymous Referee #1 for his/ her comprehensive review and such encouraging comments on our manuscript. These comments are all valuable. We have carefully addressed all the issues raised by the referee and the reply is presented below:

However, the temperature data collected from meteorological stations are actually air temperature (AT), not land surface temperature (LST). The relationship between the two temperature datasets is complicated and still not totally understood over heterogeneous land surfaces. I understand it is impossible to use actual LST collected artificially to reconstruct new datasets or for verification on large scales. Nevertheless, the relationship between AT and LST should still be investigated, and the impact on your results should also be discussed.

Response: In the past, meteorological stations usually measured air temperature (AT). In recent years, they have increased the measurement of more parameters, especially land surface temperature (LST). Therefore, to better ensure the accuracy of the data reconstruction or verification process, LST records from ground-based observations provided by the China Meteorological Administration were used in our study.

First, most meteorological stations have added observations of LST data since 2000. For sites with LST data, the LST data is used in the reconstruction or verification process. However, for some stations, LST may not be measured. For this case, we performed a regression analysis based on the MODIS LST and AT to increase the amount of LST data from the station. Second, we also took into account the situation pointed out by the referee, so the dataset we produced is a monthly scale product. Because somewhere is not always covered by the cloud, the error in monthly LST product is weakened compared to the daily LST product. Finally, as shown in Fig.11 of the original manuscript, the verification results indicate that our dataset accuracy is relatively high. Therefore, we believe that the reconstructed LST dataset can meet the research needs.

Response to referee #2

Dear professor,

Thank you very much, and your comments and suggestions for modification are very good. We will try to modify and emphasize your comments in our paper which are marked in blue.

Our work is very important and meaningful. The dataset has been downloaded 2124 times (https://zenodo.org/record/3378912#.XmwrCXK-s2w) and the method of data set paper has been cited by two papers which shows that our method is no problem, and we have received many thanks from many users for our dataset.

Temperature is one of the most important geophysical parameters in studying ecosystems. Global and regional surface temperature datasets are very important data for studying climate change, agricultural production, and urban heat island effects, and so on. At present, there are mainly two methods for obtaining global surface temperature data set. **Our method tries to combine the advantages of remote sensing and traditional methods to improve accuracy.** A detailed analysis is already made in "**AC9: 'Response to RC3', kebiao mao, 16 Mar 2020**". The point-to-point response is as follows.

Response to RC3

Summary: Data gaps, e.g. due to cloud cover or aerosol, limit the usefulness of land surface temperature products derived, for instance from MODIS aboard the EOS TERRA and AQUA satellites. Depending on region and season this applies to both daily and monthly products. This paper presents a potential improvement of this situation by proposing the development of an enhanced monthly LST product based on gap-filled daily LST data for China. Gap filling is carried out with the aid of LST observations from meteorological stations, a similarity analysis and linear regression between observed LST and elevation. The paper provides an extensive interpretation of LST trend maps on annual, seasonal and monthly temporal resolution

This paper has been submitted to the journal "Earth System Science Data". My understanding of this journal is that it is a platform to present new data sets alongside a thorough description and evaluation of the used methodology and results, the data formats and the content of the data files. To my opinion, this paper does not fit into this journal. Neither is the method described adequately so that it is easily understood, nor is the method or steps of it evaluated or illustrated enough. Examples of the new data set are not shown, instead the authors present maps of the multi-year annual mean LST, trends and correlations. Too much focus is put on harvesting the data set. I don't see a reason why I should use this data set. It is neither evaluated properly enough nor does it come with a critical discussion of limitations, uncertainties or even improvements over the data sets existing so far.

Response: We would like to thank the anonymous referee for reviewing our manuscript. These constructive comments are very important for us to improve the present manuscript.

We agree that description should focus on the introduction of the data set production method and the evaluation of the data set. So, we added more information on the reconstruction method, especially some examples of graphs in the process, so that it can be more easily understood by users. In addition, we removed the analysis part of the LST trend in the main body of the manuscript according to your advice. After careful thinking and analysis of all the questions you raised, we have replied to all these questions and comments. In this process, we also have carefully modified and improved the corresponding parts of the manuscript. Changes in our manuscript are indicated by blue slanted font. We hope will meet with approval.

General comments:

GC1: The description of the LST restoration method requires rewriting, clarification and more illustration of what is done. Several issues are unclear. Please see my specific comments.

Response: Thank you for the valuable comment. We have made a point-to-point response to your question in the specific comments. We hope these modifications can satisfy you.

GC2: Section 3 lacks a final sub-section in which the reader learns what the output of all the measures explained so far is. Neither are examples of re-constructed daily LST time series at a particular location nor gap-filled daily or monthly LST maps shown here. Missing at this place as well is a critical assessment of the validity of the obtained, gap-filled LST data. The evaluation shown in Section 5 it too global (see also GC5). The results section begins right away with the presentation and discussion of the annual national-mean LST.

Response: Thank you very much for your advice. For thermal infrared remote sensing data, there are large number of missing values (more than 60%) in daily MODIS LST image and the location of missing data is randomly distributed. In this study, we only reconstructed the missing pixels of the monthly image, resulting in many missing values still exist in the reconstructed daily MODIS

LST image, though these missing values had no much effect on the accuracy of our final monthly image. To make the reconstruction method easier to understand, we added more explanations of the reconstruction steps and the corresponding output in the manuscript. Thanks again for your suggestions.

GC3: While the data section introduces data from both sensors MODIS TERRA and MODIS AQUA, it is not clear which are shown in the results (only for Figs. 3 and 4 it is mentioned that this is TERRA). This is particularly important since local overpass times of MODIS AQUA are closer to the daily minimum and maximum LST values than of MODIS TERRA. If for some reason the LST results shown in Fig. 5 are based on a combination of both, TERRA and AQUA, then there is a critical lack of information throughout the paper which needs to be mitigated.

Response: The Terra satellite acquires data daily at 10:30 and 22:30 local time and the Aqua satellite acquires data daily at 13:30 and 1:30, resulting in four LST observations per day. We agree that the Aqua satellite can better represent the minimum/maximum LST values. For the average LST, theoretically, the more data used in a day, the more accurate it is in representing the temperature of the day. At the same time, the combination of Aqua and Terra data can reduce some systematic errors more than using only Aqua data. Therefore, after obtaining the seamless LST data at the four local overpass times after data reconstruction, we averaged the Terra and Aqua data during the day to get the daytime LST. Similarly, the average of Terra and Aqua overpass at night was used as the LST at nighttime. Finally, the final result is obtained by averaging the day and night MODIS LST. We have added a brief description in the manuscript as follows.

"After LST data restoration data reconstruction, four overpass times of images are obtained each month. Calculated the average LST at four times to represent the LST image of the month."

GC4: A large fraction of the results section 4 comprises hypothetical considerations about potential causes of the observed LST changes, supplemented by hypotheses about the potential impact the observed LST changes may have. I suggest that all these hypotheses are taken out of the paper and used to motivate a suite of follow-on studies where an improved and evaluated LST data set is compared to and interpreted with the aid of additional data, such as CO2 concentration, atmospheric re-analyses, snow cover data, land-cover change data, etc. Results of those studies can then be published in highly ranked journal such as Nature Geoscience or similar.

Response: Thanks for your good suggestions, which has helped us to improve the manuscript quality. We agree that the statement about potential causes of the observed LST changes and impact should be deleted to better highlight the data set. We also plan to combine the reconstructed LST data set with other data for further research. Thanks again for your advice.

GC5: It is clear that the re-construction method presented in Section 3 cannot be ideal and is likely to have errors. However, the verification section is very global and does not touch upon an evaluation of the steps performed in the re-construction but instead, because the biases / RMSEs apparently are not "good" enough, comes up with a bias-correction method. In order to develop and apply such an additional step, first a thorough evaluation of the re-construction method should be carried out, taking into account into which direction the re-construction and hence gap-filling of the original LST product will change the LST values. This needs to be understood first and is not convincingly enough laid out in this paper. –> One example: Lets consider that the original monthly daytime LST of a month with high insulation but also a considerable number of data gaps due to invalid daily LST values due to clouds is +35degC. If we assume that this occurs in a region with high station density, then it is likely that the actual station measurements will have a high impact on the reconstructed LST. According to your method one can expect that a substantial fraction, if not all, of the missing daily LST values would be replaced by station observations, which since these are from cloud-covered days, provide a LOWER LST, e.g. +25degC. Now, reconstructing the monthly LST with this new daily LST time series which is composed of original clear sky and hence high LST values AND re-constructed cloudy-sky lower LST values would result in a lower monthly mean LST value. And this is actually your result for many of the grid cells. Such considerations and explanations are required by a reader of this paper and user of your data set to understand what is the new, enhanced, and credible part here.

Hence, what the evaluation section really needs is A) examples of time series of the original and the re-constructed DAILY LST for several selected stations for several years / seasons - taking into account all three flavours of the reconstruction method

B) examples of maps where the authors illustrate how for a region without valid data (like shown in

Fig 3) the reconstruction method fills in LST values - again taking into account all three flavours.

C) examples which illustrate how the reconstruction method works for day-time and night-time (clouds have different impact) and in areas with high- or low open water areas and in areas with / without snow cover

D) examples of different topographic complexity which illustrate how the similarity concept and the elevation-determines-LST concept perform - ideally for two different seasons. Once this is done, I suggest a similar investigation with the monthly LST data. I as a reader and potential user of an enhanced LST data set want to see original and reconstructed monthly LST maps and not just multi-annual mean maps of trends. Last but not least a sub-section should be devoted to the true quality of the station observations in terms of the spatial representativity and other aspects I laid on the specific comments.

Response: After careful thinking and analysis of all the questions and suggestions you raised, we agree that the reconstruction method should be evaluated more comprehensively to show the credibility of the generated data set. The associated explanation has been added to the revised manuscript and can be seen in Subsection 3.3.2. We hope our revision will give you satisfaction.

GC - wording / editing:

- Please avoid usage of, e.g., "warming trends". A trend is either positive or negative, indicating an increase or decrease of the geophysical parameter assessed; in your case it is the LST, so we have an increasing LST which is a warming and we have a decreasing LST which is a cooling. The trends themselves are not warming.

Response: Thank you very much for your careful review. We have modified the words " warming trends " and " cooling trends " to the more appropriate " positive trends " " negative trends", respectively.

- You are introducing regions I through V in Figure 1 but hardly refer to those in the description and interpretation of your results. It would greatly aid the readability of your paper if you would more stringently follow your own notation of regions instead of the geographical names which may not be so familiar to readers outside of China.

Response: Thank you very much for your careful review. We also agree that the numbering of each area is easier for readers to understand. We have checked the relevant parts of the manuscript and marked with the corresponding number of the geographical name.

Specific comments:

Lines 63/65/67/70: "low-quality" ... "noise-contaminated" ... "cloud contamination pixels" ... "poor-quality" –> Please, this is not a narrative but a scientific paper. I suggest to define clearly at this stage for which pixels you will re-construct the LST, write this down in a well-structured way, and introduce terms which hold for the entire paper. "low-quality" can be due to clouds, low observation angles, aerosols, etc."; "noise-contamination" as well, even though this sounds like sensor noise and cross-talk effects as well; "cloud contamination pixels" is clear. Which of the low quality pixels will you replace by a re-constructed value for which effects causing this low quality? - clouds? / - cloud shadows? / - aerosol? / - low observation angles? / sensor noise?

Response: We appreciate the referee for his/her suggestion, which has helped us to improve the manuscript quality. The pixels which need to be reconstructed include null pixels and low-quality pixels. Low-quality pixels are caused by undetected thin clouds, atmospheric disturbance, observation geometry and instrumental problems (Wan, 2014). We agree that we should define clearly at this stage for which pixels you will re-construct the LST. So, as the reviewer suggested, we have modified these words in the revised manuscript. The revised lines 63-70 are as follows:

"Moreover, other factors can also contaminate the observation signal and cause the data to be unavailable, such as atmospheric disturbance, observation geometry and instrumental problems (Wan, 2014). In general, the abnormally low values in LST maps caused by undetected thin clouds, together with other poor-quality values, need to be identified and filtered because these values greatly reduce the accuracy of the LST data.

Cloud cover and other factors, which causes extensive amounts of missing and low-quality pixels, significantly reduces the proportion of usable LST data and poses a problem to further applications. Thus, the reconstruction of these missing and low-quality pixels is necessary for satellite-derived LST applications."

Line 78: So far with the advantages of method I. What are its disadvantages?

Response: Thank you very much for your careful review and reminder, we have added the corresponding statement in the manuscript. The first category of methods, which estimate missing MODIS LST data using only LST data, takes advantage of the similarity and interdependence of the available temporal/spatial attributes of neighboring pixels. To some extent, these methods have the advantage of simplicity and reliability. However, this category of methods is often not as reliable as expected especially in complex topographical regions and areas with many missing data, because it cannot obtain enough information for reconstruction.

"To some extent, these methods have the advantage of simplicity and reliability. However, this category of methods are often not as reliable as expected especially in complex topographical regions and areas with many missing data, because it cannot obtain enough information for reconstruction."

Line 93: Please provide a frequency here; what is meant by "high-frequency channels"?

Response: Thank you for your comments. High-frequency channels usually refer to channels with a frequency of 85 GHz and above. The radiation of the high-frequency channel mainly comes from the shallower surface emission layer, which is closer to the 0 cm surface temperature; while the low-frequency channel has better penetration, the emission layer maybe come from a certain depth of soil, and the obtained bright temperature is the volume bright temperature rather than surface temperature, so there is a large error. We also explain it in the manuscript.

Lines 111-122: I don't think this paragraph belongs into the "study area" section. I suggest to either delete it or put it into the Introduction section to underline the importance of a more accurate, medium-term LST data set.

Response: Thank you for your comments. We also agree that this paragraph shouldn't belongs into the "study area" section, so we removed this paragraph. Thank you for your guidance.

Lines 129-131: Also here I suggest to remove the hint to the crop production; this information appears not to be relevant for the paper - unless you want to refer to land surface type patterns ... which you, however, don't to for the other three regions in eastern China. So this info can be removed. Line 130: I have difficulties to believe that region I covers > 50% of China's land area as it is written currently.

Response: Thank you for your comments. The change of temperature has a significant impact on grain production. In order to better explain the impact of temperature in different regions on crop production, we have added more content of crop production. After careful consideration, we agree that these information were redundant for this study, so we removed this sentence (Lines 129-131). We are sorry for carelessness on Line 130 and we have removed it. Thank you for your guidance.

Figure 1: - The coloring of the elevations is opposite to what is usually used. Was this done on purpose? If so why? - Did you try to use smaller black dots to mark the stations? These might come out clearer. - Did you try to use white or black for the delineation of the sub-regions; currently their boundaries are somewhat hard to follow. - I note that the red ellipses denoting the key regions used for evaluation are partly obscured by the dots marking the station. I suggest to a) use a different color for the ellipses (black or white) and b) plot them on top of the stations locations. - In the caption: "spatial patterns of the meteorological stations" –> perhaps better "spatial distribution of ... ", or simply "location of ... ". One could already add the total number of these stations in the text of the caption.

Response: Thank you for your comments. We also tried some methods to match the symbols and colors to better reflect the Terrain features, the stations locations, the area divisions, and the location of the stations for accuracy verification, but none of them achieved a good effect. Thanks for your good suggestions. We changed the color of the elevations, and used the light color combination to make the boundary of the sub-regions more clearly.

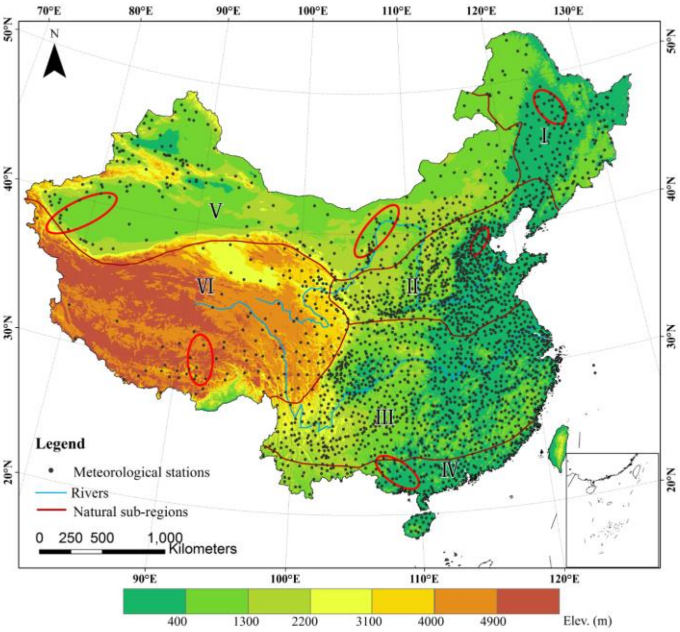

Table 1: It appears to be that the ellipses contain more stations than are actually listed in Table 1, e.g. regions c) and d). What is the reason for this?

Response: Thank you for your comments. The LST of the stations we selected (Table 1) has a significant positive/negative change trend, and these stations are distributed in areas with different climatic conditions. We think these sites are representative when assess the effectiveness of the reconstruction method. In the process of data reconstruction, we used as much reliable site data as possible to improve the accuracy of the results. The eastern part of China（I, II, III and IV）has a flat Terrain and high site density. In order for readers to be able to clarify the distribution of sites in different regions, Figure 1 contains more sites than they actually are. We have also explained this in the manuscript.

Line 149: I suggest to put in some notion about the snow cover and its duration in the various regions because reflection of incoming solar radiation as well as thermal emission are considerably different from bare and vegetated surfaces and should play a role in the retrieval.

Response: Thank you for your comments.

Lines193-198: I don't understand the meaning of this paragraph. Is this something you did with the MOD/MYD11C1 and MOD/MYD11C3 data? Possibly not because none of these data sets include brightness temperatures. Hence I find this paragraph a little confusing and not well connected to the previous one. Clarification would be welcome.

Response: Thank you for your comments. This sentence is an introduction to MODIS LST data. It indicated that the monthly (MOD11C3/MYD11C3) data are calculated and averaged by daily data (MOD11C1/ MYD11C1). This is also the basis of our research that the daily data (MOD11C1/ MYD11C1) can be used to reconstruct the monthly (MOD11C3/MYD11C3) data.

- Please mention why you don't u se data before 2003. TERRA MODIS LST data begin in Feb. 2000 and AQUA MODIS LST data begin in July 2002.

Response: Thank you for your comments. As you said, AQUA satellite did not acquire data for the whole year before 2003. It is not very reliable to take the average temperature obtained only from two overpass times as the average LST values. Moreover, the average LST values from TERRA may deviate from the value from TERRA and AQUA after 2003.

Line 203: Please provide a reference to the Jackknife method.

Response: Thank you very much for your careful review. Jackknife method refers to the random resampling of the entire observations set several times (Benali et al., 2012). We also added this reference to the manuscript.

Lines 200-209: - Did all these stations record without data gaps over the time period given?

- Is the way the land surface temperature is observed homogeneous across all stations for the entire period? It is automated of manual? Were there changes in instruments? Were there changes in location (and hence land surface properties) for any of the stations during the period? Were there changes in the location of the stations with respect to the heat island of a growing city / faculty complexes / nearby reservoirs / reforestation? In other words: How confident are you that these data provide high quality means to supplement your product and to use it for (a first) evaluation?

Response: Thank you for your comments. Thank you for your comments. Stations record were provided and subjected to strict quality control and evaluation by the China Meteorological Administration. Only a small part of the observation records are excluded due to disqualification. We have uniformly processed the surface temperature data of the observation station before it is used in this study. For the integrity of the site data, only recorded site data was used in this study, and null values were ignored. For the change of site location, due to urban expansion and other reasons, from 2003 to 2017,the detection environment of some stations was destroyed and relocated. For the relocated stations, we only retained the observation data and coordinate information of the long observation time series before / after the relocation.

- How representative are the locations of the stations in terms of the surface conditions (over which surface exactly is the LST measured in relation to the matching (co-located) CMG 0.05 degree pixel of the MODIS data?)? This is critical for your step I (see Line 225): filling the daily pixel by the in-situ observation. It has been shown that already at the scale of 500 m the evaluation of a geophysical quantity derived from a satellite sensor with an in situ observation can yield misleading results because of heterogeneous surface properties in the 500 m grid cell. Here we talk about a grid cell an order of magnitude larger!

Response: Thank you for your comments. Large-scale data includes LST and soil moisture, and there are indeed representative problems in the data verification part of ground stations. Because thermal infrared is greatly affected by clouds, if you do not use ground station observation data information, direct interpolation will result in higher interpolation results than actual results. In order to further improve the interpolation accuracy, we use as much ground station information as possible to make the ground products more consistent with the actual situation. This is currently the best selection method for such large-scale data. In order to further increase the representativeness of the site data, the number of sites will need to be increased in the future to improve accuracy where the surface type changes greatly and the Terrain is undulating. For this part of the content, we also made supplementary explanations in the paper.

- I don't understand the mentioning of / focus to the 4 equator local overpass times. China is a big country and local overpass times at the equator differ from those further north. I suggest to provide maps (4, two for AQUA, two for TERRA) of average (typical) local overpass times of your region of interest for illustration that this approach is correct.

Response: Thanks for pointing this out. Yes, we agree that four maps for illustration is more appropriate for this study. We have changed it for the whole context in the revision.

Lines 210-211: I don't understand the connection between the SRTM data and the LST; please be more specific. Could it be that your DEM had gaps which you filled with the SRTM data? Please clarify in the text.

Response: Thank you for your comments. SRTM (Shuttle Radar Topography Mission) DEM(Digital Elevation Model) data were used in this study. Temperature dem is closely related. There have been many studies on the relationship between temperature and altitude in geography. For example, Barry studied the relationship between mountain temperature and altitude (Barry, 1992). Körner redetermined the geographical significance of altitude and discussed the influence of altitude on temperature (Körner, 2007). The vertical decline law of temperature decreasing by 0.55°C when the altitude increases by 100 meters is applicable to most areas.

Line 211: I note that for the verification you are using a subset of the same data set you use for the improvement of the data set. Isn't there perhaps another, more independent means to verify your product, e.g. airborne satellite under flights, other well-calibrated IR temperature measurements?

Response: Thank you for your comments. Due to its optimal temporal and spatial resolution throughout the world, the Moderate Resolution Imaging Spectroradiometer (MODIS) sensor has become an excellent data source for satellite-derived LST data and is widely used in regional and global climate change and environmental monitoring models. We have also tried other data, but the stability and accuracy of the data are not high enough, and the data obtained by different sensors are quite different.

Line 283-290: Also here I have several concerns with the formulation as well as the content: - Whether the approach described here is viable for a 0.05 degree grid cell needs to be proven and needs to be supported with the information you provide in the revised version of this paper with respect to how representative the station measurement is with respect to the grid cell in terms of land cover, elevation, etc.

Response: Thank you for your comments. This method is to take advantage of the similarity of geographically adjacent geographical units, and the formulation has been widely used in geographic information system large-scale interpolation. It is widely used at the macro scale, please refer to the following references (Hansen et.al.,2010; Smith et.al.,2018; Hansen et.al.,1987; Hansen et.al.,1988;

Hansen et.al.,1999; Rayner et.al.,2003). We have added references to the manuscript.

- It is not correct that the LST in adjacent cloud covered grid cells is always lower than the clear-sky ones. This is only valid for daytime LST values and might also be not fully valid for snow-covered grid cells.

Response: Thank you for your comments. We revised this sentence in the revised version.

- I suggest to not write "prediction" in the context of the satellite LST observations. Likewise, I suggest to replace "predictor factors" by, e.g., "influencing factors" and add "elevation".

Response: Thank you for your comments. We revised this term in the revised version.

- How is the co-location between the MODIS grid cell and the station done? Is there a threshold distance to the grid-cell center required to use the station observation or is it sufficient if the station falls just within the approximately square-shaped grid cell? How did you measure this distance (in kilometers / meters or in degrees)?

Response: Thank you for your comments. We deal with this problem based on this principle: (1) when there is no cloud, we use MODIS temperature product data; (2) in the case of cloud, if the pixel has ground observation site data, we will calculate the difference when there have no cloud based on nearby dates between the pixel and the site data of the MODIS temperature product as a threshold to modify the site observation data as the temperature data of the pixel; (3) When the pixel has no site data, it is processed by classic interpolation methods. See references (Hansen et.al.,2010; Smith et.al.,2018; Hansen and Lebedeff, 2018).

Line 214: "... it is difficult to reconstruct the operational LST dataset under clear-sky conditions on a daily scale ..." –> I don't understand. Why do we want this in case of a clear-sky pixel?

Line 215: "and it is even more difficult to retrieve the LSTs to identify the real performance of the LST reconstruction ..." –> retrieve LSTs from what? What do you want to say with this sentence?

Response: Thank you for your comments. We are sorry for our unclear expression. We have revised sentence, and the revised Figure is as following.

"*It is difficult to reconstruct the cloudless LST dataset on daily scale, and it is even more difficult to reconstruct the dataset that can reflect the LST of the ground under the cloud cover.*"

Line 217: This "high-precision data set", does this have daily or monthly temporal resolution or both? It is not clear what the main output is.

Response: Thank you for your comments. The new data set is monthly temporal resolution, and we are sorry for our unclear expression. In addition, we also modified this sentence in the original text as follows. We create a reconstruction model that combines meteorological station data and daily and monthly MODIS LST data to reconstruct a high-precision monthly dataset that can reflect the true LST under cloud coverage. The associated explanation has been added to the revised manuscript and can be seen in Subsection 4.3

Lines 219/220: You mention "poor-" and "low-quality" pixels. Are these different?

Response: Thank you for your comments. In the original manuscript they have the same meaning, and we have modified it to "low-quality".

Line 223: What is "traversed"? What are the "corresponding daily pixels"?

Response: Thank you for your comments. The associated explanation has been added to the revised manuscript,

Line 229: I recommend that in the paragraph ending in this line you add references to the subsections (3.3.1, 3.3.2 and so forth) and note that the aspects mentioned here are explained there in more detail.

Response: Thank you for your comments. As the reviewer suggested, and we revised these sentences in the revised version.

Figure 2: - What do you mean by "traversal of daily pixels ... separately"? Please be more specific. - The MOD/MYD11C1 daily LST products come in at the side. Are these auxiliary products? - Are the steps below the diamond shaped box with "The daily pixel value valid?" repeated for every day, i.e. is this a loop? - If possible I would try to color those parts of the flowchart which belong to steps I to III described in the text with different colors. - If possible I would also try to add one more illustrative figure which better explains what you do with the missing and the poor-quality pixel (of the monthly (?) data) in connection with the daily data (possibly of the same pixel but the entire

time series). I guess what would greatly help in the understanding of your method if you would further illustrate the steps carried out.

Response: Thanks for your comment and good suggestions, which has helped us to improve the manuscript quality. "Traversal of daily pixels ... separately" means that we determine the invalid pixels in daily LST images at the same location at the corresponding time, and we revised these sentences in the revised version. In addition, as the reviewer suggested, Figure 2 has been revised to explain more clearly. It is also presented below for the ease of reviewing.

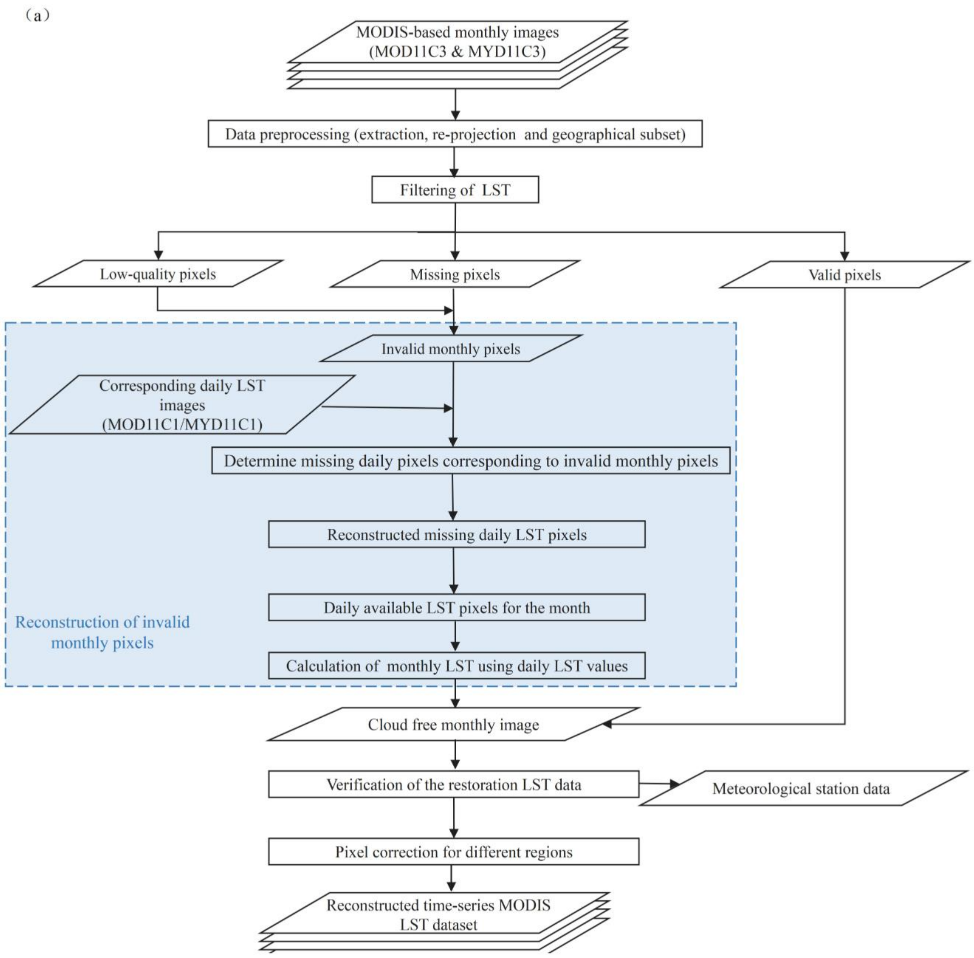

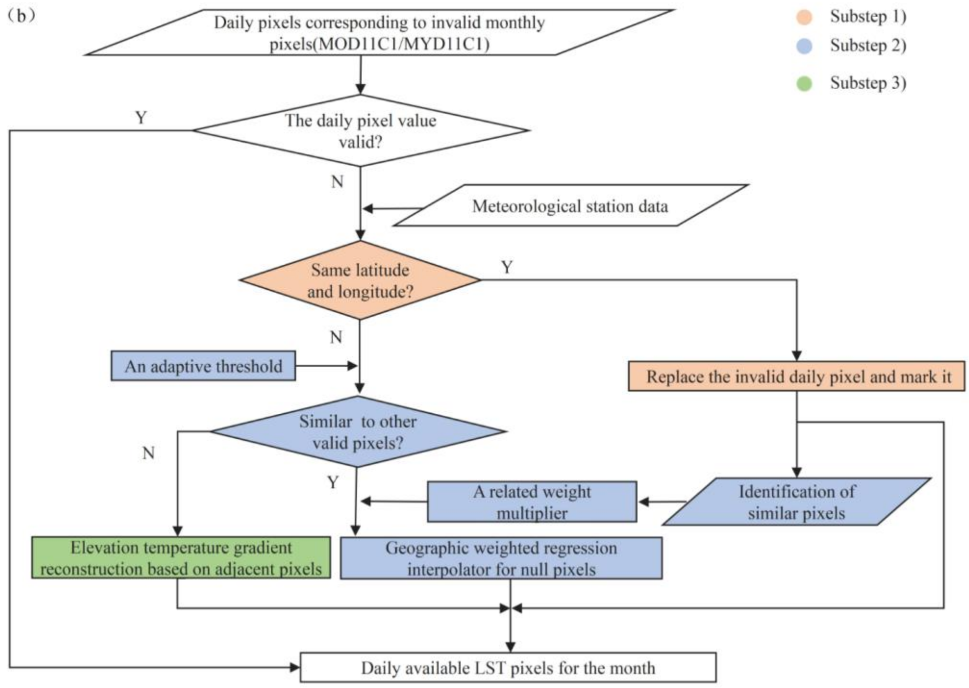

"Figure 2: (a)The summary flowchart for reconstructing MODIS monthly LST data, (b) The detailed flowchart for reconstruct missing daily pixels in (a)."

Figures 3 and 4, caption, and interpretation - I suggest to step back from the notion of an exact time for which these maps are valid and instead simply state that this is "daytime". While the local overpass time at the equator is 10:30am, China is a) further north and b) extend over a substantial latitude area. In addition, these maps are composited from MODIS data of several adjacent overpasses.

Response: Thank you for your comments. The Terra satellite passes over the China daily at 10:30 and 22:30 local time, and we agree that "daytime" is more appropriate than "10:30", and we have revised it in the manuscript.

- I suggest to harmonize the color table for both maps. Currently the same temperature range is color coded differently in a) and b). Either you use red over white to blue or red over yellow/green to blue to display the gradient from high to low temperatures. In addition it is very confusing (counter-intuitive) to have high temperatures given by bluish colors (in a). - The white areas in Fig. 3, are these the result of the filtering described in lines 256- 258? If not clarify what is shown please.

Response: Thank you for your comments. We agree that multiple colors usually indicate better. We have also tried using a color table, similar to red to white to blue, to represent the distribution of temperature values. However, due to the large difference in temperature range between the cold season (January in the manuscript) and the warm season (July as the example), July is concentrated in the high temperature range and January is in the low temperature range. Therefore, the same color coding will concentrate the colors, and the distribution of high and low LST in an image cannot be visually displayed. So, we chose two legends and used green and red to represent low-temperature January and high-temperature July, respectively. In addition, Figure 3 presents the distribution of missing values of unfiltered waves to illustrate that the daily LST data is heavily affected by the cloud.

Lines 247-260: I suggest to be more precise in your wording. - "high-precision LST dataset" should get "daily"

Response: Thank you for your comments. We are sorry for Inaccurate wording and we have modified it .

Line 251: "... composite data." –> Link to Figure 4 is missing.

Response: Thanks a lot for pointing this out. We revised it.

- "identify and reconstruct cloud-contaminated pixels" –> Sure. In which data sets? In the daily or monthly ones?

Response: Monthly LST data set is reconstructed in the text. In addition, we have modified the sentence in the original text as follows.

"It is necessary to identify and reconstruct cloud-contaminated pixels, which seriously affect the use and analysis of monthly LST data."

- Line 255 / 258: Further up you wrote "identify and reconstruct" ... here you write "eliminate to ensure the quality of the LST data" or ... "rejected". Please use one common set of expressions for filters, qualities, and actions undertaken. My assumption is that you identify low-quality pixels (or grid cells) by means of the QA filters. For further analysis you (possibly) set values in all these grid cells as missing values (preferably the same as is used for those pixels which don’t have a valid LST value anyways because of cloud coverage). Later, you are replacing the missing values by LST values derived with one of the three methods presented in Section 3.3.2

Response: Thanks a lot for pointing this out. We agree that inconsistent representations in the manuscript may confuse readers, and we have modified the sentence in the original text as follows.

“It is necessary to identify and reconstruct low-quality pixels, which seriously affect the use and analysis of monthly LST data. A reliable method for removing low-quality pixels is implemented using the data quality control information for MODIS LST data. The data quality control information is statistically calculated and stored in the corresponding QA layer and is represented by an 8-bit unsigned integer and can be found in the original MODIS LST HDF files. Therefore, we use the quality control labels for daily and monthly files as mask layers to identify low-quality pixels to ensure the quality of the LST data. Finally, pixels with QA layer labels of “the average LST error <=1 K”, “LST produced, good quality” and “the average emissivity error <=0.01” are considered to be high-quality data, and the remaining pixels are low-quality pixels and are set to missing values. Finally, we reconstructed all the invalid pixels in monthly LST data.”

Line 258: "Quality information is almost indicative; thus, sufficient information ..." –> What does this mean?

Response: Thank you for your comments. Quality control information is a reliable method to judge the quality of pixel, it is merely indicative, no other quality information were used to eliminate lower quality LST pixels (Benali et al., 2012).

Again: "poor-quality pixels" are eliminated versus "low-quality pixels" are filtered ...? So to filter is not to eliminate?

Response: Thank you for your comments. Pixel filtering is to identify low-quality pixels and set them as missing values. We have modified the sentence in the manuscript for a better understanding in Page 8 Lines 249-252.

“Therefore, we use the quality control labels for daily and monthly files as mask layers to identify low-quality pixels to ensure the quality of the LST data. Finally, pixels with QA layer

labels of "the average LST error <=1 K", "LST produced, good quality" and "the average emissivity error <=0.01" are considered to be high-quality data, and the remaining pixels are low-quality pixels and are set to missing values. Finally, we reconstructed all the invalid pixels in monthly LST data."

Lines 261-265: - Here you use a new term "invalid". Does "invalid" mean poor-quality or completely cloud covered or low-quality or eliminated or rejected or ...? - Note in line 261 that this is the monthly LST data.

Response: Thank you for your comments. Invalid pixels include missing pixels and low-quality pixels. We also have added corresponding explanations in the text as follows.

"Both missing pixels and low-quality pixels are considered invalid pixels that need to be reconstructed."

- Please go back to Figure 3 and clarify whether the white pixels there in results from your filtering or are an inherent feature of the daily LST product, i.e. in those white areas no daily LST values could be derived?

Response: Thank you for your comments. There is no daily LST values could be derived in the white area. We have revised the related contents as following.

"Figure 3: Spatial distribution of valid data for daily MODIS LST data from Terra during the daytime on (a) January 1, 2017, and (b) July 1, 2017. Areas of missing data are blank.

Figure 4: Spatial distribution of valid data after pixel filtering for monthly MODIS LST data from Terra during the daytime on (a) January and (b) July. Areas of invalid data are blank."

- In Line 275 you have "poor-quality values in monthly pixels"; in lines 280/281 you have "poor-quality daily data ... low-quality pixels in the monthly data" –> inconsistent. It is not clear what you do and why you differentiate between poor- and low-quality.

Response: Thanks a lot for pointing this out. We revised it. In the manuscript, they have the same meaning, which were determined by the pixel filtering, and we have revised them all to "low-quality" in Page 9 Lines 274 and in lines 280/281.

- Lines 275/276: "The contributions of multiple valid daily pixels, despite their good precision, are rejected along with the final poor-quality values in monthly pixels." –> I don't understand what you mean. What I assume is that you refer to a pixel in the monthly LST product, where the QA suggests, for instance, an accuracy of the LST > 2 K. Your filter identifies this pixel. Good. The monthly LST value of the grid cell is based on daily LST values, presumably those you investigate as well. Now it possibly depends on what the criteria (set by the MODIS LST production team) are to use a daily LST value to compute a monthly LST value. It seems to me that this information is not known - otherwise you would have given it. I am sure, however, that a documentation exists where it is written up to which QA flag daily LST values are used in the monthly LST product. Given the fact that this piece of information is not given it is not entirely clear which direction your approach has.

Response: Thank you for your comments. You're right, the monthly LST value of the grid cell is based on daily LST values. Because we get no missing value by reconstructing the day data, and then calculate the monthly value according to the average value of the day, which is not affected by the original method, so there is no introduction to the original data discrimination method.

- Line 281: "from the daily data" –> If I understood you correctly then this would be the "gap-filled" or reconstructed daily data, am I correct? In that case I would mention it here. If not, then I did not understand what you did.

Response: Thank a lot for the comments. You're right.

Lines 297-307: - Lines 301/302: "abrupt transformation" "wheat harvesting" ... "expansion of a city" I can agree that wheat harvesting is an abrupt transition as it happens within a day; time scales for the expansion of a city might not be days, though. Consider rewriting please.

Response: Thanks a lot for pointing this out. We revised it.

- Line 303: "nearest phase" –> What is meant here by "phase"? -

Response: Thank a lot for the comments. We are sorry for the wrong expression. We have revised "nearest phase" as "images from the other three overpass times".

After equation (1) where the target pixels is the one without a subscript and the "similar pixels" carry a subscript I became confused with the text beginning in Line 303: "for the target pixel i ...". I have difficulties to imagine where pixels i and j come from. I again recommend to add a figure illustrating the process.

Response: Thank a lot for the comments. We added a subscript for the target pixels and also added letter marks.

$$“T_t = \sum_{i=1}^{m} W_i \cdot T_i + \sum_{j=m+1}^{n} W_j \cdot T_j \quad , \tag{6}$$

where T_t is the reconstructed LST value of a target pixel, T_i and T_j represent LST values for the similar pixel i and j, the sum of W_i and W_j values is 1.“

- Why three images that are temporally closest at the same overpass time? These three images form the "reference images" ... meaning that pixel i is not on them but pixel j? No entirely clear.

- "valid pixel j" –> What is a "valid" pixel and how is it defined? - The concept of the threshold is not clear to me. How is a threshold determined?

Response: Thank a lot for the comments. Both missing pixels and low-quality pixels are considered invalid pixels that need to be reconstructed. valid pixels are reliable pixels, and they can be used in the data reconstruction process. We are sorry for our inadequate interpretation of the threshold making it difficult to understand. We added an explanation of the threshold, which can also be seen below.

“The adaptive threshold φ^{τ}, calculated from the standard deviation, indicates the local area smoothness. Local area is a certain size area centered on similar pixel, which is located in the three reference images. The closer the pixel is, the more similar the environment is, so the smoother the local area will be.”

Lines 308-315: - "spectral differences" –> so you compute spectra? From which parameter?

Response: We are sorry for carelessness and we have removed ” spectral”.

- The "similarity threshold" mentioned in Line 310 is the one referred to in the previous paragraph?

Response: Thank a lot for the comments. Yes, it is the same as mentioned above.

- Line 311: What is a "null pixel"?

Response: Thanks a lot for pointing this out. We revised it as invalid pixel.

- Line 312: "target image" –> So, in addition to the 3 (?) references images we have a target image. I assume that is the image which contains the target pixel and the i-th pixels mentioned in Equation 1? How does this fit with what is written here?

Response: Thanks a lot for pointing this out. You are right that the target image is an image which contains the target pixel.

"Missing daily pixel is defined as the target pixels T_t*, the image contains the target pixel* T_t *is target image."*

Lines 318-322: - In addition to target and valid pixels we now also get a "local pixel"–> what is this? In addition we get the "local area" mentioned in line 311 already –> which is located where? On the target or one (or each) of the reference images? The description of the steps given in these last paragraphs also leave open the question: Which parameters are actually used to define "similarity"? LST? Elevation? NDVI? All together? Is "smoothness" a measure of the spatial variability of the respective parameter in (?) the local area? - Line 321: "greater than 4" –> where? in the local area? in one image? Not clear.

Response: Thank a lot for the comments. Local pixel is the mean value of all pixels in local area. We also revised it in Page 6 Lines 26-28. The adaptive thresholdφ^{τ}, calculated from the standard deviation, indicates the local area smoothness. Local area is a certain size area centered on similar pixel, which is located in the three reference images. We set the range of the local area to 5 pixels by 5 pixels centered on the target pixel. So, the LST values used to define "similarity". It means in one image. The associated explanation has been added to the revised manuscript and can be seen in Subsection 3.3.2.

"Here, we use an adaptive threshold φ^{τ}*to determine similar pixels for each invalid pixel (Eq. 3). The adaptive threshold* φ^{τ}*, calculated from the standard deviation, indicates the local area smoothness. Local area is a certain size area centered on similar pixel, which is located in the three reference images. The closer the pixel is, the more similar the environment is, so*

the smoother the local area will be. For example, the jth valid pixel in the target image is determined to be a similar pixel of the target pixel i only when the relationship described in Eq. (2) is satisfied in the reference image τ. Simultaneously, similar pixels were determined based on all valid pixels in the image rather than a sliding window because missing values are often arbitrarily clustered in a large area rather than scattered.

$$|P_s^\tau - P_t^\tau| \leq \varphi^\tau, \tag{2}$$

$$\varphi^\tau = \sqrt{\sum_{i=1}^{n}(P_s^\tau - \varepsilon)^2}, \tag{3}$$

where P_s^τ and P_t^τ are the values of pixels corresponding to the position of the similar pixel and the target pixel in the reference image, respectively. φ^τ is the threshold used to determine similar pixels. ε is the mean value of all pixels in local area. τ is the reference image (value=1, 2, 3). Here, we set the range of the local area to 5 pixels by 5 pixels centered on the target pixel (Zeng et al., 2013). In this paper, the number of similar pixels of the target pixel in the target image should be greater than 4 to apply the GWR method to reduce the error due to an insufficient number of similar pixels."

Line 323-329: - "related weight multiplier" –> related to what? - "relative multiweight values of the ground stations were set to 3" –> Not clear ... relative is often something per 100 ... so 3 percent? I don't understant what the "relative" stands for and I am lost about the "multiweight values" –> are these determined by Eqs. 4 to 6? - In order to understand correctly what you do here: You have an area of missing LST data. You find, e.g., two stations collocated with two of the pixels of this area of missing LST data. These pixels you assign the LST values from the stations. You keep these pixels in mind [according to what you wrote these pixels would have an LST value for every time step from the station data, correct?]. For re-constructing LST values in all other pixels of the area with missing LST data you proceed with the GWR method. And in this method, you first identify similar pixels and subsequently incorporate (if present) LST (?) data from similar pixels filled with station data and clear sky (?) similar pixels with different weight coefficients M (3 and 1, respectively) to derive weights W. If there is not station around then it is a W_i; if there is a station around and included then it is a W_j ...? Question: What is the threshold or measure which determines whether a pixel filled with a station value is included such that the weights become a W_j?

Response: Thank a lot for the comments. The regression weight coefficient of a similar pixel is determined by its Euclidean distance from the target pixel. In addition， we assign a related weight multiplier to the marked ground station data based on the GWR. “Relative multiweight values of the ground stations were set to 3 ” means that for similar pixels that have been assigned to the site, the weight coefficient is obtained by the GWR method, and then multiplied by three to increase the weight of the ground site data. The weight coefficient is determined by Equation (4)-(6). We agree with what the reviewers said about the reconstruction process. The threshold is determined by Equation (2)-(3), calculated from the standard deviation.

Line 338: Is "cloudless contaminated pixel" = "clear sky"? Otherwise this is very confusing. - I note that D in eqs. 5 and 6 carries subscripts i and j while equation 4 makes no difference between i and j; I suggest to change this accordingly. How is D measured? In kilometers or meters? - How connect the W_i and W_j of Eqs. 5 and 6 to Eq. 1? Is this the same W_i? If yes, then how is it ensured that the sum of all W_i equals 1?

Response: Thanks a lot for pointing these out. You are right and we revised it. Equation 4 applies to pixels i and j at the same time. In addition, we modified it in the original text. D represents the Euclidean distance from the similar pixel (i, j) to the target pixel t. We revised the formula and adjusted the structure of this part. It can be seen in Page 6 Lines 26-28.

Lines 340-352: - Is it correct that you apply the method described here only based on the elevation and that this is the general method the be applied in case the 5x5 pixel local area (in whatever image) contains only 4 or less similar pixels? - Does this means at the same time that elevation is not among the similarity criteria used in the GWR method?

Response: Thank a lot for the comments. The elevation temperature gradient regression method was used to reconstruct the remaining low-quality pixels that did not have enough similar pixels. So, the two methods are used in different situations.

- Line 343: "spatial trend" –> It is perhaps a matter of taste but "trend" is something I connect to time series. Here you refer to the spatial variation of LST as function of the elevation, am I correct?

Response: Thank a lot for the comments. Generally, "temporal trend" is related to time series. As you said, "spatial trend" means that the temperature drops vertically when the altitude increases. In addition, similar expressions have also been found (Sun, 2016).

- While I can imagine that the pure elevation has in most cases the dominant influence I am wondering about the impact of the slope and the orientation with respect to solar illumination. Did you take this into account as well? If not, could this be the reason why you require a sliding window of 19 x 19 pixels -which is about 1 degree x 1 degree or 106 km x 106 km - to minimize your noise?

Response: Thank a lot for the comments. We agree that LST is not only closely related to altitude, but also affected by slope and aspect, especially in mountainous areas. Reconstruction of mountainous areas where the topography changes in small areas and slopes has a greater advantage. We mainly reconstructed the missing and low-quality sky pixels by GWR method. For pixels that do nsot have enough similar pixels, a reliable elevation temperature gradient regression method was used. Especially for the plain areas of eastern China, the slope and aspect have less significant influence on the surface temperature than mountain areas. In future research, we will further develop a study on the use of slope and aspect for remote sensing image reconstruction in mountainous areas. In addition, using a sliding window of 19 x 19 pixels can effectively reduce noise and increase calculation speed.

– Did you compute alpha and beta for every pixel and every day for which you need to use this method instead of the GWR method? Or do you compute global values for every grid cell of China for these parameters? Otherwise I have problems to understand the "sliding window" technique. - Did you compute alpha and beta separately for the daytime and nighttime LST data? If not then how did you take into account that nocturnal cooling often results in near surface "lakes" of cold air in areas with sufficient topography, offsetting the classical temperature-to-elevation relationship? The same applies to cases with pronounced inversions.

Response: Thank a lot for the comments. We estimate the temperature value in the area based on the linear relationship between the elevation and temperature in a certain area. The reconstructed pixel values are obtained based on neighboring pixels and elevation information. SO, we cautiously think do not need to compute alpha and beta for every pixel and every day. It is a problem for the cooling of the surface caused by the nocturnal cooling you mentioned.

- Line 344: "null pixel"? "non-empty pixels"? - Lines 350/351: What do you mean by cropping here?

Does that mean that you carry out the computation for an areas which is actually expanded by 9 pixels in each direction beyond the Chinese border?

Response: Thank a lot for the comments. We revised these words. In order to avoid insufficient data in the sliding window at the edge of the study area, we crop the geographic subset of the LST images according to latitude and longitude position of the study area during preprocessing in Section 3.1.

Line 363: "changes" ??? So you mean that, e.g. a negative LST trend during the first half of the period changing towards a positive LST trend during the second half of the period (i.e. a change) causes a large correlation value? Please clarify. Perhaps I misunderstood what Eq. 9 does ... but apparently you do not compare two different data sets but you compute the correlation of the time series with itself? ... You write that "the LST is positively correlated with the time series" ... I guess I don't get what you here ... correlating one annual mean value with the 15-year time series ... ? Perhaps you enter spatial information but I don't understand where.

Response: Thank a lot for the comments. A negative LST trend during the first half of the period changing towards a positive LST trend during the second half of the period (i.e. a change) causes a small correlation value. To some extent, the correlation coefficient can be used to reflect the reliability of the surface temperature trend over time. In order to more clearly express the significance of the trend, student's t-test was performed for different time scales. The significance maps has been added to the revised manuscript and can be seen in supplementary material.

Lines 396-408: This paragraph does not fit to an ESSD paper about a new data set. If at all it would belong either to the discussion and/or into a conclusion/outlook section; see GC4 also.

Response: Thanks for your good suggestion. We agree that the discussion /or into a conclusion/outlook section should be deleted. We believe that through the study of the changing trends of new data sets, readers can have more understanding of our data sets, so we hope this section can be kept.

Lines 409-417: - This paragraph repeats partly the paragraph where Figure 6 has been described. Please consider to delete it. I have the same view of it as I voiced for the previous paragraph; see

GC4. - Without a map where those Taihang Mountains are located it is not possible to take any added value out of what is written about it here.

Response: Thanks for your suggestions, which has helped us to improve the manuscript quality. According to your suggestions, we have deleted these contents.

Lines 418-448: Same as stated for the previous two paragraphs. This is certainly all nice and well collected information but to my opinion this journal is the wrong place to lay out these issues in that degree of detail. Consider deleting it and - if you feel it needs to be included - summarize the key messages in 3-4 sentences in the conclusions; this would be my recommendation for the while part of lines 396-448; see GC4.

Response: According to your suggestions, we have deleted these contents.

Lines 450-462 / Figure 7: - I note that you show the correlation in Fig. 7 b) but do not comment on it in your text. You might consider to not show this parameter or put it into supplementary material. However, isn't it interesting to note that while Fig. 6 a) appears to be dominated by the daytime LST changes Fig. 6 b) resembles a lot of the pattern shown by the nighttime R (Fig. 7 b). Do you / we understand why this is the case?

Response: Thank a lot for the comments. To some extent, the correlation coefficient can be used to reflect the reliability of the surface temperature trend over time. We hope that the value of r indicates the reliability of the change. In addition, according to Dr. He's opinion, we have added saliency maps in the supplementary material, hoping to provide some reference.

Yes, it is also interesting that the changes and R in the daytime LST are similar to the interannual LST, which is mainly due to the small changes of LST at night. The annual daytime positive /negative trends of LST in almost all regions from 2003 to 2017 are significantly higher than those in the evening ($-0.03<slope<0.03$); thus, the average LST positive/negative trends can be attributed to changes during the daytime.

- I note that the color bar below the panels is twice as large as for, e.g., Fig. 6 a, b but that an annotation of what is shown by the color bar is missing

Response: Thank you very much for your careful review. There is no missing comment on the content shown in the color bar we see. If there is any deviation in understanding or displaying version, please contact us and we will continue to change it.

- I suggest to tie the text closer to the Figure by explicitely referring to it as Fig. 7 a) day and Fig. 7 a) night; it might be easier actually to use panels a) through d) instead of a) and b).

Response: Thanks for your good suggestions, we revised it.

"Figure 7: Spatial dynamics of Fig. 7 a) day and Fig. 7 a) night LST change trends based on slope (a) and correlation coefficient (b)."

- I find it interesting that the negative daytime LST trend in the northern part of region IV is offset by a positive nighttime LST trend.

Response: I'm sorry we didn't find the opposite phenomenon you point out.

- Line 451: "average annual diurnal surface temperature" , also in Line 450 you use "diurnal" –> I am not convinced that usage of "diurnal" is adequate here. I suggest to separately refer to day- and nighttime LST because diurnal implies that you know more about the diurnal development of the LST - but since you only use data of one MODIS sensor here you only have two anchor points

Response: Thank you for your comments. Adopted.

- Line 454: "evening" –> "nighttime"; in addition: there appears to be a substantial fraction (25% or even more) where the absolute slope is larger than 0.3 in Fig. 7 a) night; the range given in parenthesis appears not be correct therefore.

Response: Thank you for your comments. Adopted; we are sorry for the careless expression we have revised the related contents as following.

"The annual daytime positive/negative trends of LST in most regions from 2003 to 2017 are significantly higher than those in the nighttime."

- Line 456: "daytime human activities" –> what does this have to do with LST observations?

Response: Thank you for your comments. We have changed "daytime human activities" into "daytime human production " .

Lines 464-478 / Figure 8 - Please check Figure 8 a). It cannot be that the average daytime LST in southern China is around 0degC.

Response: Thank you for your comments. I am puzzled by what you said about "0degC ". We have carefully checked Figure 8 and the average daytime LST in southern China is around 25 degC.

- I note that quite a large fraction of the LST shown in Fig. 8 b) is saturated at the lower end of the color scale shown. I suggest to expand that accordingly. I don't think it would hurt to cut off the legend at +20degC and add the respective two 5 Kelvin bins at the left hand side. - Why did you use such 5 Kelvin wide bins? Is the LST distribution too noisy otherwise? - All legends lack the annotation of what is shown in which unit.

Response: Thank you for your comments. In order to more directly reflect the difference in temperature difference between daytime, nighttime and day and night temperature difference, we use the same legend for the three figures. We cautiously believe that the current distribution of temperature in the same image and between different images can be well reflected. In addition, we will add units to all the graphs.

- Line 470/471: The stated latitudinal dependence is only evident in the eastern half of China - possibly due to its comparably smoother relief.

Response: Thanks a lot for pointing this out. We revised it.

"This result may suggests that the spatial temperature change is related to the latitude range, and also to the smooth Terrain in the east."

- Line 475: Here you use "temperature difference between day and night" –> This appears to be a better wording than diurnal. - Finally, I suggest to stress that you look at a multiple-years average of the annual mean LST and that hence individual day-to-night changes can be much larger (or smaller) depending on season - to have an adequate link to the next section。

Response: Thanks for your good suggestions. As the reviewer suggested, we have modified these words in the revised manuscript.

Lines 479-489: Same comment as for Lines 396-408. Hence, remove the Hu line in Fig. 8 c); see

GC4.

Response: Thank you for your comments. we have deleted these contents.

Section 4.2: - Please check for GC - wording/editing; there are many increasing and warming trends here. - I find this section overly long and suggest to condense the material to the key elements, omitting any links to changes in crop yield or the like and omitting attempts to explain observations with changes in atmospheric circulation / precipitation or the like. If at all then this can be included in a condensed paragraph in the conclusions.

Response: Thank you for your comments. As the reviewer suggested, we have revised the related contents as following.

"Specifically, in spring, the warming area is mainly concentrated in the northern areas (I, II, and V), while a weak negative trend is observed in the southern areas. The largest positive trend over the northern areas appears in the Inner Mongolia Plateau (slope >0.18, $P < 0.01$). In addition, rapid warming also occurred in the North China Plain in the eastern part of the North China Region (II) (especially near Beijing and some areas of Hebei Province, slope >0.12, $R > 0.6$, $P < 0.01$)f

As shown in Fig. 9, compared with the other two seasons, both summer and autumn showed weak positive trends throughout the country. In summer (Fig. 9b1, b2 and b3), there were slight increasing trends in most areas of China, while there were still negative trends in the Northeast Region (I) (details in Fig. 9). Significant increasing trends were mainly observed in the Qinghai-Tibet Plateau, North China Plain, Inner Mongolia Plateau, Tarim Basin and some areas in the north, with the largest positive trend in the Qinghai-Tibet Plateau. In autumn, the negative trends were mainly present in the Northeast Region (I) and the Northern Chinese Tianshan Mountains in the Qinghai-Tibet Plateau Region (VI). In contrast, the Qinghai-Tibet Plateau was still controlled by strong positive trends (near Lhasa city, slope=0.09, R=0.60, $P < 0.05$), especially in the southern part of the Tanggula Mountains.

In winter, 69.4 % of the areas experienced warming, which is significantly higher than in other seasons; thus, winter is the most important source of interannual increases in the average LST. The most remarkable positive trends in winter were observed in the Northwest Region (V) and the Qinghai-Tibet Plateau Region (VI)."

Lines 561/562: "dramatic" and "rapid" –> Please reconsider these formulations because "dramatic" appears not adequate and "rapid" implies that something happens particularly fast but it appears that it is rather the magnitude of the trend which strikes here. Ines.

Response: Thank you for your guidance. They're all part of the analysis of temperature effects, and they've been removed

Section 4.3: - While I see the merit to also take a look at the months it appears to me that the paper should contain an analysis of either seasonal or monthly distributions / changes in the multi-annual development of the LST. I tend to favor the seasons and to delete Figure 10 and this section for the sake of keeping more space for the illustration of the method and the evaluation.

Response: Thank you for your comments. According to your suggestion, we have deleted these contents.

Response: Thank you for your comments.

What is the temporal resolution of the MODIS LST data shown in Fig. 11? Daily or monthly? Please indicate in the figure caption. - What is the time period used?

Response: Thanks a lot for pointing this out. It is monthly MODIS LST data shown in Fig. 11. We have added descriptions of temporal resolution in the figure caption and original text.

- Single data pairs obscure each other. I suggest to plot two sets of panels, one with the re-constructed values (currently in blue) and one with the linar model corrected values (currently in grey), in which you show the count per data value bin, i.e. my suggestion is to plot a 2-dimensional histogram, using a bin-size of the LST values of 1 Kelvin and displaying the count of data pairs falling into these bins with a color code. This way one would have a better impression where data pairs concentrate. Currently, I find it un-natural that we see for all regions - excpet region I - an elongated cluster of points with an almost constant width across; only region I shows some variation here and is the most credible of the panels shown.

Response: Thank you for your comments. Although single data pairs obscure each other, it can be intuitively judged by the change of the slope of the site that the quality of the point after the linear model is stretched has been significantly improved. At the same time, we only showed a rough distribution here, and the specific difference can be obtained according to the numerical indicators(R^2, RMSE, MAE).

- Line 547: "better" can be removed.

Response: Thanks. We have revised.

- Lines 557/558: This last sentence is not supported by Figure 11.

Response: Thank you for your comments, and we have deleted these contents.

Lines 559-571: - Lines 566-571, beginning with "Simultaneously ..." can be deleted; see GC4.

Response: Thanks a lot for pointing this out. We revised it.

Lines 572-581: - Please describe how this comparison is carried out. It is not known how you computed the seasonal averages and then finally carried out the comparison. The number of seasonal LST values per station entering this comparison is not clear; one can guess that per station it is 3 months (per season) times the number of years, i.e. 15. It is furthermore not clear how you dealt with data gaps in the original LST data in this comparison. Also, when using the original LST data, did you take into account the quality flags as users should do when using the data?

Response: Thanks a lot for pointing this out. We are sorry that we have ignored the description of the division of seasons in the text.

"The original MODIS monthly LST data were used directly without filtering quality flags. For the original MODIS LST images, we averaged the LST data of the month corresponding to the season, and obtained the seasonal LST images. The pixels with missing LST values in original MODIS LST images for the corresponding months of the season were not used in the verification process. Therefore, if there is no missing value for the LST pixel corresponding to the site, each station can have a maximum of 15 values in each season."

Lines 594/595: I don't agree to this statement. Why should the reconstruction of the LST be particularly vulnerable in areas (the red ellipses) where the absolute LST changes over the period chosen are at maximum? These areas (red ellipses) in fact contain regions of large topographic complexity, yes, but this is possibly not the only error source which needs to be discussed.

Response: Thank you very much for your careful review. We are sorry for the statement on Line 594 and we have revised it as follows. Thank you for your guidance.

"We also note that the selected ground stations shown in Table 2 located in six key zones are examples of where the local LST warming/cooling rate changed by more than the average rate, and these areas actually include areas with greater Terrain complexity."

Lines 597-607: This steps is not transparently enough explained and appears not justified; see GC5.

Response: Thank you for this comment. We have revised and deleted some contents in the manuscript. The revised statement is as follows.

"Moreover, the examples indicate that the reconstruction model proposed here is effective even in the areas of complex topography."

Typos / editorial comments:

Lines 56/57: These lines read as if the sensor is used in the models but I assume it is the LST derived from the MODIS observations which is used in the models; please reformulate accordingly.

Response: Thank you very much for your careful review. As the reviewer suggested, we have modified the sentence in the revised manuscript.

"Due to its optimal temporal and spatial resolution throughout the world, the Moderate Resolution Imaging Spectroradiometer (MODIS) sensor has become an excellent data source for satellite-derived LST data, and the MODIS LST values are widely used in regional and global climate change and environmental monitoring models (Tatem et al., 2004; Wan et al., 2014)."

Line 65: "reconstruction of noise contaminated ..." –> "reconstruction of the LST of noise-contaminated ..."

Response: Thank you for your comments. we have modified the sentence in the revised version for better understanding.

"Thus, reconstruction of these missing and low-quality LST pixels low-quality is necessary for satellite-derived LST applications."

Line 154: Typo: "mm" –> needs to be micrometer

Response: Thank you for your comments. we have modified this word in the revised version.

Line 231: "a thermal infrared band" –> this contradicts the information given further up, where you explained the day/night algorithm used for MODIS LST retrieval since V006.

Response: Thank you very much for your careful review. For the LST V006 version products used in this article, seven thermal infrared bands (bands 20, 22, 23, 29, 31, 32, 33) were used for retrieving LST values. We apologize for the carelessness, and we revised this term in the revision version.

"MODIS LST data are retrieved from thermal infrared bands in clear-sky conditions and contain many missing values and low-quality values caused by clouds and other atmospheric disturbances."

Lines 232/236: You need to clarify what you mean by "atmospheric disturbance"; for some people this would be a low pressure system ... I doubt that this is what you mean as you give this in addition to clouds.

Response: Thank you for your comments. Atmospheric disturbance means the influence of atmospheric molecules and aerosols.

Line 234: Markus needs to be Markus et al.

Response: Thank you for your comments. We have revised the wording.

Line 236: Why is "illumination" a problem if we talk about IR data?

Response: Thanks a lot for pointing this out. Thermal infrared remote sensing data is not affected by illumination conditions. We have corrected this error in the revised version of the manuscript.

Line 359: "LST image time series" –> "LST time series"

Response: Thank you for your comments. We have revised the wording.

Line 360: suggestion: "A positive slope indicates an increase in LST (warming); a negative slope indicate a decrease in LST (cooling)." This avoids to write something about trends which become warmer.

Response: Thank you for your comments. As the reviewer suggested, we have modified this sentence in the revised manuscript.

Lines 384-395: - Please stick with "areas" and do not mix "areas" and "districts". - See GC - wording - Consider to use again "area" or "region" instead of "pattern".

Response: Thank you for your comments. As the reviewer suggested, we have modified these words in the revised manuscript.

- Line 391: I doubt that the area with a slope > 0.05 degC/year (panel a) coincides with the area with R > 0.6 (panel b).- Line 394: Mentioning of R < -0.6 appears to be not that informative here? - The slopes lack a unit.

Response: Thank you for the valuable comment. To some extent, the correlation coefficient can be used to reflect the reliability of the surface temperature trend over time. In order to more clearly express the significance of the trend, we further calculated the significance according to the correlation, and student's t-test was performed for different time scales. The significance maps have been added to the revised manuscript and can be seen in supplementary material. In addition, we added the unit in the revised manuscript.

- Figure 6: I particularly like panel (c). Cool! However, also here the unit of the warming / cooling regimes should be degC / year, right? Annotation "slope" and "R" in panels (a) and (b) is too small. The slope lacks a unit.

Response: Thank you for your appreciation of our Figure. We revised the units and annotation in Figure 6.

Thank you again for your efforts in reviewing our manuscript. We hope our modification will be to your satisfaction.

References:

Kilibarda, M., T. Hengl, G. B. M. Heuvelink, B. Gräler, E. Pebesma, M. Percec Tadi ˇ c, and B. Bajat (2014), ´ Spatio-temporal interpolation of daily temperatures for global land areas at 1 km resolution, J. Geophys. Res. Atmos., 119, 2294–2313, doi:10.1002/2013JD020803.

Benali, A., Carvalho, A. C., Nunes, J. P., Carvalhais, N., and Santos, A.: Estimating air surface temperature in Portugal using MODIS LST data. Remote Sens. Environ., 124, 108-121, https://doi.org/10.1016/j.rse.2012.04.024, 2012.

Sun, Z., Wang, Q., Batkhishig, O., and Ouyang, Z.: Relationship between evapotranspiration and land surface temperature under energy-and water-limited conditions in dry and cold climates. Adv. Meteorol., 1-9, 1835487, https://doi.org/10.1155/2016/1835487, 2016.

Benali, A., Carvalho, A. C., Nunes, J. P., Carvalhais, N., and Santos, A.: Estimating air surface temperature in Portugal using MODIS LST data. Remote Sens. Environ., 124, 108-121, https://doi.org/10.1016/j.rse.2012.04.024, 2012.

Barry B R G. Mountain Weather and Climate[M]// Mountain weather and climate. Routledge, 1992.

Körner C. The use of 'altitude' in ecological research[J]. Trends in Ecology & Evolution, 2007, 22(11):0-574.

Hansen, J., Ruedy, R., Sato, M. & Lo K. Global surface temperature change. Rev. Geophys. 48, RG4004, doi:10.1029/2010RG000345 (2010).

Smith, T. M., Reynolds, R. W., Peterson, T. C., & Lawrimore, J. Improvements to NOAA's historical merged land-ocean surface temperature analysis (1880-2006). J. Climate 21, 2283–2296 (2008).

Hansen, J.E. and Lebedeff, S. Global trends of measured surface air temperature. J. Geophys. Res. 92, 13345-13372, doi:10.1029/JD092iD11p13345 (1987).

Hansen, J., Ruedy, R., Sato, M. and Lo, K.: Global surface temperature change. Rev. Geophys., 48.4， 1-29, https://doi.org/ 10.1029/2010RG000345， 2010.

Smith, T. M., Reynolds, R. W., Peterson, T. C., and Lawrimore, J. Improvements to NOAA's historical merged land-ocean surface temperature analysis (1880-2006). J. Climate 21, 2283–2296, 2008.
Hansen, J.E. and Lebedeff, S. Global trends of measured surface air temperature. J. Geophys. Res. 92, 13345-13372, doi:10.1029/JD092iD11p13345 (1987).
Hansen, J. E. et al. Global climate changes as forecast by Goddard Institute for space studies three-dimensional model. J. Geophys. Res. 93(D8), 9341-9364 (1988).

Hansen, J., Ruedy, R., Glascoe, J. and Sato, M. GISS analysis of surface temperature change. J. Geophys. Res. 104, 30,997–31,022, doi:10.1029/1999JD900835 (1999).

Hansen, J. E. et al. A closer look at United States and global surface temperature change. J. Geophys. Res. 106, 23947-23963, doi:10.1029/2001JD000354 (2001).

Hansen, J. et al. Global temperature change. PNAS, 103, 14288-14293, doi:10.1073/pnas.0606291103 (2006).

Rayner, N. A., Parker, D. E., Horton, E. B., Folland, C. K., Alexander, L. V., Rowell, D. P., Kent, E. C., and Kaplan A. Global analyses of sea surface temperature, sea ice, and night marine air temperature since the late nineteenth century. J. Geophys. Res. 108(D14), 4407, 1-22, doi:10.1029/2002JD002670 (2003).

Fan, Y., and Dool, H.V.D. A global monthly land surface air temperature analysis for 1948 – present. J. Geophys. Res. 113(D01103), 1-18, doi:10.1029/2007JD008470 (2008).

Jones, P.D., New, M., Parker, D.E., Martin, S., and Rigor, I. G. Surface air temperature and its changes over the past 150 years. Rev Geophys 37, 173–199 (1999).

Ghafarian Malamiri, H.R.; Rousta, I.; Olafsson, H.; Zare, H.; Zhang, H. Gap-Filling of MODIS Time Series Land Surface Temperature (LST) Products Using Singular Spectrum Analysis (SSA). *Atmosphere* 2018, *9*, 334.

Response to short comment

Response to short comment #1

Although the development of thermal infrared remote sensing technology has made it possible to obtain surface temperature over a large area, there are still many missing values of temperature due to the influence of clouds and rainfall in most parts of China, especially in southern China. In this manuscript, the authors reconstruct a high resolution land surface temperature dataset by combining multiple source data. This dataset covers the complex climate and topographical conditions in China and is very useful for regional climate and drought research. This manuscript proposes a new idea to retrieve LST of pixels under cloudy conditions which highly suitable contribution to Earth System Science Data. The authors show the validation in annual and seasonal scale for different areas with different climatic condition, which is important to further clarify the usage limitation for end users. It also provides a good data set for our meteorological department, which provides good support for long-term regional climate change research. Overall, this is a really nice contribution. A couple of suggestions and comments to improve the paper:

Response: We would like to thank Dr. Wu for the guidelines and constructive comments to our manuscript. These feedbacks made by the reviewer will clearly help to improve the manuscript. In the following, we provide point-by-point answers to the Dr. Wu's comments.

1) Pg.13, Line 412 "R>-0.6 " should be " R<-0.6"?

Response: Many thanks for your attentions. We have revised the error in the new version of the manuscript.

2) The legend of figure 8 should be revised (add unit).

Response: Thank you for this comment. It will be corrected in the revised manuscript.

3) The average annual diurnal LST difference from 2003 to 2017 is characterized by the blue line AB, which indicates the boundary between the eastern China and western China." However, I have not seen the results.

   Response: Thanks for this comment. The expression here is that the diurnal LST difference has a tendency to distribute along the Hu Line (ie, the blue line AB): in most areas, the diurnal LST difference in the west is higher, and the diurnal LST difference in the east is lower. This is in good agreement in the southern part of China, but may not be well reflected in the north, especially in the Northeast. So we removed the statement about this part of the content in the revised manuscript.

4) According to Figure 1, Line 428 should be the warming trend of the Loess Plateau in the western part of the Taihang Mountains, not the eastern part.

   Response: Many thanks for your attentions. We have revised the error in the new version of the manuscript.

Response to short comment #2

We think that the research of your team is very significant. You have done a very good long-term sequence of surface temperature data sets in China. The data you provide will play a key role in promoting research on the thermal environment at the regional scale, and also many other related disciplines. We read your paper carefully and use your temperature dataset to do a regional-scale thermal environment analysis and find that there is a small problem in the dataset.

Response: We appreciate Dr. Liu for her/his appreciation of our study and for the valuable suggestions that helped us to clarify and improve the manuscript. Our point-by-point responses to the Dr. Liu's comments are given as follows.

We have three suggestions:

1.For dataset, not all rows and columns of data are consistent, and the number of rows and columns of 60% data is 724*864, but the number of rows and columns of 40% data is 723*863.This will affect the user's processing and analysis when they use this dataset. This problem should be caused by the software batch process. Please correct the data and re-upload it, which is more conducive to us to promote the use of this dataset. Thanks again.

Response: Thank you for pointing out this key issue. It is important to ensure the consistency of the rows and columns of the dataset as it is the basis for processing and analysis. This problem may be due to errors in the clipping process. We scrutinized the data and then all the data with 723*863 was reprocessed. In the end, all images are 724*864.

The new version of the datasets were uploaded to the repository: https://doi.org/10.5281/zenodo.3528024. At the same time, all the results in the text have been checked and corrected in the next version of the manuscript.

2. Page 5. Line 155. It will be better if this sentence is revised as "MODIS is a key sensor of Earth Observing System (EOS) program which provides a unified grid product with global coverage of the land, atmosphere and oceans. MODIS covers 36 spectral bands from the visible, near-infrared and thermal infrared ranges (from 0.4 to 14.4 um), so it is extensively used to study global marine, atmospheric, and terrestrial phenomena (Wan et al., 1997)."

Response: Thanks for this constructive comment. The sentence will be revised.

3. Page 6. Line 175. It will be better if this sentence is revised as: "Then, these day/night pairs of MODIS data are used to construct 14 nonlinear equations to retrieve the surface average emissivity and surface temperature based on a physics-based day/night LST model from the MODIS 1B data

without high accuracy atmospheric temperature and water vapor profiles (Wan and Li, 1997)."

Response: Thanks for this constructive comment. The sentence will be revised.

Response to short comment #3

Land surface temperature (LST) is one of the most important essential climate variables for climate change studies. Given the cloud contamination and discontinuous satellite observations, it is challenging to analyze the trend of LST for a specific region and time frame by solely relying on a satellite product. To tackle this issue, the study targets to provide a temporal-consistent LST dataset for China in 2003-2017 by utilizing both MODIS LST product and local LST measurements from meteorological stations. The authors applied their data reconstruction method and validated their dataset. The validation suggests that the accuracy of reconstructed LST is reasonable well for the long-term trend analysis.

Response: We would like to thank you for the comprehensive summary and constructive comments of the manuscript. A detailed response to each comment is given as follows.

I am particularly interested in the imbalanced temperature-trends for different regions and seasons in China from this study. I would have the following suggestions and look for the authors responses.

From Fig. 1, we can see that the distribution of weather stations is sparse in the western China. Can you discuss how the non-uniform distribution of weather stations affects the dataset accuracy and your potential method for improvement?

Response: Thank you for the valuable comment. There are relatively fewer meteorological stations in western China. Under the same conditions, the accuracy in western China is lower than that in areas with dense weather stations when using the surface meteorological station to reconstruct LST values under the cloudy cover conditions. As shown in Fig. 3-4, there are more clouds in the eastern China than in the western China. In this case, the number of days for LST values can be obtained from the remote sensing image in a month is very smaller in the eastern part of China than in the western China. In this study, accuracy evaluation is based on the monthly scale. The accuracy is mainly determined by the number of days of effective pixels on the monthly and annual scales, and our analysis indicates that the more days of available pixels corresponding to the pixels on the monthly scale, the higher the accuracy. No matter how cloudy or not, the higher accuracy can be achieved by increasing the number of weather stations and satellite observations.

The authors have made significant contribution in analyzing the historical temperature changes in China. The imbalanced LST trends in China are revealed. The authors have made an amount of discussions on the reasons.

First, can the author add the significance of trends to the maps (or in the supplementary materials)?

Response: Thank you for the valuable comment. To some extent, the correlation coefficient can be used to reflect the reliability of the surface temperature trend over time. In order to more clearly express the significance of the trend, student's t-test was performed for different time scales. The significance maps has been added to the revised manuscript and can be seen in supplementary material.

Second, the authors mentioned that the increase in aerosol may reduce the "cooling effect", while I think that the aerosol is recognized for the cooling effect. Can the authors clarify that?

Thanks for this comment. The effect of aerosol climate forcing is complex, because aerosols both reflect solar radiation to space (a cooling effect) and absorb solar radiation (a warming effect) (Hansen et al., 2011).

The warming effect is mainly caused by the absorption of solar radiation by black carbon aerosols. As Ramanathan and carmichae (2008) pointed out, black carbon aerosols may be the second strongest contribution to climate warming. Kühn et al. (2014) also found that recent changes (1996–2010) in aerosols forcing over China are a warming effect due to increasing black carbon concentrations, especially in the north. In this part of the manuscript (Summary and conclusions), we emphasized the contribution of human factors to climate warming, so only the warming effects of black carbon aerosols was discussed.

As Dr. He has pointed out, scattering aerosols, such as sulfate aerosols and nitrate aerosols, are expected to produce cooling effects by absorbing and scattering solar radiation. We also make a supplementary explanation for this part in the revised version of the manuscript.

Third, the authors attributed the cooling trend in Northeast China to negative Arctic oscillation;

while I found that the cooling trends are mostly located in cropland; the increasing agriculture and irrigation may contribute to increased evapotranspiration and therefore, the lower LST; more discussion is expected in this regard. I look forward to seeing your peer-reviewed and refined revision.

Response: Thanks for this constructive comment. We agree with Dr. He that the evaporation and irrigation of vegetation have a cooling effect. In our analysis, we emphasized the possible causes of temperature changes from a macro perspective, while ignoring the possible impact of changes in local land use types. In recent years, the area of unused land converted to cultivated land in the Northeast has continued to increase. Transpiration caused by increased crops and irrigation is one of the important reasons to produce a cooling effect on surface temperature. This part will be added in the revised version of the manuscript.

Some specific comments:

Fig. 1 and table 1: it is unclear from the captions what is the difference between key zone and region?

Response: Thank you for the valuable comment. We agree that the original description of the key zone is not quite clear and needs further clarification.

The study area is divided into six regions to describe the temporal and spatial characteristics of China's LST. They are: I Northeast Region, II North China Region, III Central - South China Region, IV South China, V Northwest Region, VI Qinghai-Tibet Plateau Region.

To further understand the credibility of the data and clarify the limitations of the use of our method, we further assess the performance by some meteorological station data at different sub-climate regimes and topography situations. Six key zones which shown in Fig. 1 and Table 1 are determined by interannual change trends of LST from the slope map (Fig. 6(a)), including the three most significant regions for warming (b, d, f), the two most significant regions for cooling (a, c) and the zone located in Xinjiang Province (see Fig. 6a for details), and special attention was given to area around the Taklamakan Desert (e) in Xinjiang, which has complex terrain and extensive heterogeneity.

Figs. 3 and 4: Areas of invalid data are in ‘blank’.

Response: Many thanks for your attentions. We have revised the word as suggested in the revision.

Fig. 5: need more information in the caption: is the linear trend derived from “National average”, is the “National average” derived from the corrected MODIS LST time-series?

Response: Many thanks for your attentions. We apologize for the insufficient description of Fig. 5. We have revised the caption statement in Fig. 5. The caption information is also presented below for the ease of reviewing.

Time series of annual mean LST (unit: °C) for the period of 2003-2017 from the corrected MODIS LST of China. The solid blue line indicates its linear trend. The orange dashed line shows its five-year running average trend.

Fig. 6: it is desirable to show a separate map for each pixel if the correlation is significant.

Response: Thanks for this comment. The significance map of annual mean LST change trend has been added to the revised manuscript and can be seen in Figure. S1.

Table 2: for some records, the RMSEs after corrections are increased.

Response: Thanks a lot for pointing this out. The accuracy for each pixel should be improved in the ideal situation if the region is divided into small enough. However, affected by complex sub-climate regimes and topography situations, it is difficult to use limited strategies to significantly improve the accuracy of each pixel for such a large area.

In this study, we reconstruct the surface temperature under the cloud cover by combining MODIS daily, monthly and meteorological station data, which can effectively ensure the quality of the reconstructed data. Then, we built calibration models for subregions with different climatic conditions and topographical characteristics, which can further improve the data accuracy. As Shown in table 2, about 83% of the data accuracy is improved and a small amount of accuracy is slightly decreased after the reconstructed data is corrected by the verification model.

L607: examine “Sahara Desert region”.

Response: We appreciate Dr. He for the careful reading of our manuscript and are very sorry for the carelessness. We have replaced “Sahara Desert region” with “Taklamakan Desert” in the revised manuscript. Thank you.

References

Ramanathan, V. and Carmichael, G.: Global and regional climate changes due to black carbon. Nat Geosci, 1, 221–227. https:// doi.org/10.1038/ngeo156, 2008.

Hansen, J., Sato, M., Kharecha, P., and von Schuckmann, K.: Earth's energy imbalance and implications. Atmos Chem Phys, 11, 13421-13449. https:// doi.org/10.5194/acpd-11-27031-2011, 2011.

Kühn, T., Partanen, A.-I., Laakso, A., Lu, Z., Bergman, T., Mikkonen, S., and Laaksonen, A. : Climate impacts of changing aerosol emissions since 1996. Geophys Res Lett, 41, 4711–4718. https://doi.org/10.1002/2014gl060349, 2014.

A combined Terra and Aqua MODIS land surface temperature and meteorological station data product for China from 2003–2017

Bing Zhao[1,2,†], Kebiao Mao[1,3,4,†], YuLin Cai[2], Jiancheng Shi[3], Zhaoliang Li[1], Zhihao Qin[1], and Xiangjin Meng[5]

[1]Institute of Agricultural Resources and Regional Planning, Chinese Academy of Agricultural Sciences, Beijing, 100081, China
[2]Geomatics College, Shandong University of Science and Technology, Qingdao, 266590, China
[3]State Key Laboratory of Remote Sensing Science, Jointly Sponsored by the Institute of Remote Sensing Applications of Chinese Academy of Sciences and Beijing Normal University, Beijing, 100101, China
[4]School of Physics and Electronic-Engineerring, Ningxia University, Ningchuan 750021, China
[5]School of Surveying and Geo-Informatics, Shandong Jianzhu University, Jinan, 250100, China

~~Bing Zhao[1, 2, †], Kebiao Mao[1, 3, †], YuLin Cai[1], Jiancheng Shi[3], Zhaoliang Li[2], Zhihao Qin[2], and Xiangjin Meng[4]~~

~~[1]Institute of Agricultural Resources and Regional Planning, Chinese Academy of Agricultural Sciences, Beijing, 100081, China~~
~~[2]Geomatics College, Shandong University of Science and Technology, Qingdao, 266590, China~~
~~[3]State Key Laboratory of Remote Sensing Science, Jointly Sponsored by the Institute of Remote Sensing Applications of Chinese Academy of Sciences and Beijing Normal University, Beijing, 100101, China~~
~~[4]School of Surveying and Geo-Informatics, Shandong Jianzhu University, Jinan, 250100, China~~

Correspondence to: Kebiao Mao (maokebiao@caas.cn)
†These authors contributed equally to this work and should be considered co-first authors.

Abstract. Land surface temperature (LST) is a key variable for high temperature and drought monitoring and climate and ecological environment research. Due to the sparse distribution of ground observation stations, thermal infrared remote sensing technology has become an important means of quickly obtaining ground temperatures over large areas. However, there are many missing and low-quality values in satellite-based LST data ~~caused by cloud coverage exceeding~~because clouds cover more than 60 % of the global surface every day. This article presents a unique LST dataset ~~in~~for China ~~for~~from 2003-2017~~, which~~ that filters and removes missing values and ~~poor~~low-quality LST pixel values ~~contaminated~~low-quality by clouds from raw LST images and retrieves real surface temperatures ~~under~~in areas with cloud coverage ~~by~~via a reconstruction model. We specifically describe the reconstruction model, which uses a combination of MODIS daily data, monthly data and meteorological station data to reconstruct the true LST ~~under~~in areas with cloud coverage, and ~~then~~ the data performance is then further improved by establishing a regression analysis model. The validation indicates that the new LST dataset is highly consistent with ~~the~~ in situ observations. For the six natural subregions with different climatic conditions in China, the RMSE ranges from 1.24 °C to 1.58 °C, the MAE varies from 1.23 °C to 1.37 °C, and the R^2 ranges from 0.93 to 0.99. The new dataset adequately captures the spatiotemporal variations in LST at annual, seasonal and monthly scales. From 2003-2017, the overall annual mean LST in China ~~shows~~showed a weak increase. Moreover, the ~~warming~~positive trend was remarkably unevenly distributed ~~over~~across China. The most significant warming occurred in the central and western areas of the Inner Mongolia Plateau in the Northwest Region (slope >0.10, R >0.71, P~~<~~ < 0.05), and a strong ~~cooling~~negative trend was ~~also~~ observed in some parts of the Northeast Region~~.~~ and South China Region. Seasonally, there was significant warming in ~~the~~ western ~~part~~China in winter, which was most pronounced in December. The reconstructed dataset exhibited significant improvements and can be used for the spatiotemporal evaluation of LST ~~and~~in high temperature and drought monitoring studies. The data are ~~published in the~~available through Zenodo at ~~https://doi.org/10.5281/zenodo.3378912~~https://doi.org/10.5281/zenodo.3528024 (Zhao et al., 2019).

1 Introduction

Land surface temperature (LST), which is controlled by land–atmosphere interactions and energy fluxes, is an essential parameter for the physical processes of the surface energy balance and water cycle at regional and global scales (Li et al., 2013; Wan et al., 2014; Benali et al., 2012). Accurate surface temperature datasets are not only required for high temperature and drought research over various spatial scales but also important elements for improving global hydrological and climate prediction models. In particular, temperature changes directly influence glacier reserves and water storage on the Qinghai-Tibet Plateau (Tibetan Plateau), which is known as the "World Water Tower". In turn, these changes directly affect the living conditions of nearly 40 % of the world's population (Xu et al., 2008). Therefore, LST research at regional and global scales is crucial for further improving and refining global hydroclimatic and climate prediction models. LST data, which is conventionally measured by meteorological stations or ground surveys, have the advantages of high reliability and long time series. However, the meteorological station data collected as point data with very limited spatial coverage are often sparsely and/or irregularly distributed, especially in remote and rugged areas (Neteler, 2010; Hansen et al., 2010; Gao et al., 2018). To obtain spatially continuous LST data, various geostatistical interpolation approaches are commonly applied to achieve spatialization, such as kriging interpolation and spline function methods. However, the smoothed spatial pattern obtained after interpolation may suffer from low reliability because the ground station density is far from sufficient in most regions.

In contrast to ~~the~~ground-based observations with their limited availability and discrete spatial information~~ from ground-based observations~~, images captured by satellite thermal infrared instruments have become reliable alternative data sources with the advantages of detailed spatialized surfaces and near real-time data access (Vancutsem et al., 2010). For instance, for the study of uniform continuous surface temperatures over large-scale areas, such as ~~over~~at regional and global scales, satellite remote sensing is the only efficient and feasible method (Xu et al., 2013). Satellite remote sensing obtains global ~~LST~~LSTs based on a variety of mature retrieval algorithms that have been proposed since the 1970s for use with data from thermal infrared channels~~, which dates back to the 1970s~~ (McMillin, 1975). Due to ~~the~~its optimal temporal and spatial resolution throughout the world, the Moderate~~-resolution~~ Resolution Imaging Spectroradiometer (MODIS) sensor has become an excellent data source for satellite-derived LST data, and ~~is~~the MODIS LST values are widely used in regional and global climate change and environmental monitoring models (Tatem et al., 2004; Wan et al., 2014). However, satellite-derived LST data are frequently and strongly affected by cloud cover, causing many data gaps and ~~a great deal~~large amounts of ~~poor~~low-quality values from undetected cloud ~~contamination~~ low-quality pixels. ~~In fact, cloud~~Cloud cover is frequent, and the locations of cloud cover are often uncertain. On average, at any one time, approximately 65 % of the global surface is obscured by clouds, ~~which~~leading directly ~~leads~~ to missing values over large, unevenly distributed areas in an image (Crosson et al., 2012; Mao et al., 2019). Although the integrity of the data has been greatly improved, the 8-day and monthly synthetic data still contain a number of low-quality pixels ~~that are affected by the~~and thus contain an insufficient quantity of daily LST pixels. Cloud cover and other factors, which causes extensive amounts of missing and ~~abnormal information,~~ low-quality pixels, significantly reduces the ~~usage rate~~proportion of usable LST data and poses a problem to further applications. Thus, ~~the~~ reconstruction of ~~noise-contaminated pixels, such as those contaminated by clouds,~~these missing and low-quality low-quality LST pixels low-quality is necessary for satellite-derived LST applications.

Two categories of methods have commonly been applied to reconstruct cloud ~~contamination~~ low-quality pixels from satellite-derived data in previous studies. The first category includes methods that directly reconstruct missing and ~~poor~~low-quality values using neighboring information with high similarity over temporal and spatial scales. Most temporal interpolation methods reconstruct missing and ~~poor~~low-quality LST values ~~of LST data~~ based on the periodic behavior of data, such as time series harmonic analysis (HANTS), S-G filtering, and Fourier transform (Xu and Shen, 2013; Na et al., 2014; Scharlemann et al., 2008). Crosson (2012) used another temporal interpolation method to reconstruct the LST data from the Aqua platform (afternoon overpass) using LST data from the Terra platform (morning overpass). Regarding spatial interpolation methods, previous methods have focused on geostatistical interpolation, including kriging interpolation, spline interpolation and their variants. Some researchers have also carried out other attempts; for example, Yu et al. (2015) introduced a method using a transfer function with the most similar pixels to estimate ~~null~~invalid pixels. These methods, which estimate missing MODIS LST data using only LST data, take advantage of the similarity and interdependence of the available temporal/spatial attributes of neighboring pixels. ~~Thus~~To some extent, these methods have the advantage of simplicity and reliability. However, this category of methods are often not as reliable as expected especially in complex topographical regions and areas with many missing data, because it cannot obtain enough information for reconstruction. The second category of methods solves these data gap problems by establishing correlation models for cloud ~~contamination~~ low-quality pixels and corresponding auxiliary data pixels. Neteler (2010) used a digital elevation model (DEM) as an auxiliary predictor to reconstruct MODIS LST data from nine years of data on temperature gradients, which achieved reliable results in mountainous regions. Ke et al. (2013) built a regression model that included many auxiliary predictors—latitude, longitude, elevation, and the normalized difference vegetation index (NDVI)—to estimate 8-day composite LST products. Fan et al. (2014) used multiple auxiliary maps, including land cover, NDVI, and MODIS band 7, to reconstruct LST data in flat and relatively fragmented landscape regions. Other similar algorithms have drawn support by employing many factors that affect LST, including elevation, NDVI, solar radiation, land cover, distance from the ocean, slope and aspect. Considering the complexity of the terrain and the nonuniformity of the spatial distribution of large-scale LST patterns, a reconstruction model with auxiliary data that provides rich information for missing pixels can improve the accuracy of the interpolation result.

The above studies greatly improve the usability of MODIS LST data and further add value to long-term LST trend analyses. However, despite the use of various techniques to reconstruct the LST value, existing techniques focus on the retrieval of the LST value under the assumption of clear-sky conditions instead of cloudy conditions, which cannot fulfill the need to obtain the real situation at the land surface. To address this issue, some scholars have also used microwave temperature brightness (TB) data, which are mostly derived from high-frequency channels (≥85 GHz), to obtain the real LSTs under clouds (André et al., 2015; Prigent et al., 2016). Microwave remote sensing is capable of penetrating clouds and can obtain useful radiation information for the retrieval of LST under clouds. However, the physical mechanisms of the current microwave LST retrieval models are not very mature, and the models have low resolution (Mao et al. 2007, 2018). Moreover, due to the difference in the surface properties of the land, the depth of the radiation signal detected by the microwave will differ at different locations, and it will deviate from the retrieval results of thermal infrared remote sensing when used to estimate LST values. Thus, new reconstruction methods for LST data need to be proposed to compensate for this deficiency.

On this premise, China is used as an example due to its large coverage area, heterogeneous landscape and complex climatic conditions. This paper presents a new long-term spatially and temporally continuous MODIS LST dataset for China from 2003 to 2017 that filters out missing and low-quality pixels and reconstructs them based on multisource data. We describe a data reconstruction process that is fully integrated with the benefits of the high reliability of surface observations, consistency and high accuracy of daily valid pixels and spatial autocorrelation of similar pixels. The process compensates for the insufficiency of reconstructing pixels under clear-sky conditions instead of under clouds in previous studies. The validation using data from the China Meteorological Administration observations indicates the robustness of the LST data after interpolation. The dataset is ultimately used to capture the annual, seasonal and monthly spatiotemporal variations in the LST in six natural subregions in China. It is envisioned that this dataset will help capture changes in surface temperature and will be useful for studies on high temperatures, drought and food security.

2 Study area

Insert Figure 1 here

Figure 1: The study area is divided into six natural subregions (I, II, III, IV, V, and VI), and the spatial distribution of the meteorological stations in the subregions is shown. The red circles mark the key areas where the temperature has changed significantly, and meteorological station from Subset (2) located these areas are used to validate the accuracy of the new LST dataset (a, b, c, d, e, and f).

~~Our study area of China is a large agricultural country, and its agricultural products are responsible for feeding more than 22 % of the world's population (Liu et al. 2004). However, agricultural production activities are very sensitive to climate change. In~~

设置了格式: 字体: 非加粗

~~recent years, global warming has directly affected the crop growth system, which in turn has affected many aspects such as food production, food security, farmers' income and rural social and economic development. In addition, the Qinghai-Tibet Plateau, which is known as the “World Water Tower”, supplies water for life, agriculture, and industry for nearly 40 % of the world's population through extensive glacial snow (Xu et al., 2008, Gafurov and Bárdossy, 2009, United Nations Environment Programme (UNEP), 2007). In recent years, increasing temperatures have forced glaciers in many large mountains to melt at an accelerating rate (Oku et al., 2006). The water resources from the water tower will be rapidly reduced, which will bring a series of serious water and ecological security problems. Therefore, the generation of a complete set of datasets that reflect the spatiotemporal variations in temperature will be helpful to study the temperature changes in China, especially the Qinghai-Tibet Plateau, and will be of great significance to agricultural production and drinking water supplies in neighboring countries.~~

~~Therefore, to~~To explore the temporal and spatial characteristics of China's ~~LST~~LSTs, the study area is divided into six natural subregions based on China's three major geographical divisions~~,~~: climatic conditions, landform types and tectonic movement characteristics. The eastern region is topographically characterized by ~~the topographical features of~~ plains and low mountains. This region has a variety of monsoon climate zones, which ~~travel~~, from south to north ~~and~~, include tropical, subtropical and temperate monsoon climate zones. Therefore, we divide the eastern region into the following four regions, as shown in Fig. 1. (I) The Northeast Region, which mainly covers the area to the east of Daxing'anling. This region has a temperate monsoon climate with an average annual precipitation of 400~1000 mm, and rain and heat are prevalent in the same period. ~~This large vast plain (approximately 55.8 % of the land area in China) and good climatic conditions are very conducive to the growth of crops, making the Northeast Region one of China's most important grain-producing areas.~~ (II) The North China Region ~~includes~~lies to the south of the Inner Mongolia Plateau, to the north of the Qinling Mountains and Huaihe River, and to the east of the Qinghai-Tibet Plateau. The region is dominated by a temperate monsoon climate and a temperate continental climate with four distinct seasons. This area is characterized by flat plains and plateau terrain. (III) The Central~~-South-~~Southwest China Region ~~that~~ extends from the eastern part of the Qinghai-Tibet Plateau to the western parts of the East China Sea and South China Sea, south to the Huaihe River - Qinling Mountains, and north to the area where the daily average temperature is greater than or equal to 10 °C. The accumulated temperature in this region is 7500 °C. This region is commonly dominated by a subtropical monsoon climate. (IV) The South China Region is located in the southernmost part of China and is characterized by a tropical and subtropical monsoon climate with hot and humid conditions. The area has abundant rainfall, and the average annual precipitation is approximately 1900 mm.

The western region is divided into 2 natural subregions. (V) The Northwest Region~~, which~~ includes the ~~north of the~~northern Qilian Mountain-Altun Mountains-Kunlun Mountains, the Inner Mongolia Plateau and the western part of the Greater Khingan Range. This region is located ~~inside~~in the ~~mainland with~~continental interior and features complex terrain conditions, ~~and the topography is mostly~~dominated by plateau basins and mountainous areas. This region has a tropical dry continental climate with rare rainfall. ~~This~~Consequently, this area ~~has a wide range~~features large areas of barren land, with a desertified land area of 2.183 million km^2, accounting for 81.6 % of China's desertified land area (Deng, 2018). Moreover, the Taklimakan Desert in this region is one of the ~~top ten~~10 largest deserts in the world. (VI) The Qinghai-Tibet Plateau Region is mainly located ~~in~~on the Qinghai-Tibet Plateau, which is the highest-elevation plateau ~~with the highest altitude~~ in the world. This region is mainly described ~~to have~~as having an alpine plateau climate, with ~~a~~ relatively high ~~temperature~~temperatures and ~~a large~~an extensive grassland meadow area.

3 Data and methods

3.1 MODIS data

MODIS is a key sensor of the Earth Observing System (EOS) program that provides a unified grid product with global coverage of the land, atmosphere and oceans. MODIS covers 36 spectral bands in the visible, near-infrared and thermal infrared ranges (from 0.4 to 14.4 um), so it is extensively used to study global marine, atmospheric, and terrestrial phenomena (Wan et al., 1997). The MODIS instruments are aboard two NASA satellites, Terra and Aqua, which were launched in December 1999 and May 2002, respectively. As both the Aqua and Terra satellites are near-polar orbit satellites with a flying height of approximately 705 km in sun-synchronous orbit, they provide data with a temporal resolution of twice daily. The Terra satellite passes through the equator from north to south at approximately 10:30 am and 10:30 pm local solar time and is called the morning star. The Aqua satellite passes through the equator in the opposite direction from south to north at approximately 1:30 am and 1:30 pm and is called the afternoon satellite (Christelle and Ceccato, 2010). The two satellites collect repeat observations every 1-2 days and transmit observation data to the ground in real time.

MODIS LST data are retrieved with two algorithms: the generalized split-window algorithm (Wan and Dozier, 1996; Wan et al., 2002) and the day/night algorithm (Wan and Li, 1997). The split-window algorithm is advantageous for removing atmospheric effects because the signal difference between the adjacent thermal and middle infrared channels (channel 31 with a wavelength of 10.78–11.28 μm and channel 32 with a wavelength of 11.77–12.27 μm) is caused by the differential absorption of radiation in the atmosphere (Wan et al., 2002). The latest LST V006 version data used in this article is obtained by another important algorithm: the day/night algorithm. Due to the complexity of surface reflectance and atmospheric conditions, multichannel data are utilized in day/night image pairs to derive the LST, including radiation calibration data, atmospheric temperature and water vapor data, cloud masks and geolocation information and L1B data in seven thermal infrared bands (bands 20, 22, 23, 29, 31, 32, 33) from MOD07_L2 (Wan, 2007). Then, these day/night pairs of MODIS data are used to construct 14 nonlinear equations to retrieve the surface emissivity and surface temperature based on a physics-based day/night LST model from the MODIS 1B data without high_accuracy atmospheric temperature and water vapor profiles (Wan and Li, 1997).

The day/night LST algorithm used in the LST V006 version products exhibits great advantages in retrieving LST: it not only optimizes atmospheric temperature and water vapor profile parameters for optimal retrieval but also does not require complete reversal of surface variables and atmospheric profiles (Ma et al., 2000, 2002). A comprehensive sensitivity and error analysis was performed for the day/night algorithm, which showed that the accuracy was very high, with an error of 1–2 K in most cases (0.4-0.5 K standard deviation over various surface temperatures for mid-latitude summer conditions) (Wan and Li, 1997, Wang and Liang, 2009; Wang et al., 2007).

Here, two MODIS products were chosen for research: daily LST data (MOD11C1 and MYD11C1) and monthly LST data (MOD11C3 and MYD11C3), which were available for the period from 2003–2017. The datasets include daytime and nighttime surface temperature data provided by NASA. These data are the new collection 6 series data provided in 2017, which has been fixed and substantially improved compared to the collection 5 data used in many previous studies. In collection 6 data, the identified cloud-low-quality LST pixels were removed from the MODIS Level 2 and Level 3 products, and the classification-based surface emissivity values were adjusted (Wan. 2014). Both datasets provide the global LSTs generated by the day/night algorithm with a spatial resolution of 0.05°×0.05° (approximately 5600 m at the equator), which is provided in an equal-area integerized sinusoidal projected coordinate system. The composited 8-day (MOD11C2/MYD11C2) and monthly (MOD11C3/MYD11C3) data are deduced from daily global data (MOD11C1/ MYD11C1) without cloud contamination. The global LST product MOD11C1/MYD11C1 (V006) was created by assembling daily MOD11B1/MYD11B1 tiles and resampling from 5600 m spatial resolution to a resolution of 7200 columns and 3600 rows of the latitude/longitude grid.

The preprocessing of the MODIS data mainly includes extraction of daytime and nighttime LST and the corresponding quality assessment (QA) data from 17 scientific datasets, projection conversion (reprojection of raw data from a sinusoidal projection (SIN) to an equal-area conical projection (Albers), WGS84 coordinate system), conversion of the data format (conversion from HDF to Geo-tiff), and clipping (selection of geographic subsets according to latitude and longitude position to improve the efficiency of the model). The brightness temperature is converted to real surface temperature by coefficient and offset correction.

3.2 Supplementary data

~~The~~ LST records ~~in China for~~at the hourly intervals from 2399 meteorological ground stations in China from 2003-2017 were used in this study, and they were provided and ~~underwent~~subjected to strict quality control and evaluation by the China Meteorological Administration (CMA). Meteorological station data were randomly divided into two completely independent subsets by the jackknife method~~.~~ (Benali et al., 2012). Subset (1): the number of ground stations used for the reconstruction process was 1919, accounting for 80 % of the total number of ground stations. Subset (2): the number of sites used for verification was 480, accounting for 20 % of the total. Then, the data used for the reconstruction process ~~in~~for subset (1) were created by extracting meteorological station LST data at the overpass times of Terra and Aqua (01:30, 10:30, 13:30, and 22:30). For the verification process, six key areas where warming/~~cooling~~negative trends were the most significant (i.e., shown in the red ~~ellipse~~ellipses a-f in Fig. 1 and Table 1) were selected for detailed verification to better reflect the accuracy of the LST data. All meteorological ground station data were tested for temporal and spatial consistency, which included identifying and rejecting extreme values and outliers. It is worth noting that the key areas marked by red circles contain site data from subset (1) and subset (2). Generally, there are more stations in the red circle than the sites used for verification in Table 1, especially in the Eastern China where there are a large number of stations.

设置了格式: 字体: (默认) 宋体, (中文) 宋体, (中文) 中文(中国)

Table 1 Basic information for some of the meteorological stations in key zones

Insert Table 1 here

Elevation data with 1 km resolution are available from the NASA Space Shuttle Radar Terrain Mission (SRTM) V4.1 for reconstruction of cloud-low-quality data.

3.3 LST data restoration method

For satellite-derived LST data, due to the extensive and random distribution of missing and unreliable values caused by cloud contamination in the images. It is difficult to reconstruct the cloudless LST dataset on daily scale, and it is even more difficult to reconstruct the dataset that can reflect the LST of the ground under the cloud cover. Therefore, we create a reconstruction model that combines meteorological station data and daily and monthly MODIS LST data to reconstruct a high-precision monthly dataset that can reflect the true LST under cloud coverage. The reconstruction model effectively preserves the highly accurate pixels in the original daily data, reconstructs only the low-quality daily data, and finally, replaces low-quality pixels with the composite average pixel value in the monthly data. To better describe the data processing, Fig. 2 shows a summary flowchart for the reconstruction of MODIS monthly LST data. The reconstruction model we propose is divided into two general steps: LST pixel filtering and LST data restoration. Low-quality pixel values were first identified and set to missing values for all input monthly LST images based on pixel quality filtering (see section 3.3.1 for details）. Both missing pixels and low-quality pixels are considered invalid pixels that need to be reconstructed. low-qualityFor each invalid pixel in the monthly images, we first determined the invalid pixels in daily LST images at the same location at the corresponding time. And then we reconstructed these invalid daily pixels. The reconstruction process for the invalid daily pixels is divided into three substeps low-quality(see section 3.3.2 for details）: 1) in situ LST observations at the same location, as judged from the longitude and latitude information, were used to fill the invalid pixels at the same location; 2) the geographically weighted regression (GWR) method was employed to interpolate invalid pixels based on similar pixels from multiple sources; and 3) the remaining invalid pixels were reconstructed based on regression of the elevation temperature gradient. Finally, the averages of the available daily LST pixels were calculated and filled using the corresponding monthly pixels.

Insert Figure 2 here

Figure 2: (a)The summary flowchart for reconstructing MODIS monthly LST data, (b)the detailed flowchart for reconstructing reconstruct missing daily pixels in (a).

3.3.1 Filtering of MODIS LST

MODIS LST data are retrieved from thermal infrared bands in clear-sky conditions and contain many missing values and low-quality values caused by clouds and other atmospheric disturbances. Generally, the cold top surface of a thin or subpixel cloud is difficult to detect, and the LST retrieved under such conditions usually leads to an underestimation of the temperature values in the MODIS LST data (Neteler, 2010; Markus et al., 2010; Jin and Dickinson, 2010; Benali et al., 2012). Moreover, other factors can also contaminate the observation signal and cause the data to be unavailable, such as atmospheric disturbance, observation geometry and instrumental problems (Wan, 2014). In general, the abnormally low values in LST maps caused by undetected thin clouds, together with other low-quality values, need to be identified and filtered because these values greatly reduce the accuracy of the LST data.

Cloud cover is extensive and inevitable in daily weather conditions. Statistical calculations were performed and showed that missing values for daily data reached approximately 50 % for Terra and Aqua satellites. Figure 3 shows an example representing the distribution of valid pixel values in the daytime for winter and summer. The coverage of pixels with missing data in the study area at 10:30 am during the daytime on January 1, 2017, and July 1, 2017, for the Terra platform reached 44.9 % and 51.7 %, respectively. The spatial gaps in the daily data are characterized by an arbitrary distribution and generally large aggregations. In fact, the emergence of a large number of missing values every day makes it difficult to reconstruct a high-precision daily LST images that represents real values under clouds using current techniques due to such a paucity of information, especially for areas with complex climates.

However, the random occurrence of cloud-covered areas has a much smaller impact on monthly composite products, which makes these products a reliable source for building a high-precision monthly LST dataset. Compared with daily and 8-day composite data, spatiotemporal integrity and consistency have been greatly improved in monthly composite LST data. However, for many regions, the lack of data or quality degradation caused by clouds is still common even in monthly composite data（Fig. 4）. It is necessary to identify and reconstruct low-quality pixels, which seriously affect the use and analysis of monthly LST data. A reliable method for removing low-quality pixels is implemented using the data quality control information for MODIS LST data. The data quality control information is statistically calculated and stored in the corresponding QA layer and is represented by an 8-bit unsigned integer and can be found in the original MODIS LST HDF files. Therefore, we use the quality control labels for daily and monthly files as mask layers to identify low-quality pixels to ensure the quality of the LST data. Finally, pixels with QA layer labels of “the average LST error <=1 K”, “LST produced, good quality” and “the average emissivity error <=0.01” are considered to be high-quality data, and the remaining pixels are low-quality pixels and are set to missing values. Finally, we reconstructed all the invalid pixels in monthly LST data. Quality information is almost indicative; thus, sufficient information is provided for the filtering of low-quality pixels (Benali et al., 2012). A summary flowchart of the process used to construct the LST data model is schematically illustrated in Fig. 2.

The spatial distribution pattern of invalid Terra LST data after filtering by the QA layer is shown in Fig. 4. The low-quality pixel coverage rates for January and July 2017 were 23.45 % and 19.68 %, respectively. There are more missing values in winter than in summer in the northeastern region, which may be affected by the confusion resulting from large areas of snow cover and clouds in the winter. However, the missing values are mainly concentrated in southern China in summer, which is closely related to the increased cloud cover in the hot summers in South China.

Insert Figure 3 here

Figure 3: Spatial distribution of valid data for daily MODIS LST data from Terra during the daytime on (a) January 1, 2017, and (b) July 1, 2017. Areas of missing data are blank.

Insert Figure 4 here

Figure 4: Spatial distribution of valid data after pixel filtering for monthly MODIS LST data from Terra during the daytime on (a) January and (b) July. Areas of invalid data are blank.

3.3.2 LST data restoration

Missing values caused by cloud coverage have always been an important limitation of using LST from thermal infrared (TIR) data in a wide range of applications. For daily LST data, although many attempts have been made to reconstruct the LST data under clear-sky conditions, the widespread missing values make it difficult to reconstruct high-precision daily LST pixels under clouds using the limited available information. To obtain a high-precision LST dataset that can retrieve the true temperature of the land surface under cloud cover instead of clear skies, we adopted another strategy .

Given that monthly LST data are composited from the corresponding daily data, an insufficient amount of valid daily data and low availability for some pixels will lead to quality degradation in the monthly data. The contributions of multiple valid daily pixels $\bar{P}_i$, despite their good precision, are rejected along with the final low-quality values in monthly pixels. Thus, considering the inheritance of these high-quality data, we believe that these valid daily pixels $\bar{P}_i$ can help to reconstruct high-precision estimates for LST pixels under cloudy conditions. Therefore, we uses a combination of MODIS daily data, monthly data and meteorological station data to reconstruct the true LST in areas with cloud coverage.

In the reconstruction model, we first filter the monthly image, and the locations of the cloud-low-quality pixels (i.e., the missing and low-quality monthly pixels) are determined. Then, we filter all the daily pixels from the month in which the cloud-low-quality pixels occurred. The valid pixels $\bar{P}_i$ in the daily data are retained, the low-quality daily data are reconstructed, and the low-quality pixels in the monthly data are replaced with the corresponding averaged pixel values from the daily data (Fig. 2). Missing daily pixel is defined as the target pixels T_t , the image contains the target pixel T_t is target image. The reconstruction process for the the target pixels T_t is as follows.

During the daytime, the real ground LST values in pixels obscured by clouds are usually lower than the values in the adjacent unaffected pixels, and at night it is the opposite. Many influencing factors are considered for data reconstruction. The ground meteorological station values observed at the same time as the reconstruction result are the most reliable among all influencing factors, such as NDVI, elevation, longitude and latitude. Therefore, the latitude and longitude information of the invalid pixels was first used to search for the ground stations in the same location. Invalidt pixels were filled using the values from valid ground-based LST data at the same location at the same time, and these filled pixels were marked. Then, for the invalid pixels without ground meteorological station data, we used a combination of two strategies to reconstruct the missing LST data to improve the accuracy of the result. The first strategy identified the most similar pixels by using adaptive thresholds and reconstructed them by using a GWR method.

GWR is a common and reliable method for estimating missing pixels, which quantifies the contribution of each similar pixel to contaminated pixels. This method assumes that similar pixels that are spatially adjacent to the target pixel are close in the spectrum and should be given more weight.

$$\cancel{T = \sum_{i=1}^{n} W_i \cdot T_i \ ,} \qquad \cancel{(1)}$$

~~where T is the reconstructed LST value of a target pixel, T_i is the value for the similar pixel i, W_i is the weight coefficient, and the sum of all W_i values is 1.~~

Due to the high temporal variability of thermal radiation emitted from the land surface and atmospheric state parameters, satellite sensors that measure the thermal radiation energy from different phase images at the same locations often produce different values even when the same thermal infrared sensor is used. Some of the most common regular changes in surface features, such as the vegetation spectrum changes due to seasonal changes, can be predicted using auxiliary information. However, multiple unpredictable changes that cause abrupt transformation in the thermal energy of infrared radiation are difficult to predict, such as wheat harvesting ~~and the expansion of a city. Therefore, it is only possible to determine the most accurate similarity relationship for the target pixels by selecting the image from the nearest phase. Thus~~. Therefore, for the target pixel i and a valid pixel j in the same image, the three images that are temporally closest at the same overpass time are determined as reference images, and a adaptive threshold is then used in the reference image to determine whether the pixels corresponding to pixels i and j are similar. If two pixels are judged to be similar in more than one image, the valid pixel j is identified as a similar pixel for the target pixel i.

~~As~~Because the factors that influence surface temperature (vegetation cover, sun zenith angle, microrelief, etc.) vary greatly ~~in~~among different regions and seasons, the ~~spectral~~ differences of adjacent pixels in different areas may also vary greatly. Thus, there will be large deviations in the similar pixel decision criteria if a fixed similarity threshold is used. Here, we use an adaptive threshold φ^{τ} ~~, which denotes the smoothness of the local area,~~ to determine similar pixels for each ~~null~~invalid pixel (Eq. 3). The adaptive threshold φ^{τ}, calculated from the standard deviation, indicates the local area smoothness. Local area is a certain size area centered on similar pixel, which is located in the three reference images. The closer the pixel is, the more similar the environment is, so the smoother the local area will be. For example, the jth valid pixel in the target image~~, it~~ is determined to be a similar pixel of the target pixel i only when the relationship described in Eq. (2) is satisfied in the reference image τ. Simultaneously, similar pixels were determined based on all valid pixels in the image rather than a sliding window because missing values are often arbitrarily clustered in a large area rather than scattered.

$$|P_s^\tau - P_t^\tau| \leq \varphi^\tau \ , \qquad (1)$$

(1)

$$\varphi^\tau = \sqrt{\sum_{i=1}^{n}(P_s^\tau - \varepsilon)^2}, \qquad (2)$$

~~Where~~$\varphi^\tau = \sqrt{\sum_{i=1}^{n}(P_s^\tau - \varepsilon)^2}$, (2)

where P_s^τ and P_t^τ are the values of pixels corresponding to the position of the similar pixel and the target pixel in the reference image, respectively. φ^τ is the threshold used to determine similar pixels. ε is the mean value of all pixels in local area. τ is the reference image (value=1, 2, 3). Here, we set the range of the local area to 5 pixels by 5 pixels centered on the target pixel (Zeng et al., 2013). In this paper, the number of similar pixels of the target pixel in the target image should be greater than 4 to apply the GWR method to reduce the error due to an insufficient number of similar pixels.

After determining similar pixels, the LST values of the pixels low-quality by clouds are determined through GWR. In theory, LST data from meteorological stations are the most reliable record, even in the case of thick cloud coverage. Thus, similar pixels obtained from ground stations are the most representative and can better reflect the LST under clouds than under clear-sky conditions. In the process of reconstructing missing pixels, The regression weight coefficient of a similar pixel is determined by its Euclidean distance from the target pixel. In addition，we assign a related weight multiplier to the marked ground station data based on the GWR. After selecting some of the marked pixels as experiments, it was found that the target pixels could be more accurately estimated when the relative multiweight values of the ground stations were set to 3 in this paper. Therefore, the weighting coefficients of similar pixels are determined by Eqs. (5) and (6).

$$D = \sqrt{(x - x_t)^2 + (y - y_t)^2},$$

()

$$W_i = \frac{\frac{M_c}{D_i}}{\sum_{i=1}^{m}\frac{M_c}{D_i} + \sum_{j=1}^{n}\frac{M_g}{D_j}}, \qquad (4)$$

(4)

$$W_j = \frac{\frac{M_g}{D_j}}{\sum_{i=1}^{m}\frac{M_c}{D_i} + \sum_{j=1}^{n}\frac{M_g}{D_j}},$$

(5)

where D represents the Euclidean distance from the similar pixel (i，j) to the target pixel t, x, y, x_t and y_t describe the locations of the similar pixel and target pixel. i and j represent similar pixels used to estimate the low-quality LSTs, i is a pixel that is not low-quality by clouds, and j is a pixel assigned by the ground station. W_i and W_j describe the weight that similar pixels i and j contribute to the target pixels, respectively. m is the number of similar pixels that are not low-quality by clouds, and n is the number of similar pixels that are assigned by ground stations. M_c and M_g represent the weight coefficients of clear sky pixels and ground station assignment pixels, respectively. In this paper, M_c and M_g are set at 1 and 3, respectively.

Therefore, the GWR method can be represented as follows

$$T_t = \sum_{i=1}^{m} W_i \cdot T_i + \sum_{j=m+1}^{n} W_j \cdot T_j, \tag{6}$$

where T_t is the reconstructed LST value of a target pixel, T_i and T_j represent LST values for the similar pixel i and j, the sum of W_i and W_j values is 1.

For another strategy, the elevation temperature gradient regression method was used to reconstruct the remaining low-quality pixels that did not have enough similar pixels. In general, the elevation factor has a particularly significant effect on the spatial variation at the regional scale. Elevation is recognized as the most important factor that characterizes the overall spatial trend of LST (Sun, 2016). DEM data and LST data are used to construct linear regression relationships for invalid pixels based on the clear sky pixels in the neighborhood of a certain window size; these data are then used to predict the missing value pixels by linear interpolation. After several simulations of the experimental pixel window size, the noise was found to be minimized when a sliding window of 19 by 19 pixels was used, and this window size was considered to have the best complement value.

$$T_i = \alpha \times h_i + \beta, \tag{7}$$

where T_i is the surface temperature data after interpolation (units: °C); h_i is the elevation value of pixel i (units: m); α is the influence coefficient of the elevation on the surface temperature, which is the regression coefficient; β is the estimated intercept. Finally, we accurately crop the image to a China-wide image to ensure that the sliding pixel window reaches the edge of the study area.

3.4 Analysis of the LST time series trend

In this study, the slope of a linear regression describes the rate of LST cooling/warming and is calculated by Eq. (8). The slope value and correlation coefficient (R), calculated with Eq. (9), were selected to quantify the temporal and spatial patterns in the LST variations.

$$Slope = \frac{\sum_{i=1}^{n}(iT_i) - \frac{1}{n}\sum_{i=1}^{n} i \sum_{i=1}^{n} T_i}{\sum_{i=1}^{n} i^2 - \frac{1}{n}(\sum_{i=1}^{n} i)^2}, \quad (8)$$

$$R = \frac{n\sum_{i=1}^{n}(iT_i) - \sum_{i=1}^{n} i \sum_{i=1}^{n} T_i}{\sqrt{n\sum_{i=1}^{n} i^2 - (\sum_{i=1}^{n} i)^2}\sqrt{n\sum_{i=1}^{n} {T_i}^2 - (\sum_{i=1}^{n} T_i)^2}}, \quad (9)$$

where i is the number of years, T_i is the average LST of year i, and n is the length of the LST time series; here, n is 15. A positive slope indicates an increase in LST (warming); a negative slope indicate a decrease in LST (cooling). The R values range from -1 to 1. An R value greater than 0 means that the LST is positively correlated with the time series, and an R value less than 0 means that the LST is negatively correlated with the time series. Meanwhile, the larger the absolute value of R is, the stronger the correlation with the time series changes.

4 Results

Temperature changes show significant differences at different time scales (day, night, month, season and year) and different spatial scales. Therefore, various QA methods were performed to validate the new data on the monthly and seasonal scales. Furthermore, to better understand the spatial and temporal variations in surface temperature and the reactions of different regions, we analyze the LST at yearly, seasonal and monthly scales and show the changes in temperature during the day and at night.

4.1 Annual change analysis

4.1.1 Average change

After LST data restoration data reconstruction, four overpass times of images are obtained each month. Calculated the average LST at four times to represent the LST image of the month. To obtain the overall LST trend, we averaged the LST for each year to remove seasonal effects. Fig. 5 shows the annual average LST change in China over the period from 2003-2017. The LST fluctuations in China exhibited a general weak ~~warming~~positive trend. The sliding average of the 5-year unit also showed a weakly fluctuating ~~warming~~positive trend. The lowest LST in China appeared in 2012 at 7.51 °C. The temperature reached its highest value in 2007 (9.26 °C), but after 2012, the LST remained high. This result coincides with the global warming stagnation period that was noticed from 1998-2012, and the LST increased significantly after 2012. After analyzing the LST on the seasonal and monthly scales, we found that the cooling in 2012 mainly occurred in the winter, as it was concentrated from January-February, and the cooling in the southern region was more significant than that in the other regions. In 2012, due to the abnormally strong East Asian winter monsoon, there was abnormal rainfall in the south in winter. We also observed a sudden decrease in LST in 2008 and a sudden increase in 2013. In 2008, severe persistent low-temperature snowstorm events in southern China in winter caused a decline in LST. The warming in 2013 was mainly affected by the abnormally high temperatures in the middle and lower reaches of the Yangtze River in summer.

Insert Figure 5 here

Figure 5: Annual mean LST changes in China from 2003 to 2017.

Insert Figure 6 here

Figure 6: Spatial dynamics of interannual change trends in LST from the slope (a) computed by Eq. (8), the correlation coefficient (b) computed by Eq. (9) and frequency distribution of the slope (c) during 2003-2017. In panel c, the different temperature trends (slope) are divided into 10 subinterval ranges corresponding to the ranges in panel a. The area to the left of the line AB represents the proportion of the area that experienced cooling, and the area to the right represents the proportion that experienced warming.

For a more detailed understanding of the spatial patterns and regional differences in the LST changes in different areas, the rate of annual average LST change per pixel from 2003 to 2017 was calculated, and the slope (Fig. 6a), correlation coefficient (R, Fig. 6b), frequency distribution of the slope (Fig. 6c) and the significance of the trend (P, Fig. A1) are shown. From 2003-2017, the annual average LST in China showed a weakly positive trend. The LST exhibited a strong positive trend in many regions in the north but negative trends in the south, and the positive trend in the west was greater than that in the east. Different regions showed significant regional variations. Most of China, accounting for 63.7 % of the study area, experienced a positive trend (slope >0) (corresponding to the pale yellow, yellow, light orange, orange, and red parts in Fig. 6c). Additionally, approximately 20.80 % of the pixels experienced significant warming (slope >0.05, R >0.6, $P < 0.05$). The areas with significant warming were mainly concentrated in the Inner Mongolian Plateau and areas to the south in the northwestern region. In contrast, 36.25 % of the areas showed a negative trend (slope <0, depicted in green and 4 shades of blue in Fig. 6c). The area with a significant cooling pattern (slope <-0.075, R < -0.6, $P < 0.05$) covered 6.53 % of the study area, and these areas were mainly concentrated in the northeast. The specific spatial variation characteristics of LST in different regions are summarized as follows.

In 2013, the Intergovernmental Panel on Climate Change (IPCC) noted that climate warming is clear (IPCC et al., 2013). However, some areas of the Northeast Region (I) showed a significant warming hiatus over the past 15 years, and these areas made the greatest contribution to China's ~~cooling~~negative trend. We observed widespread and relatively strong cooling regimes in most areas (i.e., the slope value ranged from -0.06 to less than -0.12, see Fig. 6a, b for details~~) except for~~), especially in the ~~northeastern part~~north of the ~~Greater Xing'an Mountains. The cooling trend in Northeast China in recent years may be related to the negative Arctic oscillations in the northeast, which are closely related to the Siberian high (SH) and the East Asian Trough (EAT) during this period (Sun et al., 2017). Attention should be paid to the~~ Northeast Plain ~~because it is China's most important region for commercial grain (corn, rice) and cash crops (soybeans, sugar beets, etc.), accounting for approximately~~

设置了格式: 字体: (中文) 宋体, 字体颜色: 深红

~~15 % of the country's total grain production (Yang et al., 2007). Intensified cold conditions will cause insufficient accumulated temperature in the crop growth period, which will cause large-scale crop yield reductions. In addition, if this rapid cooling continues in the Northeast Region, it will pose a great threat to agricultural production and the development of the regional economy. The possible impacts should be brought to the attention of the relevant agricultural sector, and appropriate preventive and regulatory measures should be taken.~~(slope < -0.1, R < -0.8, P < 0.05, see Fig. 6a, Fig. 6b and Fig. A1).

In the North China Region (II), The North China Plain and the Yangtze River Delta in the south both exhibit obvious positive trends, both of which are densely The North China Plain and the Yangtze River Delta in the south both exhibit obvious positive trends, both of which are densely The North China Plain and the Yangtze River Delta in the south both exhibit obvious positive trends, both of which are densely The North China Plain and the Yangtze River Delta in the south both exhibit obvious positive trends, both of which are densely populated areas. In addition, the Central-Southwest China Region (III) and the South China Region (IV) also showed negative trends, but the negative trend was stronger in the South China Region (most area: slope < 0.75, R < -0.8, P < 0.05) than in the Central-Southwest China Region.

In the Northwest Region (V), some areas in the Tianshan Mountains and the Inner Mongolia Plateau experienced significant In the Northwest Region (V), some areas in the Tianshan Mountains and the Inner Mongolia Plateau experienced significant In the Northwest Region (V), some areas in the Tianshan Mountains and the Inner Mongolia Plateau experienced significant In the Northwest Region (V), some areas in the Tianshan Mountains and the Inner Mongolia Plateau experienced significant In the Northwest Region (V), some areas in the Tianshan Mountains and the Inner Mongolia Plateau experienced significant In the Northwest Region (V), some areas in the Tianshan Mountains and the Inner Mongolia Plateau experienced significant In the Northwest Region (V), some areas in the Tianshan Mountains and the Inner Mongolia Plateau experienced significant In the Northwest Region (V), some areas in the Tianshan Mountains and the Inner Mongolia Plateau experienced significant In the Northwest Region (V), some areas in the Tianshan Mountains and the Inner Mongolia Plateau experienced significant In the Northwest Region (V), some areas in the Tianshan Mountains and the Inner Mongolia Plateau experienced significant In the Northwest Region (V), some areas in the Tianshan Mountains and the Inner Mongolia Plateau experienced significant In the Northwest Region (V), some areas in the Tianshan Mountains and the Inner Mongolia Plateau experienced significant In the Northwest Region (V), some areas in the Tianshan Mountains and the Inner Mongolia Plateau experienced significant In the Northwest Region (V), some areas in the Tianshan Mountains and the Inner Mongolia Plateau experienced significant In the Northwest Region (V), some areas in the Tianshan Mountains and the Inner Mongolia Plateau experienced significant In the Northwest Region (V), some areas in the Tianshan Mountains and the Inner Mongolia Plateau experienced significant

In the Northwest Region (V), some areas in the Tianshan Mountains and the Inner Mongolia Plateau experienced significant positive trends (slope > 0.10, R > 0.8, P < 0.01), and this area exhibited the strongest. positive trend in China over the past 15 years. In the Qinghai-Tibet Plateau Region (VI), the ecological environment is complex, and the unique plateau terrain and thermal properties of the surrounding areas play an important role in regulating the surrounding atmospheric circulation system. Because the Qinghai-Tibet Plateau is extremely sensitive to climate change, it is considered to be a key area of global climate change. Therefore, we have also paid close attention to the temperature changes on the Tibetan Plateau. As shown in Fig. 6a and b, an obvious positive trend was captured in the southern part of the Qinghai-Tibet region (slope >0.08), which should be emphasized. Additionally, the positive trend in the Qaidam Basin in the northeast is significantly higher (slope > 0.1) than that in the surrounding area.

4.1.2 Day and night change analysis

To more specifically assess the interannual changes in LST, we further analyzed the ~~diurnal~~day and night trends in LST. The spatial distribution of the average annual ~~diurnal surface temperature~~day and night LST in the time series is shown in Fig. ~~7.~~7, and the corresponding significance is shown in Fig. A2. During the day, the ~~warming~~positive trend mainly comes from the eastern part of North China, the central and western parts of the northwest, and the southern part of the Qinghai-Tibet Plateau. The annual daytime ~~warming/cooling~~ positive/negative trends of ~~surface temperature~~ LST in ~~almost all~~most regions from 2003 to 2017 are significantly higher than those in the ~~evening (-0.03<slope<0.03);~~ nighttime; thus, the average LST ~~warming/cooling~~positive/negative trends can be attributed to ~~the~~ changes during the daytime. The ~~diurnal variation in LST~~temperature difference between day and night also indicates that the trend of LST changes is more likely due to factors such as daytime human ~~activities~~production and sunshine hours. The effects of changes in solar radiation on the near-surface thermal conditions are the most pronounced. Among these changes, the ~~warming~~positive trend in the southern part of the Qinghai-Tibet Plateau is obvious (slope >0.09). Duan and Xiao (2015) found that since 1998, the amount of daytime cloud cover in the southern part of the Qinghai-Tibet Plateau has decreased rapidly, resulting in an increase in sunshine hours. The increase in solar radiation during the day will directly lead to an increase in surface temperature, which is an important factor leading to an increase in daytime temperature. However, compared with the ~~daytime~~trend during the day, the interannual temperature change trend at night is relatively gentle and can be considered stable.

Insert Figure 7 here

Figure 7: Spatial dynamics of Fig. 7 a) day and Fig. 7 a) night LST change trends based on slope (a) and correlation coefficient (b).

4.1.3 Analysis of the diurnal temperature difference

Figure 8 shows the spatial distribution of the average daytime LST, average nighttime LST, and day and night temperature differences. The LST shows significant spatial variation. During the day, the distribution of LST varies with surface insolation depending on the solar zenith angle (Jin and Liang, 2006). The highest LST during the day appears in the northwestern part of V and the desert area of the Tarim Basin in the Alashan Plateau (30 °C to more than 35 °C) rather than in the southern part of the low-latitude tropics, which is different from the patterns at night. Except for the Qinghai-Tibet Plateau, the nighttime LST decreases from the southern low-latitude areas to the northern high-latitude areas, and the spatial variation is roughly consistent throughout the six subregions. This result may suggests that the spatial temperature change is related to the latitude range, and also to the smooth terrain in the east..

As shown in Fig. 8c, the largest diurnal difference in LST is concentrated mainly in the mountainous area of the Qinghai-Tibet Plateau; this difference is greater than 25 °C and is especially prominent in the Qaidam Basin. The lowest diurnal LST difference of less than 5 °C can be seen at low latitudes along the southeastern coast in South China. At the same time, affected by the height of the plateau, the temperature difference between day and night in the Yunnan-Guizhou Plateau in the western part of Central China is 11-15 °C, while that in the eastern area at the same latitude is only 6-11 °C. Furthermore, compared with the inland areas at similar latitudes, the coastal areas (II and III in the eastern part of Central China and the central and eastern parts of the South China Region) usually have small diurnal LST differences.

Insert Figure 8 here

Insert Figure 8 here
Insert Figure 8 here
Insert Figure 8 here
Insert Figure 8 here
Insert Figure 8 here
Insert Figure 8 here
Insert Figure 8 here
Insert Figure 8 here
Insert Figure 8 here
Insert Figure 8 here

Insert Figure 8 here

Figure 8: Spatial dynamics of average daytime LST (a) and average nighttime LST (b) from 2003 to 2017

4.2 Seasonal change analysis

In addition to analyzing the characteristics of the interannual variation in LST, we also conducted an analysis of the seasonal variation characteristics to further reveal the LST variation patterns in detail (see Fig. 9 and Fig. A3). The variation characteristics are also described by the slope of the change and the correlation coefficient (R) proposed in Section 3.4.1. The results show that there is a significant spatial difference between the seasonal surface temperature trends, reflecting the effect of seasonal temperature changes on regional temperature changes. From 2003 to 2017, the positive trend in the four seasons was most significant in winter, which exhibited the largest warming area (accounting for 70 %), followed by that in spring and summer, and the national average LST change in autumn basically did not change. Compared with the global warming hiatus that occurred from 1998 to 2002, the positive trends in China showed large differences in the four seasons (Li et al., 2015).

Specifically, in spring, the warming area is mainly concentrated in the northern areas (I, II, and V), while a weak negative trend is observed in the southern areas. The largest positive trend over the northern areas appears in the Inner Mongolia Plateau (slope >0.18, P < 0.01). In addition, rapid warming also occurred in the North China appears in the Inner Mongolia Plateau (slope >0.18, P < 0.01). In addition, rapid warming also occurred in the North China Plain in the eastern part of the North China Region (II) (especially near Beijing and some areas of Hebei Province, slope >0.12, R > 0.6, P < 0.01)f
>0.12, R > 0.6, P < 0.01)f
>0.12, R > 0.6, P < 0.01)f
>0.12, R > 0.6, P < 0.01)f

As shown in Fig. ~~9~~9, compared with the other two seasons, both summer and autumn showed ~~nonsignificant warming~~weak positive trends throughout the country. In summer~~,~~ (Fig. 9b1, b2 and b3), there were ~~slightly~~slight increasing trends ~~almost everywhere~~ in most areas of China, while there were still negative trends ~~were still observed~~ in the Northeast Region (I) (details in Fig. ~~9). The slight warming trends might occur due to the weakening of the East Asian summer monsoon circulation caused by~~ 9). Significant increasing trends were mainly observed in the Qinghai-Tibet Plateau, North China Plain, Inner Mongolia Plateau, Tarim Basin and some areas in the ~~tropical high-altitude composition of~~north, with the ~~easterly jet (TEJ) (Ding Y et al., 2008). The Chinese atmospheric circulation system is significantly affected by the East Asian summer monsoon. The location of the monsoon movement and the pattern of changes in monsoon velocity and intensity affect the change in surface temperature. At the same time, summer precipitation~~ largest positive trend in the ~~northwestern region has increased in recent~~

~~years, which may have helped slow the rapid warming in the region (He et al., 2016).~~Qinghai-Tibet Plateau. In autumn, the ~~cooling~~negative trends were mainly ~~come from~~present in the Northeast Region (I) and the Northern Chinese Tianshan Mountains in the Qinghai-Tibet Plateau Region (VI). ~~The~~ In contrast, the Qinghai-Tibet Plateau was still controlled by ~~the~~ strong ~~warming~~positive trends (near Lhasa city, slope=0.09, R=0.60, $P~~<~~ < 0.05$), especially in the southern part of the Tanggula Mountains.

In winter, 69.4 % of the areas experienced warming, which is significantly higher than in other seasons; thus, winter is the most important source of interannual increases in the average LST. The most remarkable positive trends in winter were observed in the Northwest Region (V) and the Qinghai-Tibet Plateau Region (VI
).
).
).
).
).
).
).
).
).
).
).

Insert Figure 9 here

Figure 9: The interseasonal variability rates (slope) and correlation coefficients (R) of LST in spring (a), summer (b), autumn (c) and winter (d) from 2003 to 2017: a1, b1, c1 and d1 are the spatial distributions of the slopes in the four seasons; a2, b2, c2 and d2 are histograms of the slopes in the four seasons; and a3, b3, c3 and d3 are the spatial distributions of the correlation coefficients (R) in the four seasons.

5 Verification and discussion

~~We further analyze the interannual variation in the LST for each month in the time series. As shown in Fig. 10, in the past 15 years, the monthly average change in the LST was more significant than the seasonal and annual changes. Eight months showed warming trends (slope>0), which is obviously more than the number of months that showed cooling trends. The warming trends in the second half of the year (mainly concentrated in July, August, October, December) were significantly higher than those in the first half of the year. The largest warming trends were observed in July (slope=0.063), and 76 % of the areas showed warming trends. Relatively significant warming ($slope_{mean}$>0.04) occurred in the Northwest Region (V), North China Region (II) and Qinghai-Tibet Plateau Region (VI). December also showed a relatively higher warming trend, accounting for~~

~~72 % of the area, and the significantly warmed areas were concentrated in the northwest and Qinghai Tibetan areas. However, no significant cooling trend (slope <0.05) occurred in the 12-month period. The widest cooling trend was found in the Northeast Region and South China. In the Northeast Region, the cooling trend was captured in February and October, while in South China, January and April contributed the most to cooling.~~

~~Insert Figure 10 here~~

~~Figure 10: The monthly variability rates from slope (a) and correlation coefficients (b) of LST from 2003 to 2017.~~

5 Verification and discussion

MODIS exhibits good performance in retrieving LST data, as has been verified by various studies (Wan et al., 2004, Wan, 2008, Wan and Li, 2011, Wan, 2014). Furthermore, to better evaluate the accuracy of the new dataset, we performed verification for different regions using independent in situ data (subset (2) in Section 3.2) that was not used during the reconstruction process. Fig. 10 shows the statistical results of the difference between the two types of data in the six natural subregions (shown in blue in the scatterplot).

According to the scatterplots of the ground station data and the reconstructed monthly MODIS LST data shown in blue in Fig. 10, we employed a correction model that uses the results of linear regression analysis between the two datasets to further improve the accuracy. The goal of the calibration model is to reduce or eliminate the combined error introduced by various variables. Therefore, the six subregions with different climatic conditions are corrected separately to obtain better calibration results for the study area. Additionally, to eliminate contrasts at the boundaries among the six regions, smooth constraints are imposed on some edge pixels with significant differences to guarantee consistency among the regions. The comparisons of the corrected LST data with the ground station data are indicated by the gray points in Fig. 10. In this study, the main reason for adopting the regression analysis model is the reality that a linear model can further improve the robust reconstruction results have been obtained through a large amount of work. The results show that the model reconstruction results are highly consistent with the ground station data; thus, the problem of underestimation of MODIS LST data in some areas has been resolved.

In this study, three statistical accuracy measures are used to evaluate the accuracy of the calibration: the square root of the Pearson coefficient (R^2), root mean squared error (RMSE) and mean absolute error (MAE). All subregions showed good agreements between MODIS LST and meteorological station data. The R^2 values varied from 0.93 to 0.99, with an average of 0.97. The MAE varied from 1.23 °C to 1.37 °C, with an average of 1.30 °C. The RMSE ranged from 1.24 °C to 1.58 °C, with an average of 1.39 °C. A relatively large RMSE between the reconstructed LST and ground-based LST appeared in some sites in the Qinghai-Tibet Plateau Region, indicating that the temperature exhibited great spatial heterogeneity over the complex terrain. ~~The MAE varied from 1.23 °C to 1.37 °C, with an average of 1.30 °C.~~ As shown in Fig. 1, there are relatively few meteorological stations in western China. Under the same conditions, the accuracy in western China is lower than that in areas with dense weather stations when using surface meteorological stations to reconstruct LST values under cloudy conditions.

Figures 3 and 4 indicate that there are more clouds in eastern China than in western China. In this case, the number of days in which LST values can be obtained from the remote sensing images in a month is much smaller in eastern China than in western China. In this study, the accuracy evaluation is based on the monthly scale. The accuracy is mainly determined by the number of days of effective pixels on the monthly and annual scales, and our analysis indicates that the more days of available pixels corresponding to the pixels on the monthly scale, the higher the accuracy.

These results indicate that the reconstructed MODIS LST dataset is robust and accurate due to its high consistency with the in situ data. Therefore, we believe that the accuracy of LST data can be improved by this method.

Insert Figure 10 here

Figure 10: The scatter diagrams in six natural subregions (I, II, III, IV, V, and VI) between the ground station data and the monthly MODIS LST data. The blue points represent the verification results of the reconstructed MODIS LST, and the statistical accuracy measures (R^2, RMSE, and MAE) are also indicated. The results of the corrected linear model are indicated in gray.

To further understand the credibility of the data and clarify the limitations of the use of this method, we further assess the performance in terms of the seasonal bias and compare it with the original seasonal LST data. Verification ground stations in representative areas are selected to help illustrate the distribution of the error in the reconstructed data. Six key zones are identified, corresponding to the areas a, b, c, d, e, and f shown by the red circles in Fig. 1, and an overview of the ground stations can be found in Table 1. The six key zones are selected, including the three most significant regions for warming (b, d, and f), the two most significant regions for cooling (a and c), and the zone located in Xinjiang Province (see Fig. 6a for details). Zone (a) located in the Northeast Region and zone (b) located in the North China Region experienced the strongest negative trend and significant warming, respectively.
In particular, special attention has been given to the area around the Taklimakan Desert (e) in Xinjiang, which has complex
In particular, special attention has been given to the area around the Taklimakan Desert (e) in Xinjiang, which has complex
In particular, special attention has been given to the area around the Taklimakan Desert (e) in Xinjiang, which has complex
In particular, special attention has been given to the area around the Taklimakan Desert (e) in Xinjiang, which has complex terrain and extensive heterogeneity.

Seasonal~~-~~-scale verification was ~~evaluated~~performed using the RMSEs between the MODIS data (including the original LST and reconstructed LST data) and ground-based ~~LST RMSE~~LSTs for comparison in the six key zones, as shown in Table 2. The original MODIS monthly LST data were used directly without filtering quality flags. For the original MODIS LST images, we averaged the LST data of the month corresponding to the season, and obtained the seasonal LST images. The pixels with missing LST values in original MODIS LST images for the corresponding months of the season were not used in the verification process. Therefore, if there is no missing value for the LST pixel corresponding to the site, each station can have a maximum of 15 values in each season. Compared with that of the original LST, the average RMSE of the reconstructed LST data decreased by 18 % from 1.79 °C to 1.46 °C. Both datasets exhibited the largest RMSE in summer and the smallest in autumn, indicating that the original and reconstructed LST data have highly consistent seasonal patterns. For the reconstructed

LST data, we further found that the RMSE values at some sites in the summer were significantly higher than those at other sites. The regions that exhibited high RMSE values were mainly concentrated in the western regions (Xinjiang, Inner Mongolia and the Qinghai-Tibet Plateau), while the values in the other three regions were relatively ~~small~~low. The main reason for this difference may be the complex and diverse terrain and large climate differences in the western region. The average RMSE in autumn was the ~~smallest~~lowest at 1.07 °C. The winter RMSE ranged from 0.04 to 3.81, with an average of 1.45 °C.

For the reconstructed LST data, the distribution of the RMSE varied greatly between the eastern and western regions at the seasonal scale. The maximum RMSE values for all stations in the eastern typical zones (i.e., key zone a in the Northeast Region (I) and key zone b in the North China Region (II)) occurred in the cold winter, while the highest values for most sites in the western region occurred during the hot summer months (i.e., the remaining four zones). At the same time, the comparison results show that the mean RMSE between the ground-based observation data and the LST data was significantly higher in the western region than in the eastern region (mean 1.04 °C in eastern regions I and II and 1.69 °C in western regions IV, V, and VI). The large spatial variations in temperature caused by the complex terrain in the western region may be the cause of these large errors. At the same time, a large RMSE between the reconstructed LST data and the ground-based LST data appeared in some locations in Inner Mongolia (i.e., key zone e) in the Northwest Region, further indicating that the temperature over complex terrain exhibited great spatial heterogeneity.

We also note that the selected ground stations shown in Table 2 located in six key zones are examples of where the local LST warming/cooling rate changed by more than the average rate, and these areas actually include areas with greater terrain complexity. Moreover, the examples indicate that the reconstruction model proposed here is effective even in the areas of complex topography.

Table 2. RMSEs of seasonal LST between monthly LST data (including the original LST data and reconstructed LST data)

Table 2. RMSEs of seasonal LST between monthly LST data (including the original LST data and reconstructed LST data)
Table 2. RMSEs of seasonal LST between monthly LST data (including the original LST data and reconstructed LST data)
Table 2. RMSEs of seasonal LST between monthly LST data (including the original LST data and reconstructed LST data)
Table 2. RMSEs of seasonal LST between monthly LST data (including the original LST data and reconstructed LST data)
Table 2. RMSEs of seasonal LST between monthly LST data (including the original LST data and reconstructed LST data)
Table 2. RMSEs of seasonal LST between monthly LST data (including the original LST data and reconstructed LST data)
Table 2. RMSEs of seasonal LST between monthly LST data (including the original LST data and reconstructed LST data)
Table 2. RMSEs of seasonal LST between monthly LST data (including the original LST data and reconstructed LST data)
Table 2. RMSEs of seasonal LST between monthly LST data (including the original LST data and reconstructed LST data)
Table 2. RMSEs of seasonal LST between monthly LST data (including the original LST data and reconstructed LST data)

Table 2. RMSEs of seasonal LST between monthly LST data (including the original LST data and reconstructed LST data) and ground-based LST data (Orig. indicates original LST values at the ground stations. Recon. indicates the reconstructed LST values at the ground stations)

Insert Table 2 here

The verification results show that the dataset has reasonable consistency with the in situ measurements, indicating that the interference of cloud coverage is well eliminated. The dataset obtained after reconstruction is a large-scale, long-term, unique surface temperature dataset because it eliminates low-quality pixels caused by factors such as cloud disturbance and achieves complete coverage of the entire study region. The accuracy and spatiotemporal continuity of this dataset are much better than those of the original MODIS monthly data. Moreover, in this dataset, the true ground surface temperatures under cloud coverage are retrieved instead of reconstructing the LST under clear-sky conditions, which is better than the methods used in many previous studies.

Furthermore, the reconstruction strategy, which combines monthly data with daily data, effectively solves the problem of reconstructing real LST data under cloud coverage with very limited information and improves the accuracy of the monthly data reconstruction results. The final linear correction model improves the consistency of the LST data with terrestrial data. We believe that these datasets can be applied to research regional agricultural ecological environments and to monitor agrometeorological disasters. In a small range of practical applications, such as urban heat island monitoring, our current data may not be suitable for monitoring in great detail due to the coarse resolution, which is something we need to improve in future work.

6 Data availability

The LST dataset in China is distributed under a Creative Commons Attribution 4.0 License. The data are freely available from the Zenodo repository https://doi.org/10.5281/zenodo.3528024 (Zhao et al., 2019).

7 Summary and conclusions

Based on the Terra and Aqua MODIS land surface temperature dataset and meteorological station data, a new LST dataset over China was established for the period from 2003-2017. This dataset effectively removed approximately 20 % of the missing pixels or ~~poor~~low-quality LST pixels ~~contaminated~~low-quality by clouds in the original MODIS monthly image. A detailed comparison and analysis with the in situ measurements shows that the reconstruction results ~~has~~have high precision, the average RMSE is 1.39 °C, the MAE is 1.30 °C and the R^2 is 0.97. The data are freely available at ~~https://doi.org/10.5281/zenodo.3378912~~https://doi.org/10.5281/zenodo.3528024 (Zhao et al., 2019). We believe that this dataset will be of great use in research related to temperature, such as high temperature and drought studies, because it effectively overcomes the limitations of reconstructing the real LST under cloudy conditions in the past and achieves good spatiotemporal coverage.

The constructed high-precision monthly LST dataset for China provides a detailed perspective of the patterns of the spatial and temporal changes in LST. The LST dataset was used to analyze the regional characteristics and capture the variations in LST at the annual, seasonal and monthly scales. Our results showed that the LST showed a slight upward trend with a slope of 0.026 (approximately 63.7 % and 20.80 % of the pixels underwent warming and significant warming, respectively). There were great regional differences in the climate positive trend. The Northwest Region, the Qinghai-Tibet Plateau Region and the North China Plain experienced significant positive trends (i.e., the slope ranged from 0.025 to greater than 0.1). The impacts of human activities on warming, such as the increase in greenhouse gases and black carbon aerosol emissions from urbanization and industrial and agricultural development, are prominent. Greenhouse gases absorb infrared longwave radiation from the ground, which results in an increase in warming. Moreover, the coupling of greenhouse gases and monsoon systems can result in changes in the energy budget in the monsoon region, which affect the intensity of monsoon circulation. Additionally, the change in temperature in the short term may be caused by the increase in aerosols such as scattering aerosols and black carbon emitted along with other atmospheric pollutants. Black carbon aerosol pollution leads to heating of the air and a reduction of the cooling effect of solar radiation reaching the surface, resulting in local or even global climate changes (Kühn et al., 2014). However, scattering aerosols are expected to produce cooling effects by absorbing and scattering solar radiation. Consequently, the effect of human activities on global climate change is complex. The impact of human activities on temperature trends is expected to be especially pronounced in rapidly expanding urban areas, such as North China and the Yangtze River Delta
.

Meanwhile, a ~~cooling~~negative trend was also observed in China: most areas of the Northeast Region and South China Region became ~~markedly~~ colder, especially in the Songnen Plains in the middle of the region (i.e., slope=-0.11, R=0.61, P~~<~~ < 0.05). Some areas in South China also showed a slight ~~cooling~~negative trend~~.~~ (P < 0.05). The interannual temperature changes indicated that the daytime temperature changed more intensely than the nighttime temperature, which may be closely related to changes in solar radiation and the release of large amounts of greenhouse gases from human activities. Seasonal changes are primarily driven by Earth's rotation ~~is the factor that determines seasonal change, which is~~but are also affected by monsoon changes, ocean currents and other factors. The LST trends showed significant changes ~~in~~among the different seasons. The ~~warming~~positive trend in winter was ~~the most~~more significant ~~compared with~~than that in the other three seasons, especially in the northwestern region of the arid and semiarid zone and the Qinghai-Tibet Plateau. As a key parameter for different research fields, such as simulating land surface energy and water balance systems, LST provides important information for monitoring and understanding high~~–~~-temperature and drought conditions, which must be taken into consideration for agricultural production and meteorological research. Therefore, we believe that the LST dataset produced in this study can be useful for drought research and monitoring and can be further used for agricultural production and climate change research.

Author contributions. KM and YC designed the research and developed the methodology; BZ and XM supervised the downloading and processing of satellite images; BZ wrote the manuscript; and JS, ZL, ZQ and all other authors revised the manuscript.

Competing interests. The authors declare no conflicts of interest.

Acknowledgments. This research was funded by the National Key R&D Program Key Project (Meteorological Disaster Risk Maps and Integrated Systems for China and Typical Regions/Watersheds (2019YFC1510203), the Second Tibetan Plateau Scientific Expedition and Research Program (STEP) (Grant No. 2019QZKK0206)), Fundamental Research Funds for Central Non-profit Scientific Institution (Grant No. 1610132020014), and Open Fund of State Key Laboratory of Remote Sensing Science (Grant No. OFSLRSS201910). The authors would also like to thank the National Aeronautics and Space Administration (NASA) for their support by providing the LST product and elevation data. We also thank the China Meteorological Administration for providing the meteorological LST data.

References

References

References

References

References

References

References

References

References

André, C., Ottlé, C., Royer, A., and Maignan, F.: Land surface temperature retrieval over circumpolar arctic using ssm/i–ssmis and modis data. Remote Sens. Environ., 162, 1–10, https://doi.org/10.1016/j.rse.2015.01.028, 2015.

Benali, A., Carvalho, A. C., Nunes, J. P., Carvalhais, N., and Santos, A.: Estimating air surface temperature in Portugal using

Benali, A., Carvalho, A. C., Nunes, J. P., Carvalhais, N., and Santos, A.: Estimating air surface temperature in Portugal

Benali, A., Carvalho, A. C., Nunes, J. P., Carvalhais, N., and Santos, A.: Estimating air surface temperature in Portugal using MODIS LST data. Remote Sens. Environ., 124, 108-121, https://doi.org/10.1016/j.rse.2012.04.024, 2012.

Crosson, W. L., Al-Hamdan, M. Z., Hemmings, S. N. J., and Wade, G. M.: A daily merged MODIS Aqua–Terra land surface temperature dataset for the conterminous United States. Remote Sens. Environ., 119, 315–324, https://doi.org/10.1016/j.rse.2011.12.019, 2012.

Deng, M. J.: "Three Water Lines" strategy: Its spatial patterns and effects on water resources allocation in northwest China. J Geogr., 73, 1189-1203, https://doi.org/10.11821/dlxb201807001, 2018 (in Chinese).

Duan, A. and Xiao, Z.: Does the climate warming hiatus exist over the Tibetan Plateau? Sci Rep., 5, 13711,
Duan, A. and Xiao, Z.: Does the climate warming hiatus exist over the Tibetan Plateau? Sci Rep., 5, 13711,
Duan, A. and Xiao, Z.: Does the climate warming hiatus exist over the Tibetan Plateau? Sci Rep., 5, 13711,
Duan, A. and Xiao, Z.: Does the climate warming hiatus exist over the Tibetan Plateau? Sci Rep., 5, 13711, https://doi.org/10.1038/srep13711, 2015.

Fan, X., Liu, H., Liu, G., and Li, S.: Reconstruction of modis land-surface temperature in a flat terrain and fragmented landscape. Int. J. Remote Sens., 35, 7857–7877, https://doi.org/10.1080/01431161.2014.978036, 2014.

Gafurov, A. and Bárdossy, A.: Cloud removal methodology from MODIS snow cover product, Hydrol. Earth Syst. Sci. Data., 13, 1361–1373, https://doi.org/10.5194/hess-13-1361-2009, 2009.

Gao, L., Wei, J., Wang, L., Bernhardt, M., and Schulz, K.: A high-resolution air temperature dataset for the Chinese Tian Shan in 1979–2016. Earth Syst. Sci. Data., 10, 2097-2114, https://doi.org/10.5194/essd-10-2097-2018, 2018.

Hansen, J., Ruedy, R., Sato, M., and Lo, K.: Global surface temperature change. Rev Geophys., 48, RG4004, https://doi.org/10.1029/2010RG000345, 2010.

Jin, M. and Liang, S. L.: An improving land surface emissively parameter of land surface models using global Remote Sens
Jin, M. and Liang, S. L.: An improving land surface emissively parameter of land surface models using global Remote Sens
Jin, M. and Liang, S. L.: An improving land surface emissively parameter of land surface models using global Remote Sens
~~Hu, Z. Z.: Long-term climate variations in China and global warming signals. J Geophys Res., 108, 4614, https://doi.org/10.1029/2003JD003651, 2003.~~

Jin, M. and Liang, S. L.: An improving land surface emissively parameter of land surface models using global Remote Sens observations J. Clim., 19, 2867–81, https://doi.org/10.1175/jcli3720.1, 2006.

Jin, M. L. and Dickinson, R. E.: Land surface skin temperature climatology: benefitting from the strengths of satellite observations. Environ. Res. Lett., 5, 044004, https://doi.org/10.1088/1748-9326/5/4/044004, 2010.

Ke, L., Ding, X., and Song, C.: Reconstruction of Time-Series MODIS LST in Central Qinghai-Tibet Plateau Using Geostatistical Approach. IEEE Geosci. Remote Sens Lett., 10, 1602-1606, https://doi.org/10.1109/LGRS.2013.2263553, 2013.

Li, B., Chen, Y., and Shi, X.: Why does the temperature rise faster in the arid region of northwest China? J Geophys Res-Atmos., 117, 1-7, https://doi.org/10.1029/2012JD017953, 2012.

Li, Q., Yang, S., Xu, W., Wang, X. L., Jones, P., Parker, D., Zhou, L. M., Feng, Y., and Gao, Y.: China experiencing the recent warming hiatus. Geophys Res Lett., 42, 889-898, https://doi.org/ 10.1002/2014GL062773, 2015.

Liu, H., Li, X., Fischer, G., and Sun, L.: Study on the Impacts of Climate Change on China's Agriculture. Climatic Change., 65, 125-148, https://doi.org/125–148,10.1023/B:CLIM.0000037490.17099.97, 2004.

Li, Z. L., Wu, H., Wang, N., Qiu, S., Sobrino, J.A., Wan, Z., Tang, B. H., and Yan, G.: Land surface emissivity retrieval from satellite data. Int. J. Remote Sens., 34, 3084–3127, https://doi.org/10.1080/01431161.2012.716540,2013.

Ma, X. L., Wan, Z. M., Moeller, C. C., Menzel, W. P., Gumley, L. E., and Zhang, Y.: Retrieval of geophysical parameters from Moderate Resolution Imaging Spectroradiometer thermal infrared data: evaluation of a twostep physical algorithm. Applied Optics., 39, 3537 – 3550, https://doi.org/10.1364/AO.39.003537, 2000.

Ma, X. L., Wan, Z. M., Moeller, C. C., Menzel, W. P., and Gumley, L. E.: Simultaneous retrieval of atmospheric profiles and land-surface temperature, and surface emissivity from Moderate Resolution Imaging Spectroradiometer thermal infrared data: extension of a two-step physical algorithm. Applied Optics., 41, 909 – 924, https://doi.org/10.1364/AO.41.000909,2002.

Mao, K. B., Shi, J. C., Li, Z. L., Qin, Z. H., Li, M. C., and Xu, B.: A physics-based statistical algorithm for retrieving land surface temperature from AMSR-E passive microwave data,Sci China Ser D-Earth Sci., 50, 1115-1120, https://doi.org/ 10.1007/s11430-007-2053-x, 2007.

Mao, K. B., Zuo, Z.Y., Shen, X. Y., Xu, T. R., Gao, C.Y., and Liu,G.: Retrieval of Land-surface Temperature from AMSR2 Data Using a Deep Dynamic Learning Neural Network, Chinese Geogr Sci., 28, 1-11, https://doi.org/1–11,10.1007/s11769-018-0930-1, 2018.

Mao, K. B., Yuan, Z.J., Zuo, Z.Y., Xu, T. R., Shen, X. Y., and Gao, C.Y.: Changes in Global Cloud Cover Based on Remote Sens Data from 2003 to 2012, Chinese Geogr Sci., 29, 306–315, https://doi.org/CNKI:SUN:ZDKX.0.2019-02-011, 2019.

Markus, M., Duccio, R and Markus, N.: Surface Temperatures at the Continental Scale: Tracking Changes with Remote Sensing at Unprecedented Detail. Remote Sens., 2, 333-351, https://doi.org/10.3390/rs6053822,2010.

McMillin, L. M.: Estimation of sea surface temperature from two infrared pixel window measurements with different absorptions. J. Geophys. Res., 80, 5113–5117, 1975.

Na, F., Gaodi, X., Wenhua, L., Yajing, Z., Changshun, Z., and Na, L.: Mapping air temperature in the lancang river basin using the reconstructed modis LST data. J. Res. Ecol., 5, 253–262, https://doi.org/10.5814/j.issn.1674-764x.2014.03.008, 2014.

Neteler, M.: Estimating daily land surface temperatures in mountainous environments by reconstructed MODIS LST data, Remote Sens., 2, 333–351,https://doi.org/10.3390/rs1020333, 2010.

Oku, Y., H. Ishikawa, S. Haginoya., and Y. Ma. : Recent trends in land surface temperature on the Tibetan Plateau, J. Clim., 15, 2995– 3003,https://doi.org/10.1175/JCLI3811.1, 2006.

Prigent, C., Jimenez, C., and Aires, F.: Toward “all weather” long record, and real-time land surface temperature retrievals from microwave satellite observations. J. Geophys. Res. Atmos., 121, 5699–5717. 24, 2016.

Scharlemann, J.P., Benz, D., Hay, S.I., Purse, B.V., Tatem, A.J., Wint, G.R., and Rogers, D.J.: Global data for ecology and epidemiology: A novel algorithm for temporal Fourier processing MODIS data. PLoS One., 3: e1408-10.1371, https://doi.org/10.1371/journal.pone.0001408, 2008.

Shi, Y.F., Shen, Y.P., Kang, E., Li, D.L., Ding, Y.J., Zhang, G.W., and Hu, R.J.: Recent and future climate change in northwest

Shi, Y.F., Shen, Y.P., Kang, E., Li, D.L., Ding, Y.J., Zhang, G.W., and Hu, R.J.: Recent and future climate change in

Shi, Y.F., Shen, Y.P., Kang, E., Li, D.L., Ding, Y.J., Zhang, G.W., and Hu, R.J.: Recent and future climate change in northwest China. Climatic Change, 80, 379–393. https://doi.org/10.1007/s10584-006-9121-7, 2007.

Stocker, T.F., Qin, D., Plattner, G.-K., Tignor, M., Allen, S.K., Boschung, J., Nauels, A., Xia, Y., Bex, V, and Midgley, P.M. (Eds.): IPCC, 2013: Climate Change 2013: The Physical Science Basis. Contribution of Working Group I to the Fifth Assessment Report of the Intergovernmental Panel on Climate Change. Cambridge University Press, Cambridge, United Kingdom and New York, NY, USA, 2013.

Sun, L., Chen, Z., Gao, F., Anderson, M., Song, L., Wang, L., Hu, B., and Yang, Y.: Reconstructing daily clear-sky land surface temperature for cloudy regions from modis data. Comput. Geosci., 105, 10–20, https://doi.org/10.1016/j.cageo.2017.04.007, 2017.

Sun, X., Ren, G., Ren, Y., Fang, Y., Liu, Y., Xue, X., and Zhang, P.: A remarkable climate warming hiatus over Northeast China since 1998. Theor Appl Climatol., 133, 579–594. https://doi.org/10.1007/s00704-017-2205-7, 2017.

Sun, Z., Wang, Q., Batkhishig, O., and Ouyang, Z.: Relationship between evapotranspiration and land surface temperature under energy-and water-limited conditions in dry and cold climates. Adv. Meteorol., 1-9, 1835487, https://doi.org/10.1155/2016/1835487, 2016.

Tatem, A.J., Goetz, S.J., and Hay, S.I.: Terra and Aqua: new data for epidemiology and public health. Int. J. Appl. Earth Obs. Geoinf., 6, 33-46, https://doi.org/10.1016/j.jag.2004.07.001, 2004.

Vancutsem, C., Ceccato, P., Dinku, T., and Connor, S. J.: Evaluation of MODIS land surface temperature data to estimate air temperature in different ecosystems over Africa. Remote Sens. Environ., 114, 449–465, https://doi.org/10.1016/j.rse.2009.10.002, 2010.

Wan, Z. M.: Collection-5 MODIS Land Surface Temperature Products Users' Guide [EB/OL], 2007.

Wan, Z. M.: New refinements and validation of the MODIS landsurface temperature/emissivity products. Remote Sens. Environ., 112, 59–74 https://doi.org/ 10.1016/j.rse.2006.06.026, 2008.

Wan, Z. M.: New refinements and validation of the collection-6 MODIS land-surface temperature/emissivity product. Remote Sens. Environ., 140, 36–45, https://doi.org/10.1016/j.rse.2013.08.027,2014.

Wan, Z. M. and Dozier, J.: A generalized split-window algorithm for retrieving land-surface temperature from space. IEEE T Geosci Remote., 34, 892–905, https://doi.org/ 10.1109/36.508406, 1996.

Wan, Z. M. and Li, Z. L.: A physics-based algorithm for retrieving landsurface emissivity and temperature from EOS/MODIS data. IEEE T Geosci Remote., 35, 980– 996, https://doi.org/10.1109/36.602541, 1997.

Wan, Z. M. and Li, Z. L.: MODIS land surface temperature and emissivity. Remote Sens. and Digital Image Proc., 11, 563-577, https://doi.org/ 10.1007/978-1-4419-6749-7_25, 2011.

Wan, Z. M., Zhang, Y., Zhang, Q., and Li, Z. l.: Validation of the land-surface temperature products retrieved from Terra Moderate Resolution Imaging Spectroradiometer data. Remote Sens. Environ., 83, 163–180, https://doi.org/10.1016/j.rse.2009.10.002, 2002.

Wan, Z. M., Zhang Y, Zhang Q., and Li Z L.: Quality assessment and validation of the MODIS global land surface temperature. Int J Remote Sen S., 25, 261–274 https://doi.org/ 10.1080/0143116031000116417, 2004.

Wang, K. and S. Liang.: Evaluation of ASTER and MODIS land surface temperature and emissivity products using long-term surface longwave radiation observations at SURFRAD sites, Remote Sens. Environ., 113, 1556–1565, https://doi.org/10.1016/j.rse.2009.03.009, 2009.

Wang, K., Wan, Z., Wang, P., Sparrow, M., Liu, J., and Haginoya, S.: Evaluation and improvement of the MODIS land surface temperature/emissivity products using ground-based measurements at a semi-desert site on the western Tibetan Plateau, Int. J. Remote Sens., 28, 2549–2565, https://doi.org/10.1080/01431160600702665, 2007.

Xu, Y. and Shen, Y.: Reconstruction of the land surface temperature time series using harmonic analysis. Comput. Geosci., 61, 126–132, https://doi.org/10.1016/j.cageo.2013.08.009, 2013.

Xu, X., Lu, C., Shi, X., and Gao, S.: World water tower: an atmospheric perspective. Geophysical Research Letters., 35, L20815, https://doi.org/10.1029/2008GL035867, 2008.

Yang, X., Lin, E., Ma, S. M., Ju, H., Guo, L. P., Xiong., Li, Y., and Xu, Y. L.: Adaptation of agriculture to warming in Northeast China. Climatic Change., 84, 45-58, https://doi.org/10.1007/s10584-007-9265-0, 2007.

Yu, W. J., Nan, Z. T., Wang, Z. W., Chen, H., Wu, T. H., and Zhao, L.: An Effective Interpolation Method for MODIS Land Surface Temperature on the Qinghai–Tibet Plateau. IEEE J. Sel. Topics Appl. Earth Observ. Remote Sens., 8, 4539-4550, https://doi.org/10.1109/JSTARS.2015.2464094, 2015.

Zeng, C., Shen, H., and Zhang, L.: Recovering missing pixels for Landsat ETM+ SLC-off imagery using multitemporal regression analysis and a regularization method, Remote Sens. Environ., 131, 182–194, https://doi.org/10.1016/j.rse.2012.12.012, 2013.

Zhao, B., Mao, K. B., Cai, Y. L., Shi, J. C., Li, Z. L., Qin, Z. H., and Meng, X. J.: A combined Terra and Aqua MODIS land surface temperature and meteorological station data product for China from 2003–2017 [Dataset], Zenodo, https://doi.org/10.5281/zenodo.3378912, 2019.

Zhao, X., Tan, K., Zhao, S., and Fang, J.: Changing climate affects vegetation growth in the arid region of the northwestern China. J Arid Environ, 75, 946–952. https://doi.org/10.1016/j.jaridenv.2011.05.007, 2011.

Zhao, X., Tan, K., Zhao, S., and Fang, J.: Changing climate affects vegetation growth in the arid region of the northwestern China. J Arid Environ, 75, 946–952. https://doi.org/10.1016/j.jaridenv.2011.05.007, 2011.

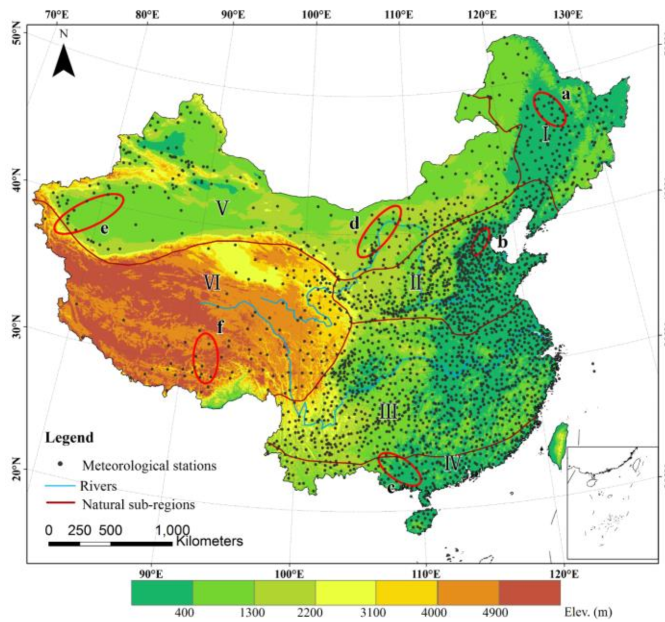

Figure 1: The study area is divided into six natural subregions (I, II, III, IV, V, and VI), and the spatial patterns of the meteorological stations in the subregions is shown. The red circles mark the key areas where the temperature has changed significantly, and meteorological station from Subset (2) located these areas are used to validate the accuracy of the new LST dataset (a, b, c, d, e, and f).

设置了格式: 字体: (默认) Times New Roman, (中文) Times New Roman, 英语(美国)

(a)

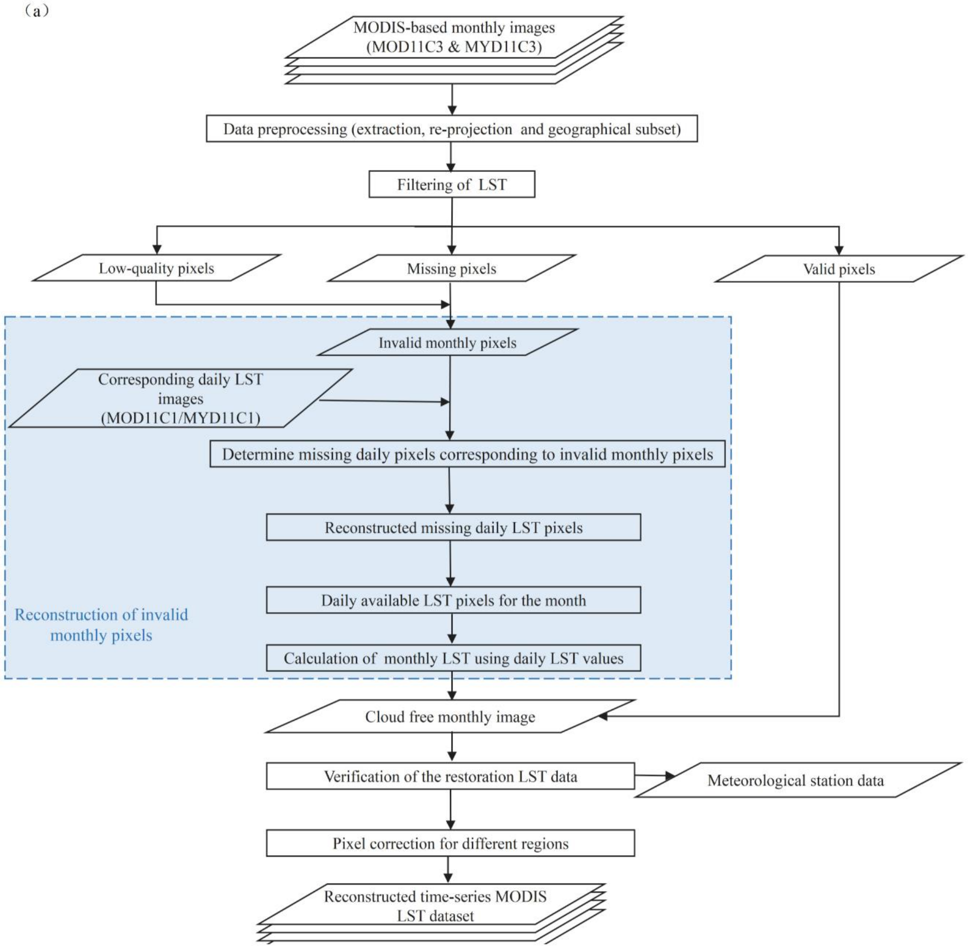

MODIS-based monthly images (MOD11C3 & MYD11C3)
Data preprocessing (extraction, re-projection and geographical subset)
Filtering of LST
Low-quality pixels
Missing pixels
Valid pixels
Invalid monthly pixels
Corresponding daily LST images (MOD11C1/MYD11C1)
Determine missing daily pixels corresponding to invalid monthly pixels
Reconstructed missing daily LST pixels
Daily available LST pixels for the month
Reconstruction of invalid monthly pixels
Calculation of monthly LST using daily LST values
Cloud free monthly image
Verification of the restoration LST data
Meteorological station data
Pixel correction for different regions
Reconstructed time-series MODIS LST dataset

960

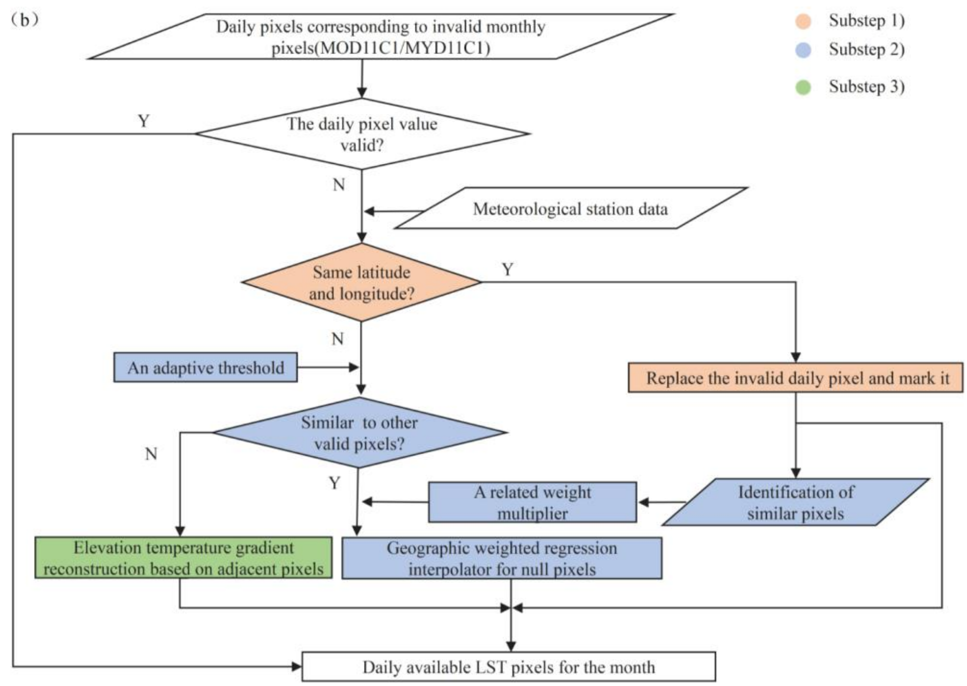

Figure 2: (a)The summary flowchart for reconstructing MODIS monthly LST data, . (b) The detailed flowchart for reconstruct missing daily pixels in (a).

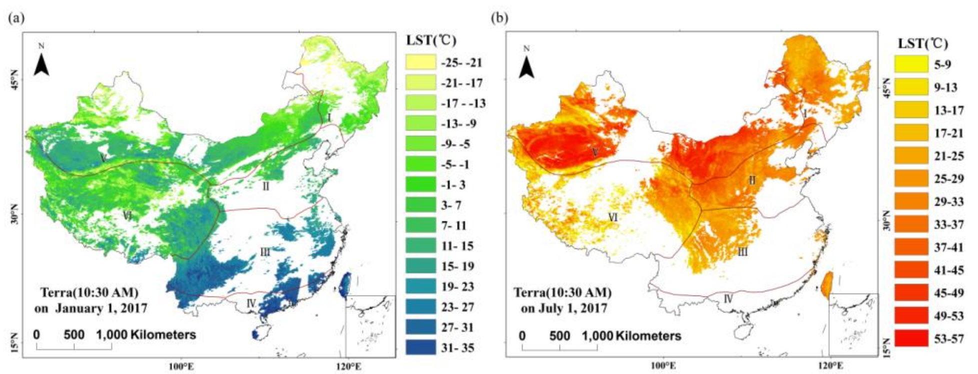

Figure 3: Spatial distribution of valid data for daily MODIS LST data from Terra during the daytime on (a) January 1, 2017, and (b) July 1, 2017. Areas of missing data are blank.

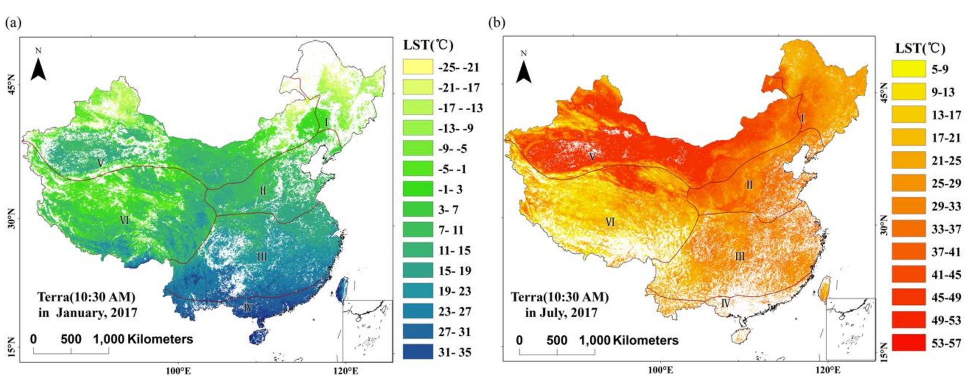

Figure 4: Spatial distribution of valid data after pixel filtering for monthly MODIS LST data from Terra during the daytime on (a) January and (b) July. Areas of invalid data are blank.

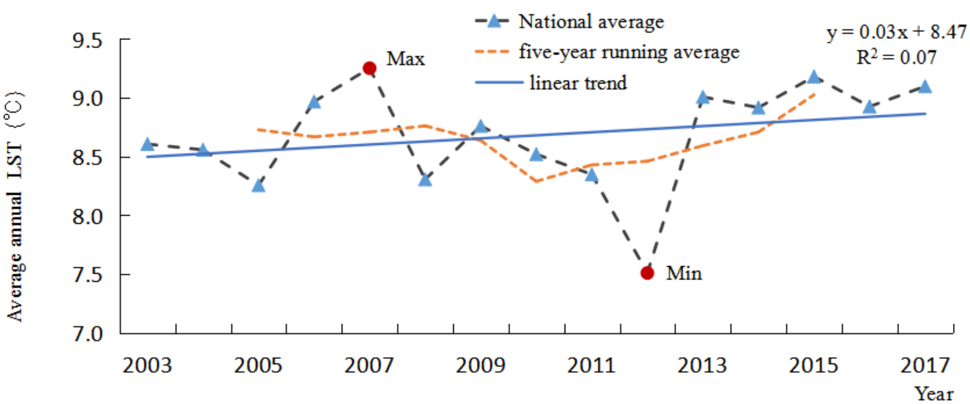

Figure 5: Time series of annual mean LST (unit: °C) for the period of 2003-2017 based on corrected MODIS LST data for China. The solid blue line indicates the linear trend. The orange dashed line shows the five-year running average trend.

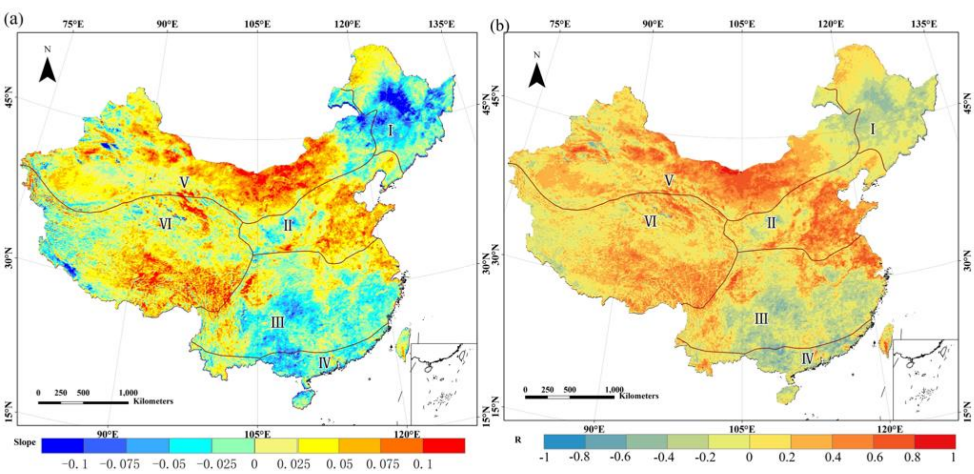

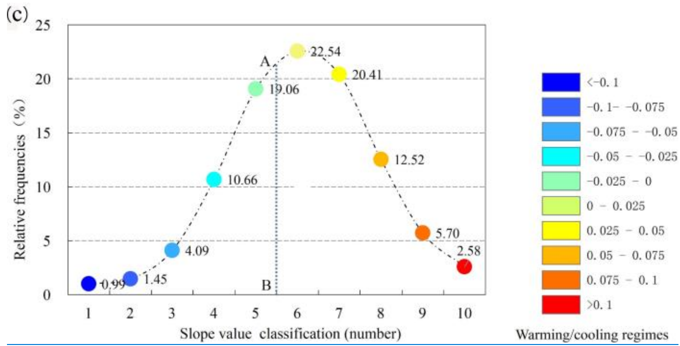

Figure 6: Spatial dynamics of interannual change trends in LST from the slope (a) computed by Eq. (8), the correlation coefficient (b) computed by Eq. (9) and frequency distribution of the slope (c) during 2003-2017. In panel c, the different temperature trends (slope) are divided into 10 subinterval ranges corresponding to the ranges in panel a. The area to the left of the line AB represents the proportion of the area that experienced cooling, and the area to the right represents the proportion that experienced warming.

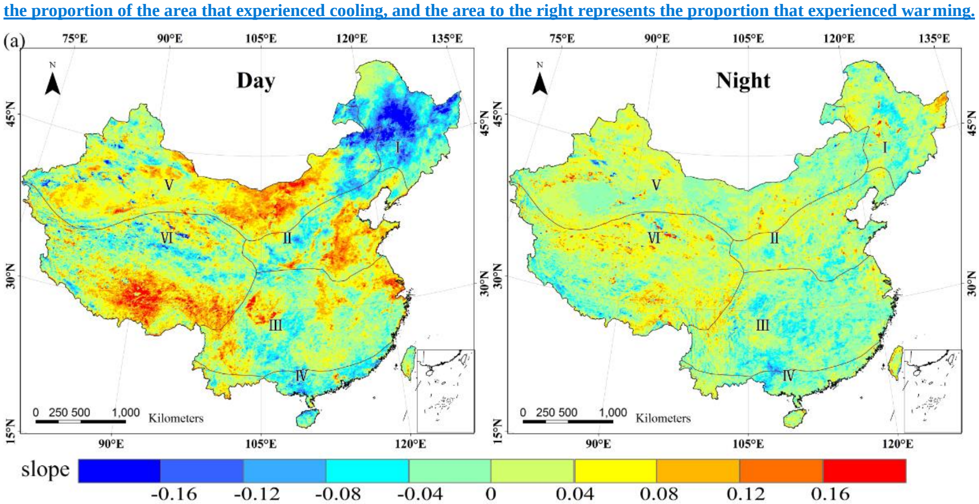

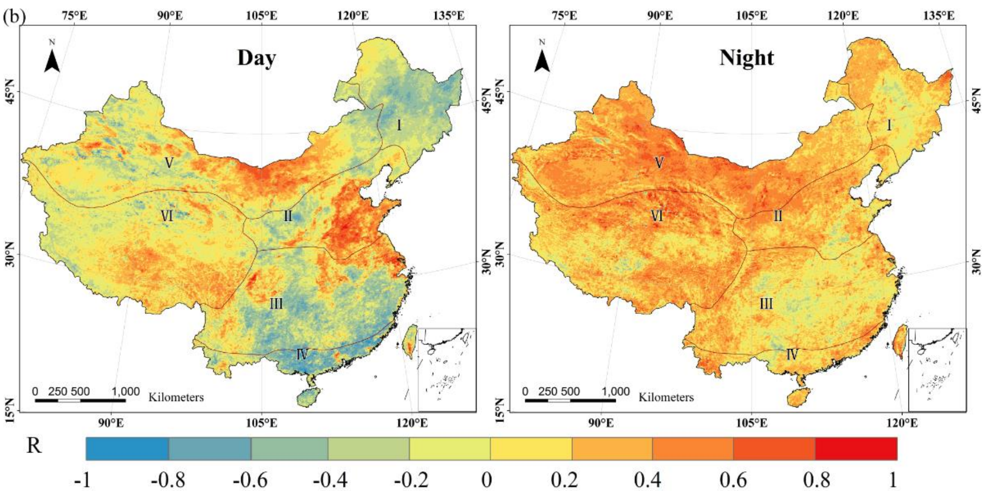

Figure 7: Spatial dynamics of (a) day and (b) night LST change trends based on slope (a) and correlation coefficient (b).

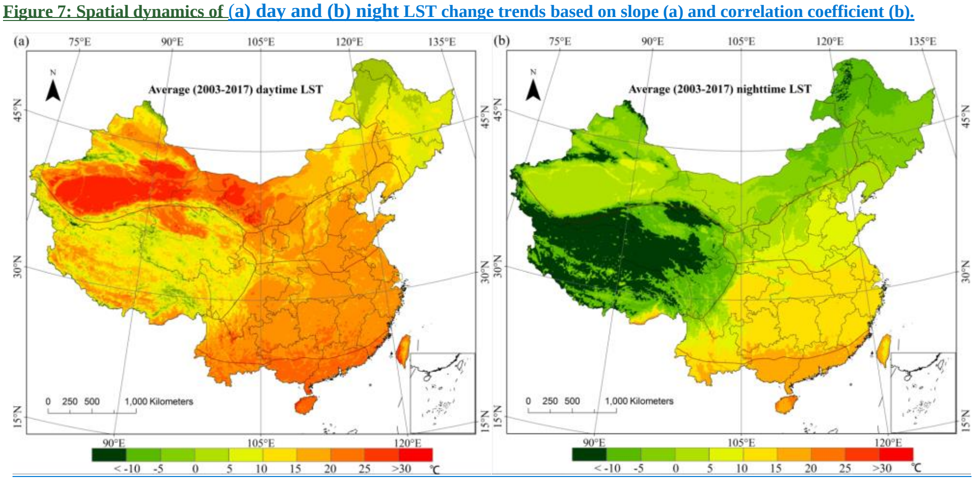

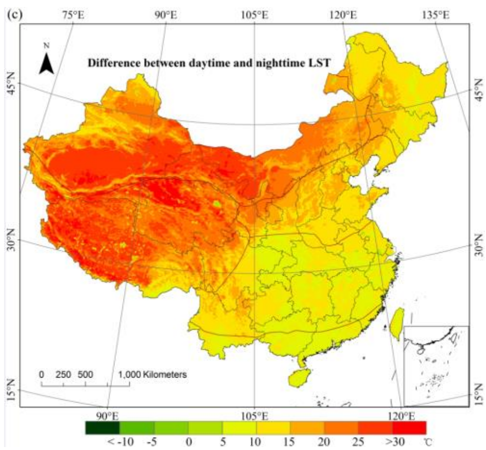

Figure 8: Spatial dynamics of average daytime LST (a) and average nighttime LST (b) from 2003 to 2017.

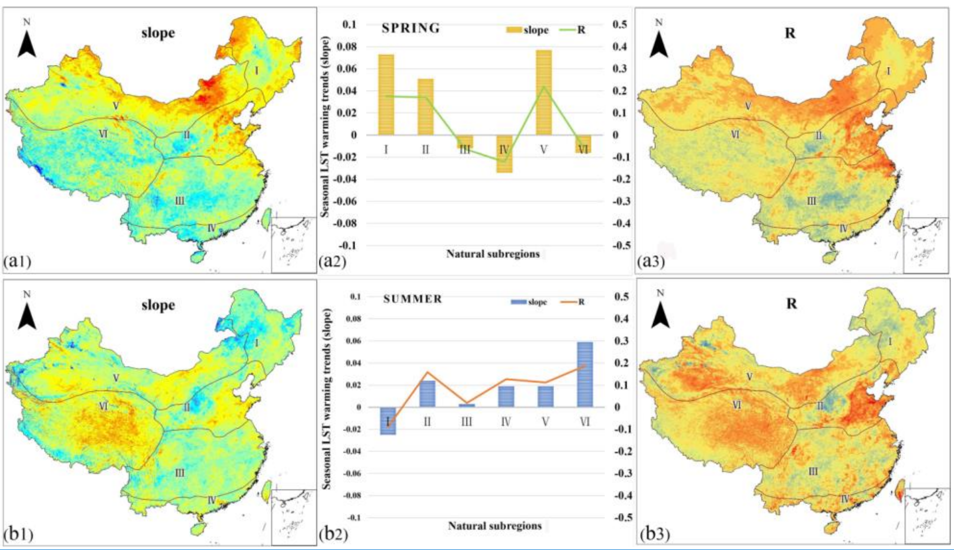

N
slope
I
V
VI
II
III
IV
(a1)
SPRING
slope
R
Seasonal LST warming trends (slope)
Natural subregions
(a2)
R
(a3)
SUMMER
(b1)
(b2)
(b3)

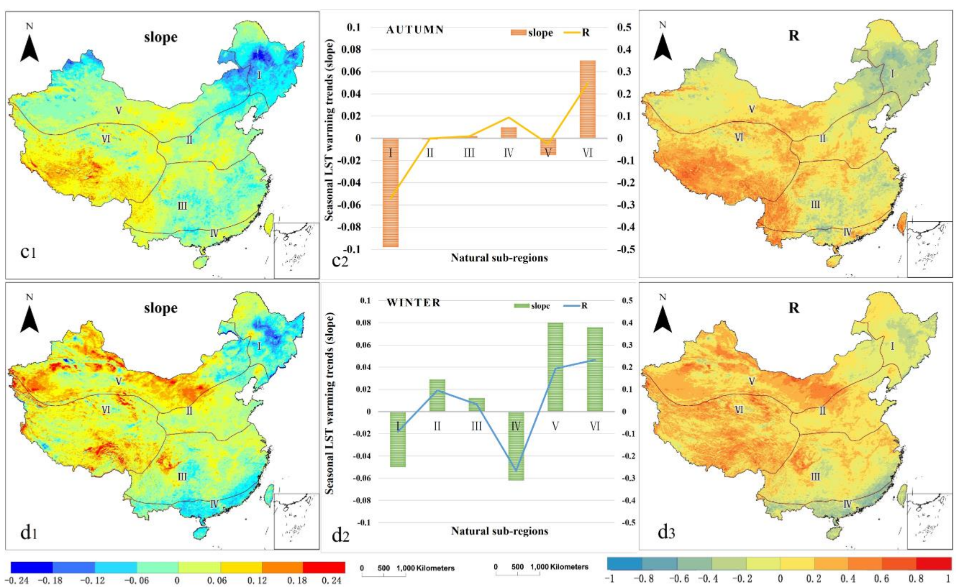

Figure 9: The interseasonal variability rates (slope) and correlation coefficients (R) of LST in spring (a), summer (b), autumn (c) and winter (d) from 2003 to 2017: a1, b1, c1 and d1 are the spatial distributions of the slopes in the four seasons; a2, b2, c2 and d2 are histograms of the slopes in the four seasons; and a3, b3, c3 and d3 are the spatial distributions of the correlation coefficients (R) in the four seasons.

995

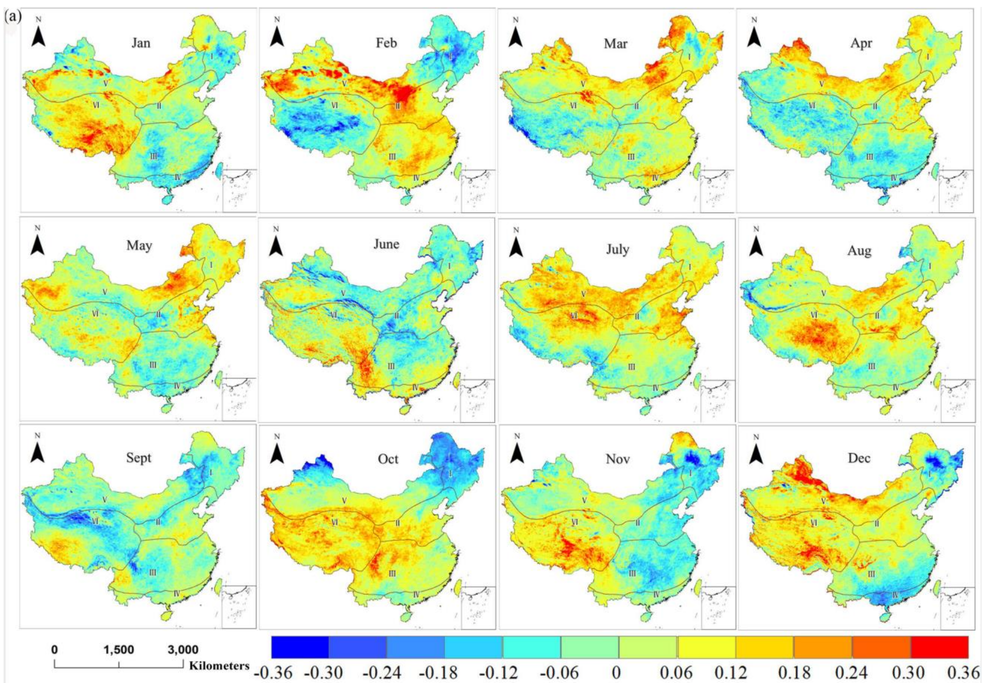

(a)
Jan
Feb
Mar
Apr
May
June
July
Aug
Sept
Oct
Nov
Dec
N
0 1,500 3,000 Kilometers
-0.36 -0.30 -0.24 -0.18 -0.12 -0.06 0 0.06 0.12 0.18 0.24 0.30 0.36

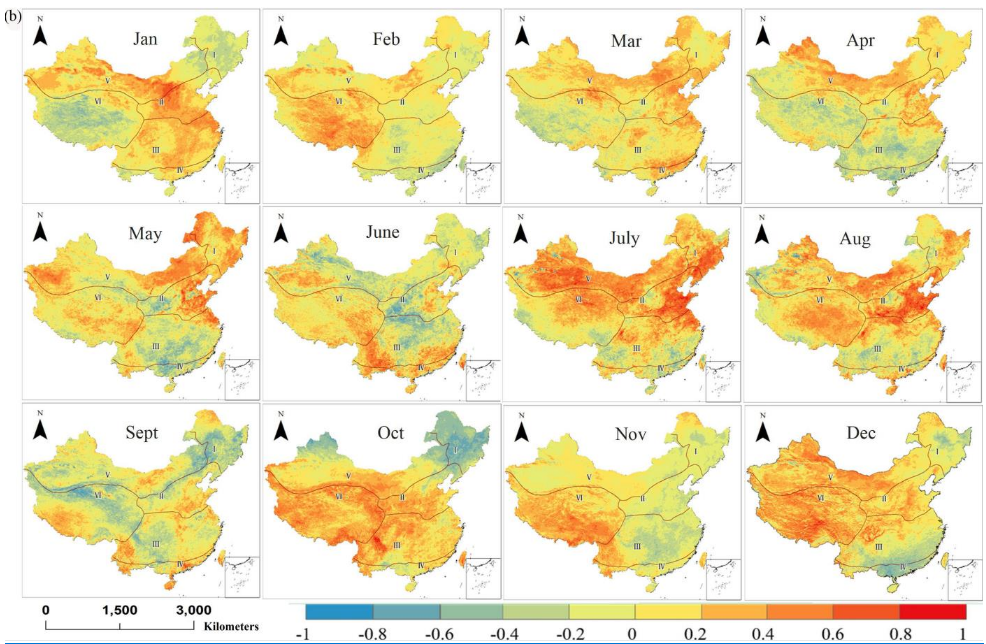

Figure 10: The monthly variability in the slope (a) and correlation coefficient (b) of LST from 2003 to 2017.

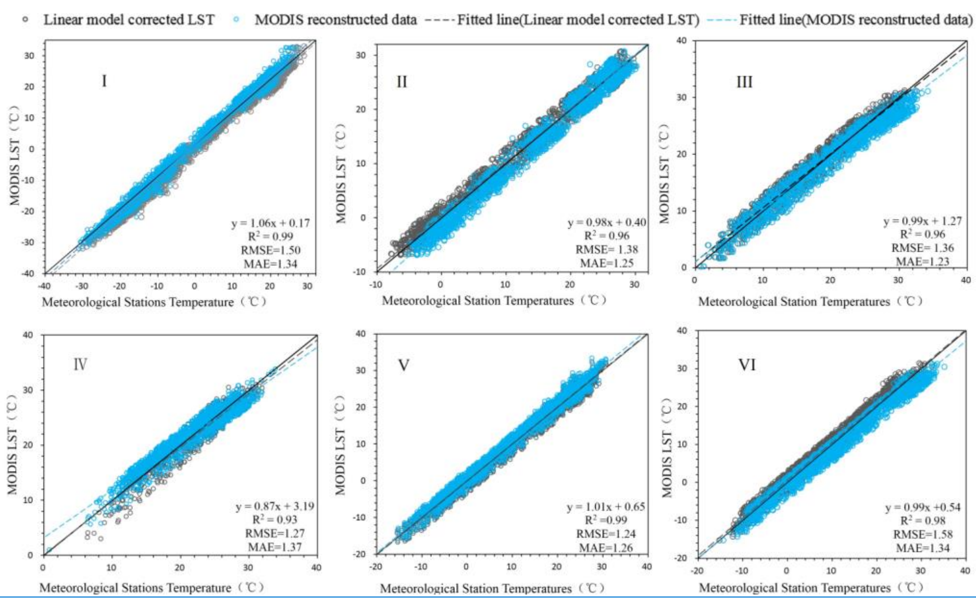

Figure 10: The scatter diagrams in six natural subregions (I, II, III, IV, V, and VI) between the ground station data and the monthly MODIS LST data. The blue points represent the verification results of the reconstructed MODIS LST, and the statistical accuracy measures (R^2, RMSE, and MAE) are also indicated. The results of the corrected linear model are indicated in gray.

Table 1 Basic information for some of the meteorological stations in key zones

Region	Key zone	ID	Latitude (°)	Longitude (°)	Elevation (m)
~~**Table 1 Basic information for some of the meteorological stations in key zones**~~					
~~Region~~	~~key zone~~	~~ID~~	~~Latitude (°)~~	~~Longitude (°)~~	~~Altitude (m)~~
I Northeast Region	a	50758	47.10	125.54	249
I Northeast Region	a	50658	48.03	125.53	237
I Northeast Region	a	50756	47.26	126.58	239
I Northeast Region	a	50656	48.17	126.31	278
I Northeast Region	a	50548	49.05	123.53	282
II North China Region	b	54525	117.28	39.73	5
II North China Region	b	54527	117.05	39.08	3
II North China Region	b	54518	116.39	39.17	8

II North China Region	b	54511	116.19	39.57	52
II North China Region	b	54624	117.21	38.22	7
II North China Region	b	54623	117.43	38.59	6
IV South China	c	59431	22.63	108.22	122
IV South China	c	59242	23.45	109.08	85
IV South China	c	59037	23.93	108.10	170
IV South China	c	59228	23.32	107.58	108
IV South China	c	59446	22.42	109.30	66
V Northwest Region	d	53336	41.40	108.48	1275
V Northwest Region	d	53446	40.34	109.50	1044
V Northwest Region	d	53602	38.52	105.34	1561
V Northwest Region	d	53513	40.48	107.30	1039
V Northwest Region	e	51730	40.33	81.19	1012
V Northwest Region	e	51716	39.48	78.34	1117
V Northwest Region	e	51810	38.56	77.40	1178
V Northwest Region	e	51811	38.26	77.16	1231
VI Qinghai-Tibet Plateau Region	f	55279	31.48	89.40	4700
VI Qinghai-Tibet Plateau Region	f	55591	29.42	91.08	3648
VI Qinghai-Tibet Plateau Region	f	55598	29.15	91.47	3560
VI Qinghai-Tibet Plateau Region	f	56106	31.53	93.48	4022

Table 2. RMSEs of seasonal LST between monthly LST data (including the original LST data and reconstructed LST data) and ground-based LST data (Orig. indicates original LST values at the ground stations. Recon. indicates the reconstructed LST values at the ground stations)

~~**Figure 2: The summary flowchart for reconstructing MODIS monthly LST data.**~~

~~**Figure 3: Spatial distribution of valid data for daily MODIS LST data from Terra at 10:30 am (a) January 1, 2017, and (b) July 1, 2017. Areas of invalid data are in white.**~~

~~**Figure 4: Spatial distribution of valid data for monthly MODIS LST data from Terra at 10:30 am in (a) January and (b) July. Areas of invalid data are in white.**~~

Table 2. RMSEs of seasonal LST between monthly LST data (including the original LST data and reconstructed LST data) and ground-based LST data (Orig. indicates original LST values at the ground stations. Recon. indicates the reconstructed LST values at the ground stations)

~~**Figure 5: Annual mean LST changes in China from 2003 to 2017.**~~

~~**Figure 6: Spatial dynamics of interannual change trends in LST from the slope (a) computed by Eq. (8), the correlation coefficient (b) computed by Eq. (9) and frequency distribution of the slope (c) during 2003-2017. In panel c, the different temperature trends**~~

[illegible]
ground-based LST data (Orig. indicates ~~the~~ original LST ~~located~~values at the ground stations. Recon. indicates the reconstructed LST ~~located~~values at the ground stations)

Table 2. RMSEs of seasonal LST between monthly LST data (including the original LST data and reconstructed LST data) and ground-based LST data (Orig. indicates original LST values at the ground stations. Recon. indicates the reconstructed LST values at the ground stations)

Table 2. RMSEs of seasonal LST between monthly LST data (including the original LST data and reconstructed LST data) and ground-based LST data (Orig. indicates original LST values at the ground stations. Recon. indicates the reconstructed LST values at the ground stations)

Table 2. RMSEs of seasonal LST between monthly LST data (including the original LST data and reconstructed LST data) and ground-based LST data (Orig. indicates original LST values at the ground stations. Recon. indicates the reconstructed LST values at the ground stations)

~~**Figure 9: The interseasonal variability rates (slope) and correlation coefficients (R) of LST in spring (a), summer (b), autumn (c) and winter (d) from 2003 to 2017, a1, b1, c1 and d1 are the spatial distributions of the slopes at the four seasons, a2, b2, c2 and d2 are histograms of the slope of the four seasons, and a3, b3, c3 and d3 are the spatial distribution of the correlation coefficient (R) at the four seasons.**~~

Table 2. RMSEs of seasonal LST between monthly LST data (including the original LST data and reconstructed LST data) and ground-based LST data (Orig. indicates original LST values at the ground stations. Recon. indicates the reconstructed LST values at the ground stations)

~~**Figure 10: The monthly variability rates from slope (a) and correlation coefficients (b) of LST from 2003 to 2017.**~~

~~**Figure 11: The scatter diagrams in six natural subregions (I, II, III, IV, V, VI) between the ground station data and the MODIS LST data. The blue scatter indicates the verification result of the reconstructed MODIS LST, and its statistical accuracy measures (R^2, RMSE, MAE) are also indicated. The result of the linear model corrected corrected is indicated in gray.**~~

Table 2. RMSEs of seasonal LST between monthly LST data (including the original LST data and reconstructed LST data) and ground-based LST data (Orig. indicates ~~the~~ original LST ~~located~~values at the ground stations. Recon. indicates the reconstructed LST ~~located~~values at the ground stations)

~~Region~~	~~key zone~~	~~ID~~	~~Spring~~		~~Summer~~		~~Autumn~~		~~Winter~~	
Region	Key zone	ID	Spring		Summer		Autumn		Winter	
			Orig.	Recon.	Orig.	Recon.	Orig.	Recon.	Orig.	Recon.
I Northeast Region	a	50758	2.11	1.48	1.36	1.23	1.16	0.61	3.80	3.81
I Northeast Region	a	50658	2.33	1.03	1.61	0.63	0.29	0.27	4.32	3.20
I Northeast Region	a	50756	3.51	0.23	1.03	0.43	0.51	0.26	3.91	3.52

I Northeast Region	a	50656	0.65	0.65	0.90	0.92	0.42	0.04	3.63	3.67
I Northeast Region	a	50548	0.82	0.89	1.09	0.61	0.51	0.40	0.15	0.15
II North China Region	b	54525	3.11	2.26	3.30	2.23	2.11	1.51	2.11	0.94
II North China Region	b	54527	1.30	1.11	1.24	1.25	0.93	0.54	2.36	0.14
II North China Region	b	54518	3.64	1.64	0.52	0.51	0.45	0.15	0.71	0.04
II North China Region	b	54511	1.06	1.26	0.33	0.32	0.50	0.66	1.07	1.27
II North China Region	b	54624	1.99	1.55	1.15	0.49	0.84	0.33	0.40	0.46
II North China Region	b	54623	0.13	0.06	0.48	0.17	1.31	1.06	2.65	2.02
IV South China	c	59431	1.71	2.73	0.12	0.06	1.05	1.02	2.91	2.91
IV South China	c	59242	2.0	1.08	2.52	1.86	0.03	0.09	2.91	2.59
IV South China	c	59037	1.08	0.73	1.26	0.94	0.78	0.78	1.00	1.01
IV South China	c	59228	0.92	0.38	1.99	1.75	1.61	0.84	0.75	0.28
IV South China	c	59446	2.01	1.30	0.97	0.78	0.49	0.49	2.40	2.39
V Northwest Region	d	53336	3.88	3.88	3.04	3.04	3.53	2.81	1.90	1.82
V Northwest Region	d	53446	2.00	2.01	3.78	3.18	1.96	1.65	0.35	0.35
V Northwest Region	d	53602	4.48	4.28	3.91	3.75	3.97	3.47	1.65	1.65
V Northwest Region	d	53513	1.55	1.48	5.33	5.15	5.01	4.93	2.04	2.24
V Northwest Region	e	51730	3.01	2.97	4.09	5.08	1.48	1.06	2.63	2.10
V Northwest Region	e	51716	0.80	0.75	0.47	0.15	0.74	0.09	0.66	0.32
V Northwest Region	e	51810	2.33	1.29	1.20	0.76	0.33	0.32	1.24	0.28
V Northwest Region	e	51811	0.57	0.57	0.52	0.90	0.62	0.36	1.34	0.39
VI Qinghai-Tibet Plateau Region	f	55279	3.63	3.44	1.37	1.74	1.83	1.45	0.99	0.99
VI Qinghai-Tibet Plateau Region	f	55591	1.76	1.79	5.56	4.08	2.99	2.59	1.95	0.41
VI Qinghai-Tibet Plateau Region	f	55598	0.85	0.85	4.37	4.62	2.95	2.91	0.63	0.69
VI Qinghai-Tibet Plateau Region	f	56106	0.52	0.58	1.44	1.44	0.88	0.68	2.11	1.99
Average			1.92	1.51	1.96	1.72	1.40	1.12	1.88	1.49

Appendix A

设置了格式: 默认段落字体, 字体: (默认) Times New Roman, (中文) 楷体, 小四, 加粗, 字体颜色: 自动设置, 英语(美国), 图案: 清除

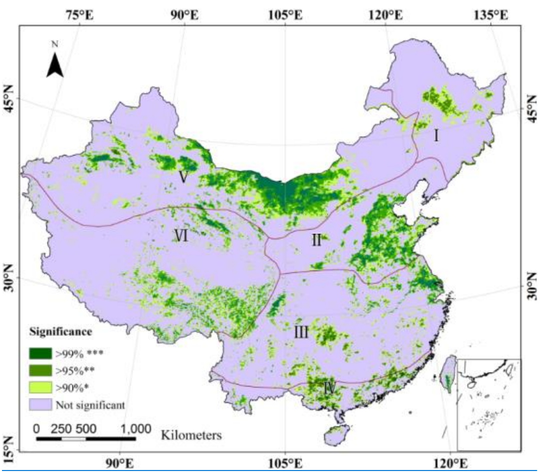

Figure A1: Significance of the spatial distribution of annual average LST trends based on an independent-samples t-test in China from 2003 to 2017. Note that the symbols *, **, and * explain that there are increasing/ decreasing tendencies averaged over China at the 99 %, 95 % and 90 % confidence level, respectively (same as below).**

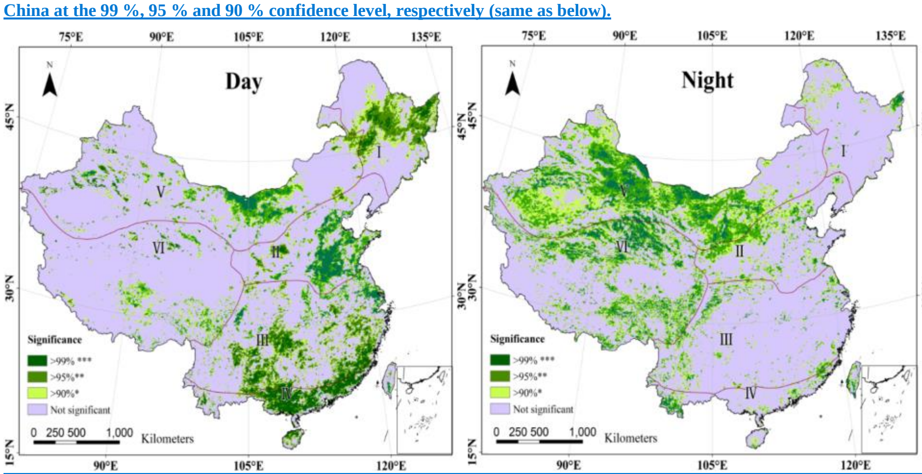

Figure A2: Distribution of diurnal LST change trends significance during 2003 - 2017

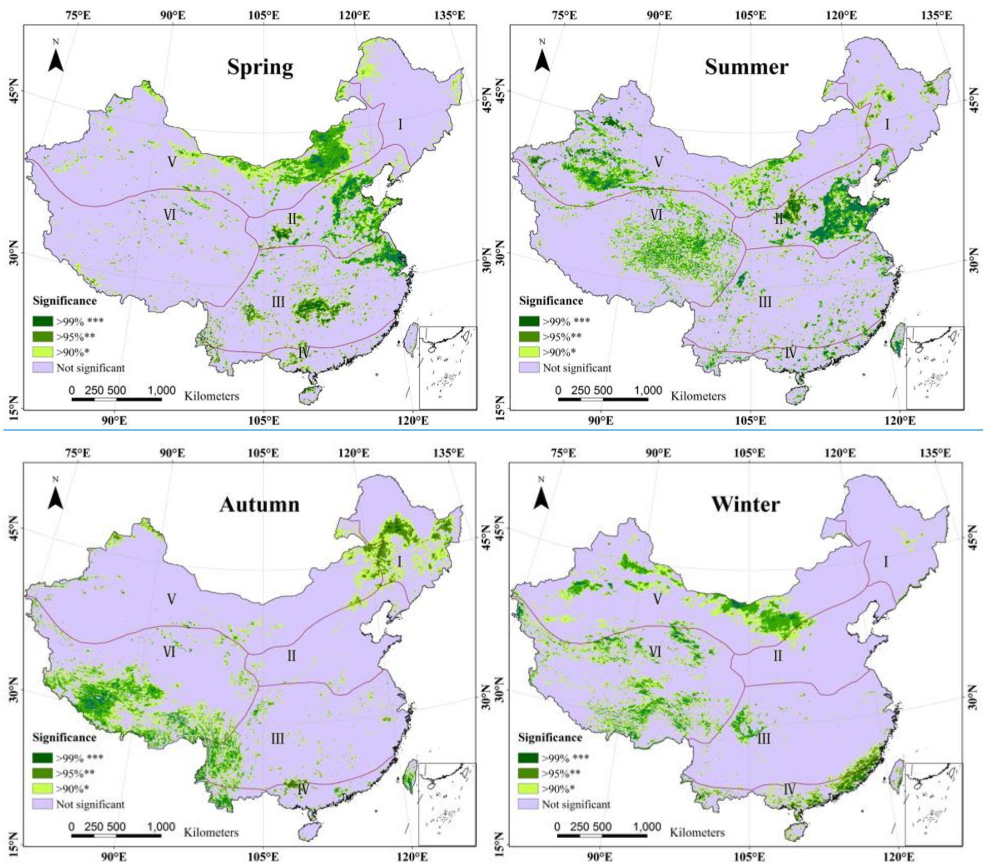

Figure A3: Distribution of seasonal LST trends significance during 2003 - 2017.